REGENERATION OF PERIPHERAL NERVES USING NEUROINDUCTIVE BIOMATERIAL SCAFFOLDS

By

PAULINA SIERPINSKI HILL

A Dissertation Submitted to the Graduate Faculty of
WAKE FOREST UNIVERSITY GRADUATE SCHOOL OF ARTS AND SCIENCES

in Partial Fulfillment of the Requirements

for the Degree of

DOCTOR OF PHILOSOPHY

Molecular Medicine and Translational Science

May 2009

Winston-Salem, North Carolina

Approved By:

Mark Van Dyke, PhD., Advisor _____

Examining Committee:

Anthony Atala, M.D., Mentor _____

Cesar Santos, M.D., Chairman _____

Tom Smith, Ph.D. _____

Shay Soker, Ph.D. _____

TABLE OF CONTENTS

ACKNOWLEDGEMENTS.....iii

DEDICATION.....vii

LIST OF FIGURES AND TABLES..... viii

ABBREVIATIONS.....ix

ABSTRACT..... xv

CHAPTER I - Introduction to Nerve Regeneration.....1

CHAPTER II – Introduction to Keratin Biomaterials.....32

CHAPTER III – Regeneration of Peripheral Nerves Using Structurally Modified Acellular Grafts.....51

CHAPTER IV – Properties and Biocompatibility of Keratin Biomaterials Derived from Human Hair Part I: Kerateine.....80

CHAPTER V – The Use of Keratin Biomaterials Derived from Human Hair for the Promotion of Rapid Regeneration of Peripheral Nerves.....110

CHAPTER VI – Peripheral Nerve Regeneration Using a Keratin-Based Scaffold: Long-Term Functional and Histological Outcomes in a Mouse Model.....145

CHAPTER VII – Repair of Critical Size Peripheral Nerve Defects in Rabbits Using Keratin Hydrogel Scaffolds.....167

CHAPTER VIII – Structural Dependence of Keratin Biomaterials on Integrin-Mediated Activation of Schwann Cells.....192

CHAPTER IX – Discussion.....220

SCHOLASTIC VITAE.....229

ACKNOWLEDGEMENTS

This thesis is the end of a long journey in obtaining my doctoral degree in Molecular Medicine. Both personally and professionally, I have been blessed to be surrounded by an amazing group of individuals, without whom this work would not be possible. Mentors and colleagues, friends and family; all of you deserve my utmost thanks and appreciation for the love, support and guidance that you have provided over the years. First and foremost, I would like to express my most sincere gratitude to my thesis advisor, Mark Van Dyke. There is no single individual who has had more of an impact on the successful completion of my graduate school work than you. Thank you for teaching me so much more than just how to make keratin! Thank you for your mentorship, guidance and endless support along every step of this process. Thank you for providing me with the perfect balance of independence and direction from the day I stepped foot in the lab through the completion of my last experiments. More importantly, thank you for always knowing what that perfect balance was. Thank you for constantly pushing me to do more, but also for recognizing when I had enough on my plate, even when I would not admit it. Thank you for providing me with the best example of how to treat and manage others. Your dedication, commitment and hard work to accomplishing whatever task is at hand to the best of your ability, is inspirational, and something I will always strive for. Thank you, Mark, for everything that you have done and continue to do to ensure my professional success. Without you this work truly would not have been possible.

To Anthony Atala, thank you for giving me the opportunity to receive training in one of the best labs in the world. The environment that you have created at WFIRM is

revolutionary and I couldn't have asked for a better place in which to complete my doctoral research. My experiences at WFIRM have provided me with invaluable skills that I will take with me into my postdoctoral fellowship and beyond.

To the rest of my committee members, thank you for your guidance during the course of my graduate school work. To Cesar Santos, thank you for your willingness to act as chair of my committee. To Shay Soker and Tom Smith, thank you for serving on my committee and providing scientific expertise during the progression of my research.

Thank you to the WFIRM lab members, both past and present. Many of you have become some of my closest friends, others have taught me invaluable research skills and techniques that I will use for the rest of my scientific career. Collectively, you have made WFIRM a stimulating and challenging environment that is a true pleasure to work in. Thank you for being the best group of colleagues and friends that one could ever ask for in a laboratory setting.

To the Molecular Medicine graduate program, thank you for giving me the opportunity to be a part of such a great program. Thank you to Sherrie Brazier for all your hard work and support over the years. To past and present chairs of the program: Kevin High, Bridget Brosnihan and Linda McPhail - your devotion to the program and its students is remarkable and gratefully appreciated.

To everyone else at Wake Forest who has supported me during this whole process. To Susan Pierce, thank you for everything you do behind the scenes to make our lives easier. To the

Orthopaedics department, for providing me with training, technical assistance and surgical expertise to carry out my animal studies. To all my great undergraduate and medical students who I have had the privilege of working with: Jacquie Burnell, Vamsy Bobba, Bernard Tawfik, Sarah DeLeo and Rawad Hamzi. Thanks for all your hard work!

To the wonderful life-long friends who I am so grateful to have made over the last five years. To Jill, thank you for being the kind of friend that only comes along once in a lifetime. It is not often that one meets their true best friend at this stage of life, and I consider myself truly lucky to have had that happen. Thank you for being such an amazing individual, and a shining example of what it means to "Work hard, play hard"! I definitely would not have made it through graduate school without you! To my closest Wake Forest girls - Dawn, Regina, Julie and Lizzy, and the best college friends ever – Andrea, Allison, Meredith, Mary, Kate, and Lauren.

Most importantly, I am deeply grateful to my family, who has molded me into the person that I am today. To Filip, thank you for always being such a great brother. To my wonderful parents, to whom this work is dedicated - words cannot express the appreciation and gratitude that you are due for all that you have done for me. Mom and dad, thank you for sacrificing so much to give me every opportunity I could ever ask for. Thank you for never being satisfied and always pushing me to do more. Thank you for never allowing me to settle for mediocrity and for always challenging me to be better in everything I do. And above all, thank you for providing me with a living example of the saying "We make a living by what we get, but a life by what we give" *~Winston Churchill.*

Lastly, I would like to thank my husband (of less than a year!). Thank you, Jonathan, for your unconditional love. Thank you for being the kind of husband that one can only dream of, but never have. Thank you for always appreciating me, understanding me, and treating me like gold since the very first day we met. Thank you for teaching me the concept of balance so early on in our relationship, and for helping me realize what is truly important in life. Thank you for always wanting what is best for me, and for making me a better person every day that we're together. Thank you for always being there for me, and for talking to me about everything but science. I cannot thank you enough for your constant encouragement and endless support in everything I do, no matter how crazy it is! I am truly blessed to have you as my husband and eagerly await the marvelous things that God has in store for our life together.

DEDICATION

This work is dedicated to my parents, Ewa and Richard Sierpinski.

Thank you for everything you have done.

LIST OF FIGURES AND TABLES

CHAPTER I - Introduction to Nerve Regeneration

Figure 1 – Anatomical organization of the PNS.

Figure 2 – Nerve degeneration and regeneration following injury

Figure 3 – Surgical end-to-end repair of damaged nerve ends

Figure 4 – Repair of peripheral nerve defects with a nerve guidance conduit

CHAPTER II - Introduction to Keratin Biomaterials

Figure 1 – Cellular structure of a hair fiber

CHAPTER III - Regeneration of Peripheral Nerves Using Structurally Modified Acellular Grafts

Figure 1 – Histological analysis of decellularized and native rabbit nerves

Figure 2 – DNA content in native and decellularized rabbit nerves

Figure 3 – SEM analysis of decellularized and oxidized nerves

Figure 4 – H&E staining of the distal segment of regenerated nerve grafts

Figure 5 – NF-200 immunostaining of neurofilaments within regenerated nerves

Figure 6 – S100β immunostaining for Schwann cells

Figure 7 – Toluidine blue cross-sections of the distal segments of regenerated nerves

Figure 8 - Histomorphometric analysis of distal nerve cross-sections

CHAPTER IV – Properties and Biocompatibility of Keratin Biomaterials Derived From Human Hair Part I: Kerateine

Figure 1 – Schematic of a wool fiber

Figure 2 – SDS-PAGE of reductively-extracted keratins

Figure 3 – Gross and SEM analysis of lyophized kerateine disks prior to implantation

Figure 4 – *In vitro* degradation of kerateine biomaterials

Figure 5 – Cytotoxicity of kerateine biomaterials

Figure 6 – 3T3 fibroblast adhesion to a kerateine coating

Figure 7 – 3T3 fibroblast proliferation on a kerateine substrate

Figure 8 – Gross examination of sub-cutaneoulsy implanted kerateine disks

Figure 9 – Hematoxylin & eosin (H&E) staining of kerateine biomaterial implants

Figure 10 – Masson's trichrome staining of kerateine implants for collagen deposition

Table 1 – Amino acid composition of kerateine biomaterials

CHAPTER V – The Use of Keratin Biomaterials Derived from Human Hair for the Promotion of Rapid Regeneration of Peripheral Nerves

Figure 1 – Schematic of a wool fiber

Figure 2 – Scanning electron microscopy (SEM) of keratin hydrogels

Figure 3 – *In vitro* cytocompatibility assessment by an MTS proliferation assay

Figure 4 – *In vitro* migration of Schwann cells in response to keratin

Figure 5 – *In vitro* adhesion of Schwann cells to a keratin substrate

Figure 6 – Gene expression changes in Schwann cells exposed to keratin

Figure 7 – Nerve fiber regeneration 6 weeks after nerve injury and repair

Figure 8 – Electrophysiology testing following 6 weeks of regeneration

Figure 9 – Muscle force generation testing at 6 weeks

Figure 10 – Toluidine blue staining of regenerated nerve cross-sections

Figure 11 – Histomorphometric analysis of regenerated nerve cross-sections

Figure 12 – Histomorphometric analysis of vascularization within regenerated nerves

CHAPTER VI– Peripheral Nerve Regeneration Using a Keratin-Based Scaffold: Long-term Functional and Histological Outcomes in a Mouse Model

Figure 1 – Placement of the keratin hydrogel in the conduit

Figure 2 – Diagram of electrode placement and setup for CMAP recording

Figure 3 – Summary of CMAP results

Figure 4 – Representative photomicrographs of regenerated nerve segments

Figure 5 – Average axon density

Figure 6 – Average axon diameter

Table 1 – Complete histomorphometry data

CHAPTER VII– Repair of Critical Size Peripheral Nerve Defects in Rabbits Using Keratin Hydrogel Scaffolds

Figure 1 – Implantation of keratin hydrogel-filled collagen nerve guides

Figure 2 – Electrophysiological testing three months following injury and repair

Figure 3 – Muscle atrophy following three months regeneration

Figure 4 – Representative images of toluidine blue stained nerve cross sections

Figure 5 – Histomorphometric analysis of nerve cross sections

CHAPTER VIII – Structural Dependence of Keratin Biomaterials on Integrin-Mediated Activation of Schwann Cells

Figure 1 – Overview of keratin fractionation process

Figure 2 – Structural analysis of proposed amino acid sequences of human hair keratins

Figure 3 – Schwann cell proliferation in response to crude and fractionated keratins

Figure 4 – Immunoblot of Schwann cell lysates probed for integrins β1 and αV

Figure 5 – Immunoblot of Schwann cell lysates probed for MAPK and pMAPK

Table 1 – Amino acid composition of crude and fractionated keratin biomaterials

ABBREVIATIONS

CNS	central nervous system
PNS	peripheral nervous system
FGF	fibroblast growth factor
NGF	nerve growth factor
IGF	interleukin-like growth factor
CNTF	ciliary neurotrophic factor
BDNF	brain-derived neurotrophic factor
VEGF	vascular endothelial growth factor
CSPG	chondroitin sulfate proteoglycan
ECM	extracellular matrix
MMP	matrix metalloprotease
FDA	Federal Drug Association
kDa	kilodalton
KIF	keratin intermediate filament
KAP	keratin associated protein
RGD	arginine-glycine-aspartic acid
LDV	leucine-aspartic acid-valine
SEM	scanning electron microscopy
NBF	neutral buffered formalin
CMAP	compound muscle/motor action potential
NIH	National Institute of Health
H&E	hematoxylin & eosin

NF	neurofilament
ANOVA	analysis of variance
SEM	standard error of the mean
PA	peracetic acid
ChABC	Chondroitinase
DI	deionized
SDS	sodium dodecyl sulfate
PTC-AA	phenylthiocarbamyl-amino acid
PBS	phosphate buffered saline
FBS	fetal bovine serum
MTS	3-(4,5-dimethylthiazol-2-yl)-5-(3-carboxymethoxyphenyl)-2-(4-sulfophenyl)-2H-tetrazolium)
ACUC	Animal Care and Use Committee
SDS-PAGE	sodium dodecyl sulfate polyacrylamide gel electrophoresis
ATCC	American Type Culture Collection
qRT-PCR	quantitative reverse transcriptase polymerase chain reaction
GAPDH	glyceraldehyde 3-phosphate dehydrogenase
L1CAM	L1 cell adhesion molecule
GFAP	glial fibrillary acidic protein
CI	confidence interval
HHK	human hair keratin
MAPK	mitogen-activated protein kinase
pMAPK	phosphorylated mitogen-activated protein kinase
DEAE	diethylaminoethyl cellulose

GDS	glycine-aspartic acid-serine
GDV	glycine-aspartic acid-valine
LDS	leucine-aspartic acid-serine
EDV	glutamic acid-aspartic acid-valine
EDS	glutamic acid-aspartic acid-serine
HPLC	high performance liquid chromatography
TBST	Tween-20 Tris-buffered saline
RIPA	RadioImmuno precipitation assay
BSA	bovine serum albumin
PVDF	polyvinylidene fluoride

ABSTRACT

Paulina Sierpinski Hill

Regeneration of Peripheral Nerves Using Neuroinductive Biomaterial Scaffolds

Dissertation under the direction of

Mark Van Dyke, Ph.D., Assistant Professor
Wake Forest Institute for Regenerative Medicine

Over 18 million extremity injuries are recorded in the United States each year, resulting in a substantial number of peripheral nerve injuries that account for more than $150 billion in health care costs. Clinically, treatment consists of direct surgical repair, implantation of a nerve guidance conduit or the use of an autograft. However, less than 50% of individuals that undergo surgical repair regain useful function, and for many patients permanent or long-term disability is a frequent prognosis. Biomaterial scaffolds are promising for use in neural reconstruction, but to date, no neuroinductive biomaterials capable of acting directly on regenerative cells to stimulate nerve growth have been identified. The goal of this dissertation work was to develop and investigate the effectiveness of novel biomaterials for neural tissue engineering applications. This dissertation work has resulted in the development of two distinct scaffold-based guidance strategies for bridging peripheral nerve defects. The first strategy is based on a classic tissue engineering approach, and involves the use of modified acellular grafts interposed across a nerve gap. The second strategy introduces keratin made from human hair as a promising, neuroinductive biomaterial for use in neural regeneration. Keratin biomaterials were found to be highly biocompatible and able to promote Schwann cell adhesion, proliferation and migration. Implantation of a keratin hydrogel into a nerve guidance conduit resulted in a 150-300% improvement in motor function recovery in a small animal model at an early time point. Long-term functional and histological assessment confirmed improved neuromuscular regeneration in keratin-treated nerves. Furthermore, keratin was found to promote functional regeneration over a critical size defect in a large animal model. Investigations into the mechanism by which keratins act on regenerative cells suggest that activation of Schwann cells is integrin-mediated and dependent on the structural characteristics of human hair keratins. Thus, keratin biomaterials derived from human hair represent a neuroinductive scaffold-based conduit filler that may be used as an “off-the-shelf” product for treatment of peripheral nerve injuries. This dissertation work justifies the translation and clinical development of a keratin-based hydrogel filler as a complimentary product for use in existing nerve conduits, and suggests that keratin biomaterials may be capable of bridging peripheral nerve defects beyond current clinical limits.

CHAPTER I

Introduction to Nerve Regeneration

Paulina Sierpinski Hill

THE CLINICAL PROBLEM

Peripheral nerve injury is a serious clinical problem that accounts for more than $150 billion in health care costs in the United States each year (1). Nerve injuries are caused by motor vehicle accidents, sports injuries, gunshot and stab wounds, work and home accidents, and tumor resection. Nerve damage can also result from underlying conditions such as carpal tunnel syndrome, diabetes, toxicity, infection, as well as many other systemic and congenital diseases. Approximately 5% of all open wounds in the extremities are complicated by peripheral nerve trauma, many of which result in nerve gaps (2). Regardless of severity, nerve injuries are debilitating and interfere with an individual's ability to function at work and in daily life. Besides functional impairment, nerve injuries often result in pain, dysesthesia (itching or burning), paresthesia (tingling or numbness) and cold intolerance (3). Fewer than 60% of individuals return to work after suffering a median or ulnar nerve injury and considerably fewer individuals regain a normal quality of life in cases of brachial plexus injury (4,5). In the United States, approximately 360,000 individuals suffer from upper extremity paralysis each year resulting in 8.6 million days of restricted activity and 4.9 million disability days (6). Over 200,000 of these patients undergo surgical intervention annually (7). Despite over one and a half centuries of experience in surgical management of peripheral nerve injuries, there has been little improvement in the outcome following nerve injury and repair (8). Less than 50% of individuals that undergo surgical repair regain useful function (9), and for many patients permanent or long-term disability is a frequent prognosis. Research in the nerve regeneration field has been extensive, but to date, few experimental therapies have been translated clinically.

Thus, a critical need remains for the development of novel and effective bridging strategies for peripheral nerve repair.

PHYSIOLOGY AND ORGANIZATION OF THE NERVOUS SYSTEM

The central nervous system (CNS) and peripheral nervous system (PNS) differ in their function, physiology and ability to regenerate following injury. The CNS consists of the brain and spinal cord, whereas the PNS consists of all of the extremity nerves including all craniofacial, spinal and sensory nerves. Unlike in the CNS, peripheral nerves have the ability to spontaneously regenerate, provided the injury is minor and surgically repaired. Anatomically, a peripheral nerve consists of a protective collagenous cushion, the epineurium, which surrounds several nerve fascicles (Figure 1). Each fascicle is surrounded by a collagen-rich sheath called the perineurium and is composed of many individual axons. Each axon is surrounded by a lipid-rich myelin sheath which is formed from dense layers of the Schwann cell membrane. The myelin sheath insulates the axons and serves to increase the propagation velocity of the action potential. The myelin sheath contains periodic 1 μm length gaps called nodes of Ranvier at which the axon membrane generates electrical potentials that are transmitted down the length of the axon to the neuromuscular junction. Each axon represents an extended process from the nerve cell body situated in the dorsal root ganglion (sensory neuron) or in the ventral horn of the spinal cord (motor neuron). Sensory or afferent neurons, are responsible for stimulus reception, and motor or efferent neurons, control end organs and tissues such as glands and

muscles. The functional unit of the neuromuscular system is the motor unit, which consists of a lower motor neuron in the spinal cord, the axon of that neuron, and the multiple muscle fibers it innervates. Muscles with highly refined movements, such as the extrinsic muscles of the eye, have a high neuron-to-muscle-fiber ratio (1:10); those with relatively coarse movements such as the gastrocnemius muscle of the leg, may have one neuron innervating as many as 1000 muscle fibers (3).

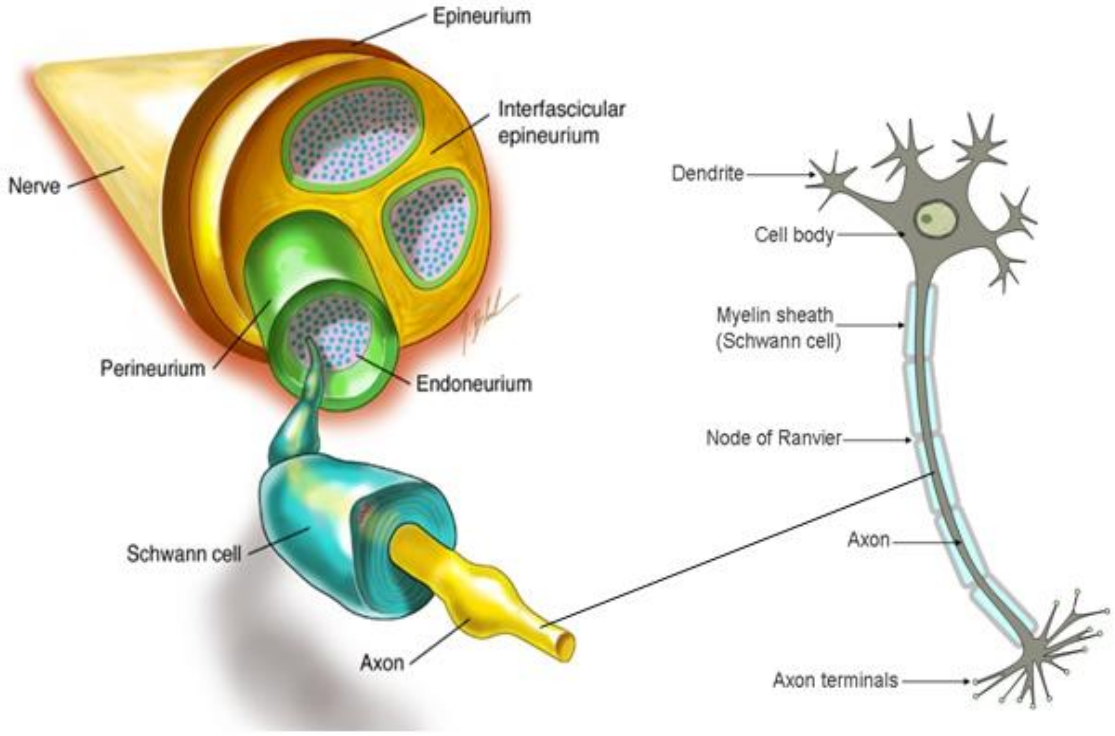

Figure 1. Anatomical organization of the PNS. A peripheral nerve consists of many fascicles grouped together by the epineurium, an outer sheath of loose collagenous tissue. Each fascicle is enclosed by the perineurium and consists of many individual axons bundled together. Each axon is surrounded by a myelinating Schwann cell sheath and a layer of oriented collagen fibers called the perineurium. Each axon has a cell body that is located in the spinal cord, and axon terminals that form neuromuscular junctions with target end organs.

PERPIPHERAL NERVE INJURY

Nerve injuries complicate successful rehabilitation more than any other form of trauma (10). In the PNS, axons have the ability to regenerate over small defects when appropriate surgical repair techniques and guiding strategies are used. The age of the individual is the most important predictor of outcome following nerve injury and repair. Children often regain normal function after injury, but adults and elderly individuals experience slow or absent functional recovery. More than half of individuals over the age of 50 do not achieve any functional recovery after nerve repair (11). Besides clinical factors such as age and health of the patient, the outcome of the injury is dependent on the site of the lesion, the degree of disruption of the surrounding tissue, the integrity of the vascular network and the degree of cellular damage (12).

The severity of a nerve injury can be classified according to a system developed by Seddon in the 1950's into three major groups: neuropraxia, axonotmesis and neurotmesis (13). Neuropraxia refers to a physiological block within the axons where axon continuity is preserved. Axonotmesis is an anatomical interruption of the axons with preservation of the perineurium and epineurium, although to varying degrees. Neuropraxia and axonotmesis are frequently the result of nerve compression syndromes from a crush injury or neuroma formation. In such cases, regeneration typically takes place within 4-6 weeks, provided the underlying condition does not persist over time (14). The most severe injury is a complete transection of the nerve that results in neurotmesis. Neurotmesis is a complete anatomical

disruption of both the axons and all of the surrounding connective tissue. Without surgical intervention, regeneration does not occur due to scar formation and axon misguidance. Classification of nerve injuries was further refined by Sunderland on the basis that axonotmesis injuries had variable prognoses depending on the source, duration and severity of the anatomical block (15).

DEGENERATION AND REGENERATION FOLLOWING INJURY

When axons are completely severed, a series of changes take place both proximally and distally to the lesion site (Figure 2). Within hours after injury, the ends of the severed axons seal themselves off and swell. The proximal end of each axon degenerates proximally to the next node of Ranvier. Centrally, approximately 40-50% of severed neurons apoptose (16,17). This phenomenon closely resembles that of fetal development where approximately 50% of post mitotic neurons naturally die off (18). Distally, the axon cytoskeleton and membrane disintegrate and Schwann cells shed their myelin sheaths in a process called Wallerian degeneration that is initiated 24-48 hours after transection (19). Macrophages enter the site of injury through the vascular network and activate Schwann cells to dedifferentiate into a rapidly proliferating state. Together with macrophages, Schwann cells begin phagocytosis of myelin debris. Following debris clearance, Schwann cells in the distal segment line up in columns called bands of Bungner and secrete growth factors such as fibroblast growth factor (FGF), nerve growth factor (NGF), interleukin-like growth factor (IGF), ciliary neurotrophic factor

(CNTF), brain-derived neurotrophic factor (BDNF) and vascular endothelial growth factor (VEGF) (20-22). The laminin and fibronectin present within the basal lamina of the Schwann cells and the secreted neurotrophic factors guide sprouting axons into the endoneurial columns. The specialized growth cone at the tip of each axon sprout contains multiple filopodia that adhere to the basal lamina of the Schwann cell and use it as a guide. Further advancement of the growth cone is stimulated by a combination of insoluble and soluble cues in the extracellular environment (23). Inhibitory factors such as netrins, semaphorins, ephrins and proteoglycans such as chondroitin sulfate proteoglycans (CSPGs) play an important role in repulsion and prevent axonal sprouting down certain paths (24-26). These mechanisms of contact and chemotactic attraction and repulsion determine the fate of regenerating axons. The first signs of axon regrowth into the distal segment may be seen as early as 24 hours post injury, or may be delayed for weeks in more severe injury. In addition to the soluble and insoluble cues provided by the microenvironment of the regenerating nerve, the rate of axonal regeneration is determined by changes within the cell body, the stability of the growth cone at the tip of the axon sprout, and the resistance of the injured tissue between cell body and end organ (27). Axons that successfully enter the endoneurial tubes in the segment distal to the injury site stand a good chance of reaching the end organ, given reasonable growth conditions. The distal regeneration rate is slower if the endoneurial tubes have been disrupted because axon sprouts must first find their way into the tubes before advancing. Each severed axon produces a large number of regenerating sprouts and at times, because several small axon sprouts may enter the same endoneurial tube, a regenerated nerve fiber may contain more axons than the original

nerve. These daughter axons are typically pruned away during the axon maturation process and usually do not all make their way into the target end organ (28).

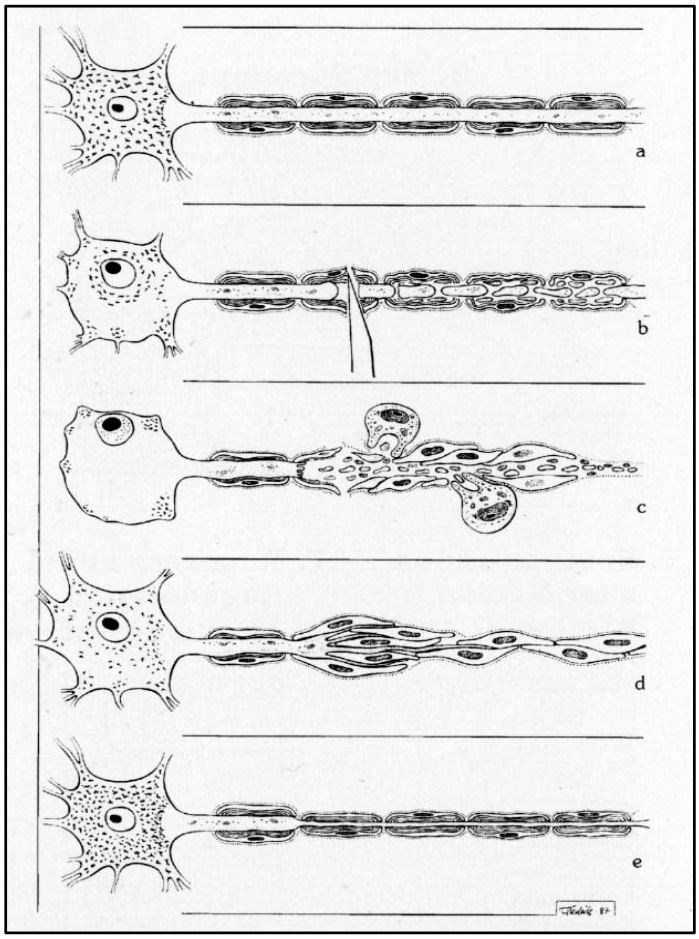

Figure 2. Nerve degeneration and regeneration following injury (29). When an intact peripheral nerve (A) is severed (B), the distal portion of the nerve degrades as a result of protease activity in a process known as Wallerian degeneration (C). Macrophages and Schwann cells migrate into the defect site, become phagocytic and clear axonal and myelin debris. Following debris clearance, Schwann cells lay down bands of Bungner, or endoneurial tubes (D), that guide regenerating axons from the proximal end across the defect, into the distal stump (E) and down to the target end organ.

The rate of axonal regeneration has been assumed to be constant and, in clinical situations, is generally estimated to be 1 mm per day (30). Reported rates of regeneration, however, vary broadly from 0.5 to 9 mm per day (27). This variability is due to several factors. For one, the rate of axon growth decreases with increasing distance from the cell body to the advancing axon tip. It is well documented that axon regeneration is faster in distal injuries and that prognosis improves the more distal the injury. Secondly, the severity and type of the injury significantly affects nerve growth. The rate of axonal outgrowth is much faster in crush injuries than in the case of a complete transection. The disparities in observed regeneration rates are also largely dependent on the animal model and methods for measuring regeneration. Moreover, the rate of regeneration can depend on the duration of denervation, survival of central neurons, the degree of vascularization and the condition of the peripheral tissues (31). Aging has also been shown to retard the rate of axonal regrowth (11).

Clinically, both demyelination and axonal degeneration result in disruption of the sensory and/or motor function of the injured nerve. However, axonal regeneration is not synonymous with return of function. A process of maturation precedes functional recovery. Morphological changes of maturation proceed along the regenerating axon at a slower rate than axon regrowth and continue for up to 2 years following repair (32). The axon's diameter increases progressively until normal dimensions are reached, but this enlargement is dependent on the establishment of functional connections between the axon tip and the appropriate end organ. Recovery of function occurs with remyelination and with axonal growth as well as

reinnervation of the sensory receptors and muscle end plates. Return of function takes place in the following order: sympathetic, pain, temperature, proprioception and motor (9).

If a functional end organ is not reached, further development and remyelination do not occur. Similarly, if the end organ has undergone degenerative changes that do not allow re-establishment of functional neuromuscular junctions due to prolonged denervation, axonal development and maturation will not take place (33). If entry of regenerating axons into the distal segment is delayed more than 3-6 months, permanent, irreversible changes may take place at the neuromuscular junction (34). Muscle fibers atrophy rapidly, with an average 70% reduction in cross-sectional area by 2 months (35). Prolonged denervation of the Schwann cells themselves also makes them unreceptive to axon regeneration. This has been shown to be the single most important contributor to poor end organ reinnervation (36).

Regeneration of nerves following injury involves a complex series of events consisting of degeneration, host cell migration and proliferation, debris clearance, axon guidance and maturation, as well as reinnervation of target end organs. Each of these processes affects the final outcome following nerve injury and repair. When designing novel bridging strategies, it is important to consider the basic neurobiology of regeneration in the PNS and develop guidance systems that accelerate and optimize each step of this multifaceted process.

SURGICAL REPAIR OF PERIPHERAL NERVE INJURIES

Primary Repair

Primary tensionless repair is the surgical treatment of choice for minor nerve injuries. This type of repair consists of surgical reconnection of the damaged nerve ends and is performed over small defects where tension-free repair is possible. The edges of the damaged proximal and distal stumps are debrided, the fascicles are aligned, and the nerve ends are reconnected by epineurial and/or perineurial suturing (Figure 3) (37). However, end-to-end coaptation is only effective for small defects that can be repaired in a tension-free manner since any tension at the anastamosis site is known to result in increased scar tissue formation, compression of regenerating axons and decreased microvascular flow (38). When the proximal and distal segments do not freely reach each other, as is frequently the case due to retraction of severed nerve ends following transection and resection of scarred nerve tissue at the site of injury, an autograft must be used to bridge the defect.

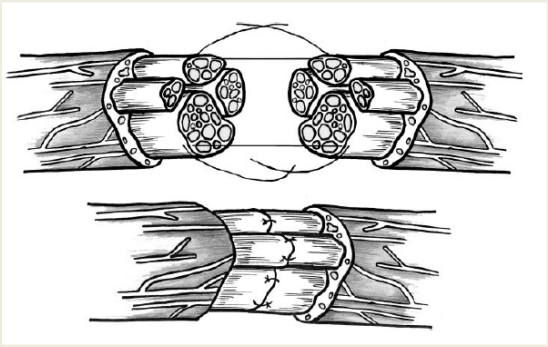

Figure 3. Surgical reconnection of damaged nerve ends. End-to-end repair consists of microsurgically suturing individual fascicles within the nerve cable together in a tension-free manner.

Sensory Nerve Autografts

The sensory nerve autograft is the most widely used technique for bridging peripheral nerve defects (39). Grafts are typically harvested from the sural or saphenous nerves, two sensory cutaneous nerves. The nerve to be repaired is often of a larger diameter than the donor nerve, therefore multiple cable grafts are used so that complete coverage of the transected nerve fascicles is achieved. Multiple small grafts are preferred because they readily receive neo-vascularization from the surgical bed and promote survival of transplanted Schwann cells (40). The axons in the nerve grafts degenerate, leaving the endoneurial tubes and Schwann cells to receive regenerating axons from the proximal nerve stump. The remaining endoneurial tubes serve as a physical matrix for host cell migration and axonal outgrowth. Although regenerating axons typically traverse the defect, studies have shown that poor motor function recovery is obtained through sensory nerves (41,42). A retrospective study of 60 patients found that only 20.1% of individuals who underwent a lower extremity injury and repair with a sural nerve autograft regained favorable functional outcomes. If surgical repair was delayed, only 11.1% of subjects showed a satisfactory return of function (43). Implantation of an autograft is also a technically demanding procedure associated with long surgical times, donor site morbidity and limited graft availability (44). These disadvantages justify the continued search for a more acceptable nerve graft substitute.

Acellular Allografts

Due to the many disadvantages with using autologous tissue, non-autologous tissue and extracellular matrix (ECM)-based grafts have been investigated for bridging nerve defects. Allografts have several potential clinical advantages: 1) grafts can be banked; 2) there is no need for sacrifice of a donor nerve; and 3) surgical procedures are quicker without the need to harvest a graft. However, allografts are not as effective as autografts, mainly due to the immunogenic host response. To overcome these limitations, thermally and chemically decellularized nerve allografts were developed. A method for decellularizing allografts was first reported about 25 years ago, when small segments of pre-degenerated mouse sciatic nerves were shown to be devoid of viable cells after exposure to a repeated freeze-thaw cycles (45). Implantation of thermally decellularized grafts across a <1 cm sciatic nerve defect was shown to support axon regeneration. Subsequent studies showed that chemical decellurization methods could be used to create a functional acellular basal lamina scaffold without the residual cell debris left by the freeze-thaw method (46,47). The use of chemically treated grafts has been shown to result in improved regeneration in rodent models compared to thermally treated grafts (47).

Acellular grafts are advantageous because they can be derived from motor nerves and possess many of the necessary ECM components specifically required for motor nerve regeneration. Because the cellular and myelin components are removed prior to implantation, acellular grafts have reduced immunogenicity while still providing a basal lamina for the regenerating nerve (48). Numerous studies have shown that acellular grafts are able to promote

regeneration over 1-2 cm defects in a rat sciatic model (49-54). However, few studies have achieved similar results over longer defects in large animal models. Evaluation of published studies utilizing a rat sciatic nerve injury model shows that even over 1-2 cm, axons do not always reach the distal segment of the graft. Moreover, the use of decellularized grafts to regenerate nerve across gaps larger than 2 cm has been largely unsuccessful. (55,56). One obvious reason for this is the absence of growth promoting cells within the scaffold. A second reason that has recently been proposed is the dense architecture of the decellularized nerve (57). Scaffold porosity is particularly important in the case of nerve regeneration to allow for migration of Schwann cells and outgrowth of axons toward distal muscle targets. Acellular scaffolds are known to possess a dense architecture that may require extensive matrix remodeling upon implantation *in vivo*. Previous studies have shown that predegradation of extracellular matrix components by matrix metalloproteases (MMPs) prior to graft implantation significantly improves axonal outgrowth (58). This suggests that partial degradation of an acellular graft prior to implantation may result in a more porous microarchitecture that is conducive to cell infiltration and regeneration over short and long distances. Furthermore, the use of a graft with a more permissive architecture for host cell infiltration and migration of regenerating axons may increase the effective length of acellular grafts. One goal of this dissertation work was to determine if acellular grafts could be structurally modified *in vitro,* and if implantation of grafts with a more favorable microarchitecture could promote axon regeneration across large nerve gaps.

Nerve Conduits

Primary repair and autografting is the standard treatment of care for peripheral nerve injuries. Prerequisites are a clean wound, good vascular supply, no crush component of the injury, and adequate soft-tissue coverage. Unfortunately, in many instances of severe trauma, infection or delay in repair, these requirements are not met (59). Entubulation strategies using hollow cylindrical tubes arose out of these limitations. Experimental work with animals was first reported by Gluck in 1880 and Vanlair in 1882 using decalcified bone as a tube (60). In the early 1900's other investigators described successful regeneration through arterial grafts (61,62), and the term nerve conduits was adopted to describe any hollow tube capable of guiding peripheral nerves across a defect (Figure 4). In the 1940's nerve conduits were extensively used to repair extremity injuries resulting from battlefield wounds. Since then, it has been recognized that a peripheral nerve has the capacity to regenerate over small distances when appropriate entubulation strategies are used. However, it was not until the 1980's that the validity of the nerve guide for bridging short nerve gaps was confirmed. In 1982, a group of researchers led by Goran Lundborg introduced the silicone tube model system as an experimental tool for characterizing the temporal and spatial effects of regeneration through a conduit (63). When a silicone tube was used to bridge a 10 mm rat sciatic nerve defect, the result was spontaneous formation of a new nerve trunk of normal appearance bridging the defect inside the conduit. However, when this distance was increased to 15 mm, no regeneration occurred within the conduit (63,64). Although silicone tubes have little clinical use due to chronic nerve compression, irritation and inflammation at the implant site requiring removal, and

impermeability to many nutrients, they adequately introduced the concept of entubulation to the scientific community (65). Following the general concept of physiological nerve regeneration, the idea of inserting luminal fillers as a surrogate provisional matrix to further facilitate regeneration was introduced shortly thereafter. In 1987, Williams, *et al.* showed that silicone tubes filled with dialyzed plasma led to a three- to five-fold increase in functional recovery compared to saline-filled conduits (66). In recent years, numerous studies have shown that cellular, neurotrophic or structural based matrices inserted into a nerve conduit promote regeneration to varying degrees (67,68).

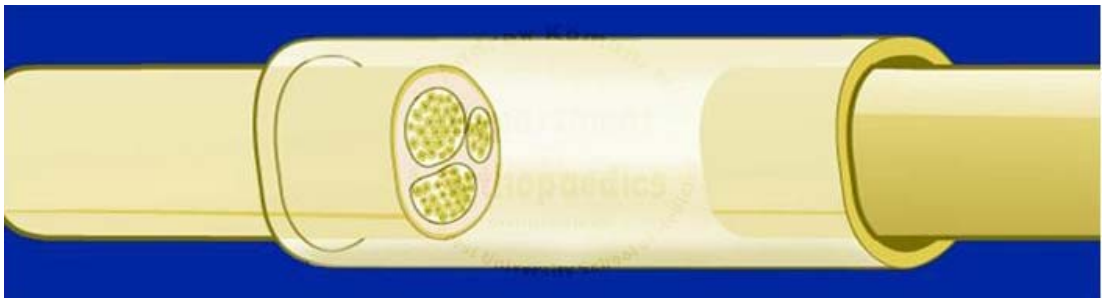

Figure 4. Repair of peripheral nerve defects with a nerve guidance conduit. The conduit allows for tension-free repair of the damaged nerve ends, prevents the invasion of scar tissue, directs sprouting axons, and provides a protected environment for migration of regenerative cells and diffusion of growth factors.

Luminal Fillers for Nerve Conduits

The purpose of a nerve guide is to provide a channel between the proximal and distal ends without introducing any tension into the nerve tissue. Guidance tubes also simplify the surgical procedure, prevent the invasion of scar, direct axons sprouting from the proximal end

and facilitate the diffusion of trophic factors (69). Three bioabsorbable nerve guides made of collagen (NeuraGen, Integra LifeSciences), polyglycolic acid (GEM Neurotube, Synovis Micro Companies Alliance) and poly(dl-lactide-ε-caprolactone) (Neurolac, Polyganics) are currently approved for clinical use (70-72). With the commercialization of highly biocompatible, bioabsorbable conduits, the experimental focus has recently shifted from the development of novel conduit materials to the addition of biologically active substrates as luminal fillers inside existing conduits. These conduits fillers are being developed on the premise that there are three major components necessary for enhancing nerve regeneration across a defect: support cells, neurotrophic factors and a scaffold for cell and axon migration.

Cell-based luminal fillers

Schwann cells, bone stromal cells, fibroblasts and other cellular components have been investigated as nerve conduit fillers (73). In 1992, Guenard, *et al.* investigated the use of autologous and non-autologous Schwann cells suspended in Matrigel™ to bridge an 8 mm rat sciatic nerve defect (74). Implantation of autologous Schwann cells resulted in significantly more myelinated axons than in empty conduits, with total myelinated axon numbers reaching 25% of that observed through a sural nerve autograft. Insertion of allogeneic Schwann cells resulted in a strong immune response and poor axon regeneration. Other studies investigating the use of autologous Schwann cells within a nerve conduit have successfully obtained axon growth in defects as high as 4 cm and 6 cm in a rabbit tibial and peroneal model, respectively

(75,76). Bone stromal cells and fibroblasts have proven to be minimally effective over small defects but have not been investigated in larger animal models (77-79). Although Schwann cells have proven to be a promising nerve conduit filler, the use of autologous Schwann cells in nerve regeneration therapy is impractical. Primary Schwann cells are difficult to isolate and expand e*x vivo*, so cell culture rarely yields enough cells for implantation *in vivo*. Furthermore, harvest of autologous Schwann cells has many of the same disadvantages as the use of a nerve autograft.

Growth factor-based luminal fillers

Soluble neurotrophic factors known to be important for regeneration of nervous tissue have been incorporated into nerve conduit lumens. NGF, FGF, CNTF, VEGF as well as other growth factors, have been investigated in rat sciatic defects of 0.5-1.5 cm. In 1989, Rich *et al.* showed that injection of NGF into a silicone conduit increased the number and thickness of myelinated axons by 58% (80). These results were later confirmed by other investigators over defects up to 2.5 cm (81-83). In 1993, Walter *et al.* found that injection of FGF into a nerve guide resulted in motor function recovery over a 1.5 cm defect in a rat compared to no functional recovery in empty conduit controls (84). Midha, *et al.* showed that the use of FGF in combination with a collagen matrix produced results comparable to that of autograft over a 10 mm gap (85). The use of CNTF and VEGF in a silicone conduit to bridge 1 cm rat defects has

also been shown to result in significantly larger axon diameters, more myelinated axons and slight improvements in motor function recovery over empty conduit controls (86,87).

Each of these growth factors provide trophic support to the regenerating nerve in at least one of three ways: 1) By increasing the survival of neurons, 2) By having a mitogenic and/or chemotactic effect on regenerating cells, or 3) By stimulating collateral sprouting and guiding axons towards their distal muscle target. Unfortunately, growth factor therapies face several scientific, regulatory and financial hurdles that must be overcome prior to therapeutic use. For example, NGF is known to cause undesirable effects such as weight loss, pain and Schwann cell migration into the spinal cord when administered systemically (88,89). Therefore, one example of an important scientific challenge that must be overcome is bioengineering a system which allows for the local delivery of growth factors in sufficient quantities with a consistent dose and rate of administration, while avoiding any adverse side effects associated with growth factors making it into the circulatory system (90).

Scaffold-based luminal fillers

Attempts have been made to use a variety of natural and synthetic materials as a supporting structure for axon outgrowth. Fillers composed of synthetic polyamide, polydioxanone and polyglactin filaments inserted into a silicone conduit have been shown to increase the effective regeneration length from 10 mm to 15 mm in a rat sciatic nerve model

(73). Natural materials are generally advantageous over synthetics because they are highly biocompatible, have decreased toxic effects and are more effective at regulating cell behavior. But, natural materials can also have their share of disadvantages such as an undesirable immune response, batch to batch variation and an inability to control processing techniques (91). Naturally occurring polysaccharides such as alginate, chitosan and hyaluronic acid, as well as ECM proteins like collagen, laminin and fibronectin in the form of gels, fibers and sponges inserted into a nerve guide have been shown to promote regeneration (92-94). In general, these materials have been shown to be neuroconductive, in that they are capable of supporting regeneration to varying degrees without the addition of cellular or growth factor components, but not neuroinductive, in that they are not capable of acting on regenerative cells to promote regeneration beyond current clinical limits. In 1985, Madison, *et al.* found that a gel composed of 80% laminin increased the number of regenerating cells within the conduit at 2 weeks (95). In a subsequent study published two years later, Madison *et al.* confirmed that a laminin gel increases the initial rate of axonal outgrowth but that the presence of the laminin gel actually inhibits the same regeneration process at 6 weeks (96). It has been shown that the concentration of collagen and laminin used within the conduit is critical to regeneration outcomes (97). Mixed results ranging from poor to excellent have been reported using different concentrations of collagen and laminin gels over short and long defects (95,98,99). The most impressive results were obtained using a laminin-soaked collagen sponge introduced into a synthetic conduit to span an 80 mm peroneal defect in a canine model (100). Matsumoto, *et al.* showed that dogs treated with a collagen-laminin sponge had near-normal walking patterns at

12 months following injury and immediate surgical repair. As impressive as these results were, no similar outcomes have been reported using a collagen-laminin filler in the 9 years since this study was published, and much skepticism remains as to the effectiveness of such a scaffold due to its potentially inhibitory effects.

The Need For Novel Biomaterial Based Nerve Conduit Fillers

Despite many reported successes on the use of cellular, neurotrophic and scaffold-based fillers, few investigators have been able to consistently demonstrate regeneration of gaps exceeding the 2 cm limit. In 1987, Williams *et al.* first demonstrated that insertion of a "filler" into the nerve guide significantly improves functional outcomes, and yet more than 20 years later, clinicians are still implanting empty or saline filled nerve guides . Almost a decade after the successful bridging of an 8 cm defect in a canine model using a collagen-laminin sponge, no off-the-shelf nerve conduit filler exists for use in patients. Translational research in this field has been muted, and as a result, the clinical use of nerve conduits remains limited to relatively small defects with suboptimal functional outcomes. This suggests that few, if any, of the fillers that have been experimentally tested to this point have potential for clinical translation and justifies the continued search for novel nerve conduit fillers. To avoid the many challenges associated with cell and growth factor delivery, the ideal luminal filler would be scaffold-based. In addition to being highly biocompatible, the optimal biomaterial filler would also be bioactive, cell instructive, non-xenogenic and degrade in a timely fashion. For ease of FDA approval and

clinical translation, such a material would also be safe, readily available, easy to obtain, "off-the-shelf" and have a long shelf life. Thus, there is a great need for a non-cell-, non-neurotrophic-based biomaterial filler that is not only neuroconductive in its ability to provide an adequate environment for regeneration, but neuroinductive in that it actively stimulates nerve growth. Such a biomaterial would serve as an ideal scaffold for nerve regeneration, potentially allowing for repair of large defects with full functional recovery.

Keratin biomaterials are one group of novel, naturally derived biomaterials that have recently emerged as promising scaffold for tissue engineering, and specifically as a candidate nerve conduit filler matrix. Keratin biomaterials are naturally derived scaffolds made from human hair that meet many of the scientific, regulatory and commercialization requirements of the ideal biomaterial filler, while avoiding the challenges associated with cellular and neurotrophic based therapies. One of the main goals of this dissertation work was to investigate the use of a keratin-based hydrogel scaffold as a nerve conduit filler for regeneration of peripheral nerve defects.

REFERENCES

(1) Praemer, A Furner S, Rice DP. In: Musculoskeletal conditions in the United States. *American Academy of Orthopaedic Surgeons.* 1999;3-162.

(2) IJkema-Paassen J, Jansen K, Gramsbergen A, Meek MF. Transection of peripheral nerves, bridging strategies and effect evaluation. *Biomaterials.* 2004;25(9):1583-1592.

(3) Lundborg G. Nerve Injury and Repair. Elsevier Inc., 1988.

(4) Lundborg G. A 25-year perspective of peripheral nerve surgery: evolving neuroscientific concepts and clinical significance. *J Hand Surg [Am].* 2000;25(3):391-414.

(5) Kline DG. Surgical repair of brachial plexus injury. *J Neurosurg.* 2004;101(3):361-363.

(6) Kreiger N, Kelsey JL, Harris C, Pastides H. Injuries to the upper extremity: patterns of occurrence. *Clin Plast Surg.* 1981;8(1):13-19.

(7) Marga F, Hubbard B, McEwan E et al. Construction of a Bioprinted Fully Biological Nerve Graft. *Biophysical Journal.* 9 A.D.;96(3).

(8) Evans GRD. Challenges to nerve regeneration. *Seminars in Surgical Oncology.* 2000;19(3):312-318.

(9) Lee SK, Wolfe SW. Peripheral nerve injury and repair. *J Am Acad Orthop Surg.* 2000;8(4):243-252.

(10) Heath CA, Rutkowski GE. The development of bioartificial nerve grafts for peripheral-nerve regeneration. *Trends Biotechnol.* 1998;16(4):163-168.

(11) Verdu E, Ceballos D, Vilches JJ, Navarro X. Influence of aging on peripheral nerve function and regeneration. *J Peripher Nerv Syst.* 2000;5(4):191-208.

(12) Hall S. The response to injury in the peripheral nervous system. *Journal of Bone and Joint Surgery-British Volume.* 2005;87B(10):1309-1319.

(13) Seddon HJ. Peripheral nerve injuries in Great Britain during World War II; a review. *Arch Neurol Psychiatry.* 1950;63(1):171-173.

(14) Seddon HJ. Methods of investigating nerve injuries. *Spec Rep Ser Med Res Counc (G B).* 1954;282:1-15.

(15) Sunderland S. A classification of peripheral nerve injuries producing loss of function. *Brain.* 1951;74(4):491-516.

(16) Aldskogius H, Arvidsson J. Nerve cell degeneration and death in the trigeminal ganglion of the adult rat following peripheral nerve transection. *J Neurocytol.* 1978;7(2):229-250.

(17) Tornqvist E, Aldskogius H. Motoneuron survival is not affected by the proximo-distal level of axotomy but by the possibility of regenerating axons to gain access to the distal nerve stump. *J Neurosci Res.* 1994;39(2):159-165.

(18) Terzis JK, Sun DD, Thanos PK. Historical and basic science review: Past present, and future of nerve repair. *Journal of Reconstructive Microsurgery.* 1997;13(3):215-225.

(19) Chaudhry V, Glass JD, Griffin JW. Wallerian degeneration in peripheral nerve disease. *Neurol Clin.* 1992;10(3):613-627.

(20) Mirsky R, Jessen KR. The neurobiology of Schwann cells. *Brain Pathol.* 1999;9(2):293-311.

(21) Ide C. Peripheral nerve regeneration. *Neurosci Res.* 1996;25(2):101-121.

(22) Ishii DN, Glazner GW, Pu SF. Role of Insulin-Like Growth-Factors in Peripheral-Nerve Regeneration. *Pharmacology & Therapeutics.* 1994;62(1-2):125-144.

(23) Chilton JK. Molecular mechanisms of axon guidance. *Dev Biol.* 2006;292(1):13-24.

(24) Yang LJ, Schnaar RL. Axon regeneration inhibitors. *Neurol Res.* 2008;30(10):1047-1052.

(25) Morgenstern DA, Asher RA, Naidu M et al. Expression and glycanation of the NG2 proteoglycan in developing, adult, and damaged peripheral nerve. *Mol Cell Neurosci.* 2003;24(3):787-802.

(26) Tessier-Lavigne M. Axon guidance by diffusible repellants and attractants. *Curr Opin Genet Dev.* 1994;4(4):596-601.

(27) Makwana M, Raivich G. Molecular mechanisms in successful peripheral regeneration. *Febs Journal.* 2005;272(11):2628-2638.

(28) Jiang BG, Yin XF, Zhang DY et al. Maximum number of collaterals developed by one axon during peripheral nerve regeneration and the influence of that number on reinnervation effects. *Eur Neurol.* 2007;58(1):12-20.

(29) Schmidt CE, Leach JB. Neural tissue engineering: Strategies for repair and regeneration. *Annual Review of Biomedical Engineering.* 2003;5:293-347.

(30) McDonald D, Cheng C, Chen Y, Zochodne D. Early events of peripheral nerve regeneration. *Neuron Glia Biol.* 2006;2(2):139-147.

(31) Midha R, Zager EL. Nerve regeneration and nerve repair. *Neurol Res.* 2008;30(10):997-998.

(32) Sanders FK, Whitteridge D. Conduction velocity and myelin thickness in regenerating nerve fibres. *J Physiol.* 1946;105(2):152-174.

(33) Carlson BM, Borisov AB, Dedkov EI et al. Effects of long-term denervation on skeletal muscle in old rats. *J Gerontol A Biol Sci Med Sci.* 2002;57(10):B366-B374.

(34) Carlson BM. Denervation, reinnervation, and regeneration of skeletal muscle. *Otolaryngol Head Neck Surg.* 1981;89(2):192-196.

(35) Midha R, Munro CA, Chan S et al. Regeneration into protected and chronically denervated peripheral nerve stumps. *Neurosurgery.* 2005;57(6):1289-1299.

(36) Sulaiman OA, Midha R, Munro CA et al. Chronic Schwann cell denervation and the presence of a sensory nerve reduce motor axonal regeneration. *Exp Neurol.* 2002;176(2):342-354.

(37) Lee SK, Wolfe SW. Peripheral Nerve Injury and Repair. *J Am Acad Orthop Surg.* 2000;8(4):243-251.

(38) Lundborg G. Alternatives to autologous nerve grafts. *Handchir Mikrochir Plast Chir.* 2004;36(1):1-7.

(39) Millesi H. Microsurgery of peripheral nerves. *Ann Chir Gynaecol.* 1982;71(1):56-64.

(40) Matejcik V. Peripheral nerve reconstruction by autograft. *Injury.* 2002;33(7):627-631.

(41) Nichols CM, Brenner MJ, Fox IK et al. Effects of motor versus sensory nerve grafts on peripheral nerve regeneration. *Exp Neurol.* 2004;190(2):347-355.

(42) Birch R, Raji ARM. Repair of Median and Ulnar Nerves - Primary Suture Is Best. *Journal of Bone and Joint Surgery-British Volume.* 1991;73(1):154-157.

(43) Matejcik V. Peripheral nerve reconstruction by autograft. *Injury.* 2002;33(7):627-631.

(44) Johnson EO, Zoubos AB, Soucacos PN. Regeneration and repair of peripheral nerves. *Injury-International Journal of the Care of the Injured.* 2005;36:S24-S29.

(45) Ide C. Nerve regeneration and Schwann cell basal lamina: observations of the long-term regeneration. *Arch Histol Jpn.* 1983;46(2):243-257.

(46) Sondell M, Lundborg G, Kanje M. Regeneration of the rat sciatic nerve into allografts made acellular through chemical extraction. *Brain Res.* 1998;795(1-2):44-54.

(47) Dumont CE, Hentz VR. Enhancement of axon growth by detergent-extracted nerve grafts. *Transplantation.* 1997;63(9):1210-1215.

(48) Rovak JM, Bishop DK, Boxer LK et al. Peripheral nerve transplantation: the role of chemical acellularization in eliminating allograft antigenicity. *J Reconstr Microsurg.* 2005;21(3):207-213.

(49) Frerichs O, Fansa H, Schicht C et al. Reconstruction of peripheral nerves using acellular nerve grafts with implanted cultured Schwann cells. *Microsurgery.* 2002;22(7):311-315.

(50) Haase SC, Rovak JM, Dennis RG et al. Recovery of muscle contractile function following nerve gap repair with chemically acellularized peripheral nerve grafts. *J Reconstr Microsurg.* 2003;19(4):241-248.

(51) Kim BS, Yoo JJ, Atala A. Peripheral nerve regeneration using acellular nerve grafts. *J Biomed Mater Res A.* 2004;68(2):201-209.

(52) Krekoski CA, Neubauer D, Zuo J, Muir D. Axonal regeneration into acellular nerve grafts is enhanced by degradation of chondroitin sulfate proteoglycan. *J Neurosci.* 2001;21(16):6206-6213.

(53) Krekoski CA, Neubauer D, Graham JB, Muir D. Metalloproteinase-dependent predegeneration in vitro enhances axonal regeneration within acellular peripheral nerve grafts. *J Neurosci.* 2002;22(23):10408-10415.

(54) Rovak JM, Mungara AK, Aydin MA, Cederna PS. Effects of vascular endothelial growth factor on nerve regeneration in acellular nerve grafts. *J Reconstr Microsurg.* 2004;20(1):53-58.

(55) Haase SC, Rovak JM, Dennis RG et al. Recovery of muscle contractile function following nerve gap repair with chemically acellularized peripheral nerve grafts. *J Reconstr Microsurg.* 2003;19(4):241-248.

(56) Neubauer D, Graham JB, Muir D. Chondroitinase treatment increases the effective length of acellular nerve grafts. *Exp Neurol.* 2007;207(1):163-170.

(57) Brenner MJ, Hess JR, Myckatyn TM et al. Repair of motor nerve gaps with sensory nerve inhibits regeneration in rats. *Laryngoscope.* 2006;116(9):1685-1692.

(58) Krekoski CA, Neubauer D, Graham JB, Muir D. Metalloproteinase-dependent predegeneration in vitro enhances axonal regeneration within acellular peripheral nerve grafts. *J Neurosci.* 2002;22(23):10408-10415.

(59) Rummler LS, Gupta R. Peripheral nerve repair: a review. *Current Opinion in Orthopaedics.* 2004;15:215-219.

(60) Suematsu N. Tubulation for Peripheral-Nerve Gap - Its History and Possibility. *Microsurgery.* 1989;10(1):71-74.

(61) Foramitti C. Zur Technik der nervenaht. *Arch Kil Chir.* 1915;73:643-648.

(62) Kirk EG, Lewis D. Fascial tubulization in the repair of nerve defects. *JAMA.* 1915;65:486-492.

(63) Williams LR, Longo FM, Powell HC et al. Spatial-temporal progress of peripheral nerve regeneration within a silicone chamber: parameters for a bioassay. *J Comp Neurol.* 1983;218(4):460-470.

(64) Lundborg G, Dahlin LB, Danielsen N et al. Nerve regeneration across an extended gap: a neurobiological view of nerve repair and the possible involvement of neuronotrophic factors. *J Hand Surg [Am].* 1982;7(6):580-587.

(65) Strauch B. Use of nerve conduits in peripheral nerve repair. *Hand Clinics.* 2000;16(1):123-+.

(66) Williams LR. Exogenous Fibrin Matrix Precursors Stimulate the Temporal Progress of Nerve Regeneration Within A Silicone Chamber. *Neurochemical Research.* 1987;12(10):851-860.

(67) Tohill M, Terenghi G. Stem-cell plasticity and therapy for injuries of the peripheral nervous system. *Biotechnology and Applied Biochemistry.* 2004;40:17-24.

(68) Frostick SP, Yin Q, Kemp GJ. Schwann cells, neurotrophic factors, and peripheral nerve regeneration. *Microsurgery.* 1998;18(7):397-405.

(69) Belkas JS, Shoichett MS, Midha R. Peripheral nerve regeneration through guidance tubes. *Neurological Research.* 2004;26(2):151-160.

(70) Rosson GD, Williams EH, Dellon AL. Motor nerve regeneration across a conduit. *Microsurgery.* 2009;29(2):107-114.

(71) Farole A, Jamal BT. A bioabsorbable collagen nerve cuff (NeuraGen) for repair of lingual and inferior alveolar nerve injuries: a case series. *J Oral Maxillofac Surg.* 2008;66(10):2058-2062.

(72) Bertleff MJ, Meek MF, Nicolai JP. A prospective clinical evaluation of biodegradable neurolac nerve guides for sensory nerve repair in the hand. *J Hand Surg [Am].* 2005;30(3):513-518.

(73) Chen MB, Zhang F, Lineaweaver WC. Luminal fillers in nerve conduits for peripheral nerve repair. *Annals of Plastic Surgery.* 2006;57(4):462-471.

(74) Guenard V, Kleitman N, Morrissey TK et al. Syngeneic Schwann cells derived from adult nerves seeded in semipermeable guidance channels enhance peripheral nerve regeneration. *J Neurosci.* 1992;12(9):3310-3320.

(75) Raimondo S, Nicolino S, Tos P et al. Schwann cell behavior after nerve repair by means of tissue-engineered muscle-vein combined guides. *J Comp Neurol.* 2005;489(2):249-259.

(76) Zhang F, Blain B, Beck J et al. Autogenous venous graft with one-stage prepared Schwann cells as a conduit for repair of long segmental nerve defects. *J Reconstr Microsurg.* 2002;18(4):295-300.

(77) Phillips JB, Bunting SC, Hall SM, Brown RA. Neural tissue engineering: a self-organizing collagen guidance conduit. *Tissue Eng.* 2005;11(9-10):1611-1617.

(78) Zhang P, He X, Zhao F et al. Bridging small-gap peripheral nerve defects using biodegradable chitin conduits with cultured schwann and bone marrow stromal cells in rats. *J Reconstr Microsurg.* 2005;21(8):565-571.

(79) Keilhoff G, Goihl A, Langnase K et al. Transdifferentiation of mesenchymal stem cells into Schwann cell-like myelinating cells. *Eur J Cell Biol.* 2006;85(1):11-24.

(80) Rich KM, Alexander TD, Pryor JC, Hollowell JP. Nerve growth factor enhances regeneration through silicone chambers. *Exp Neurol.* 1989;105(2):162-170.

(81) Mohammad JA, Warnke PH, Pan YC, Shenaq S. Increased axonal regeneration through a biodegradable amnionic tube nerve conduit: effect of local delivery and incorporation of nerve growth factor/hyaluronic acid media. *Ann Plast Surg.* 2000;44(1):59-64.

(82) He C, Chen Z, Chen Z. Enhancement of motor nerve regeneration by nerve growth factor. *Microsurgery.* 1992;13(3):151-154.

(83) Pu LL, Syed SA, Reid M et al. Effects of nerve growth factor on nerve regeneration through a vein graft across a gap. *Plast Reconstr Surg.* 1999;104(5):1379-1385.

(84) Walter MA, Kurouglu R, Caulfield JB et al. Enhanced peripheral nerve regeneration by acidic fibroblast growth factor. *Lymphokine Cytokine Res.* 1993;12(3):135-141.

(85) Midha R, Munro CA, Dalton PD et al. Growth factor enhancement of peripheral nerve regeneration through a novel synthetic hydrogel tube. *J Neurosurg.* 2003;99(3):555-565.

(86) Hobson MI, Green CJ, Terenghi G. VEGF enhances intraneural angiogenesis and improves nerve regeneration after axotomy. *J Anat.* 2000;197 Pt 4:591-605.

(87) Zhang J, Lineaweaver WC, Oswald T et al. Ciliary neurotrophic factor for acceleration of peripheral nerve regeneration: an experimental study. *J Reconstr Microsurg.* 2004;20(4):323-327.

(88) Tuszynski MH, HS U, Alksne J et al. Growth factor gene therapy for Alzheimer disease. *Neurosurg Focus.* 2002;13(5):e5.

(89) Tuszynski MH. Growth-factor gene therapy for neurodegenerative disorders. *Lancet Neurol.* 2002;1(1):51-57.

(90) Kemp SW, Walsh SK, Midha R. Growth factor and stem cell enhanced conduits in peripheral nerve regeneration and repair. *Neurol Res.* 2008;30(10):1030-1038.

(91) Hudson TW, Evans GR, Schmidt CE. Engineering strategies for peripheral nerve repair. *Clin Plast Surg.* 1999;26(4):617-28, ix.

(92) Toba T, Nakamura T, Shimizu Y et al. Regeneration of canine peroneal nerve with the use of a polyglycolic acid-collagen tube filled with laminin-soaked collagen sponge: A comparative study of collagen sponge and collagen fibers as filling materials for nerve conduits. *Journal of Biomedical Materials Research.* 2001;58(6):622-630.

(93) Lee DY, Choi BY, Park JH et al. Nerve regeneration with the use of PLGA coated collagen tube filled with collagen gel. *Journal of Cranio-Maxillofacial Surgery.* 2006;34:50-56.

(94) Madison RD, Dasilva CF, Dikkes P. Entubulation Repair with Protein Additives Increases the Maximum Nerve Gap Distance Successfully Bridged with Tubular Prostheses. *Brain Research.* 1988;447(2):325-334.

(95) Madison R, Da Silva CF, Dikkes P et al. Increased rate of peripheral nerve regeneration using bioresorbable nerve guides and a laminin-containing gel. *Exp Neurol.* 1985;88(3):767-772.

(96) Madison R, Da Silva CF, Dikkes P et al. Peripheral nerve regeneration with entubulation repair: comparison of biodegradable nerve guides versus polyethylene tubes and the effects of a laminin-containing gel. *Exp Neurol.* 1987;95(3):378-390.

(97) Labrador RO, Buti M, Navarro X. Peripheral nerve repair: role of agarose matrix density on functional recovery. *Neuroreport.* 1995;6(15):2022-2026.

(98) Rosen JM, Padilla JA, Nguyen KD et al. Artificial nerve graft using collagen as an extracellular matrix for nerve repair compared with sutured autograft in a rat model. *Ann Plast Surg.* 1990;25(5):375-387.

(99) Satou T, Hashimoto S. Experimental studies on peripheral nerve repair: a possibility of application to cure nerve complication of Hansen's disease. *Nihon Hansenbyo Gakkai Zasshi.* 1999;68(2):77-82.

(100) Matsumoto K, Ohnishi K, Kiyotani T et al. Peripheral nerve regeneration across an 80-mm gap bridged by a polyglycolic acid (PGA)-collagen tube filled with laminin-coated collagen fibers: a histological and electrophysiological evaluation of regenerated nerves. *Brain Res.* 2000;868(2):315-328.

CHAPTER II

Introduction to Keratin Biomaterials

Paulina Sierpinski Hill

KERATINS

Keratins are a family of tough, fibrous proteins found in most vertebrate and some invertebrate structures. They are the most abundant structural protein and form the protective outer layer of all epidermal tissues. Keratins are the major constituent of hair, wool, horns, nails, hooves and other appendages that grow through the skin of mammals. In birds and reptiles, they form protective structures such as scales, shells, claws, feathers and beaks (1). Keratins are intermediate filament proteins that are present in nearly all mammalian cells. In addition to the cells of hair fibers, horns and nails, keratins have been shown to occur in both the nuclei and cytoplasm of almost all differentiated cells, including epithelial, neuronal and glial cells (2).

Keratins are present in living organisms in soft or hard form. Soft keratins, or cytokeratins, are found in the epidermis of the skin as flattened non-nucleated scales that slough continually. Hard keratins form non-mineralized structures that are the major constituent of hair, wool and nails. Both hard and soft keratins contain a complex mixture of proteins arranged in a filament matrix structure which is stabilized by the formation of disulfide bonds (3). The main difference between hard and soft keratins is that soft keratins are relatively easy to break down, whereas hard keratins are highly resistant to degradation by proteolytic enzymes and difficult to solubilize by standard chemical means (4). This observed difference arises primarily from their sulfur content. All keratins have a relatively high mole percentage of cysteine, the main amino acid responsible for inter- and intramolecular bonding, compared to other proteins. However, soft keratins have a much lower cysteine content than hard keratins, 2.3% vs. 7.6% respectively (5). Because hard keratins have three times the amount of cysteine,

they form more, permanent, thermally-stable crosslinks (6). As a result, hard keratins are insoluble and form tissues with higher tensile strength that have relatively little flexibility.

HUMAN HAIR KERATINS

Human hair is a highly stable and robust structural tissue that is relatively impervious to environmental insult. In addition to providing protection, human hair is responsible for thermoregulation, collection of sensory information, social communication and mimicry (7). Approximately 90% of human hair is keratin, which is mainly composed of heavily cross-linked hard keratins that are difficult to disaggregate and dissolve (8). Each hair fiber is an elongated keratinized structure, the diameter of which varies from person to person, but is usually around 50-90 μm (9). The hair fiber is made up of three layers - the cuticle, the cortex and the medulla. The outermost layer of the hair shaft is the cuticle and is composed of a tough tubular layer of flattened cells arranged in an overlapping structure. The cuticle is primarily composed of beta-keratins that function to protect the hair fiber from physical and chemical damage . The innermost layer is called the medulla and is composed of large, loosely connected keratinized cells. The middle layer of the hair fiber is called the cortex and is made from elongated, spindle shaped cells that contain many keratin intermediate filaments. The strength, color and texture of a hair fiber is provided by the cortex layer of the hair shaft.

THE HAIR FIBER

Human hair fiber shows a fibrous organization from the micrometer to the nanometer scale (Figure 1), (10). The keratin intermediate filaments within the cortex of the hair shaft self-assemble to form strong filamentous polymers. Monomeric α-helical domains first dimerize to form a coiled-coil structure. Dimerized coils associate to form tetramers that further self-assemble to form octamers, ultimately forming rope-like assemblies of fibrous polypeptides (11). These fibrous keratin structures are referred to as microfibrils and are bound together with an amorphous keratin matrix (12). The proteins that comprise the microfibrils and matrix material are referred to as alpha and gamma keratins, respectively. Alpha keratins have an average molecular weight of approximately 50-85 kDa and are low in sulfur content. Gamma keratins are globular, lower in molecular weight (approximately 15 kDa) but have a relatively high cysteine content (13). In addition to having a different structure, alpha and gamma keratins also vary in function. The alpha keratins self-assembled into long filamentous fibers that impart toughness to the hair fiber. Gamma keratins function primarily as a disulfide crosslinker, holding the cortical super structure of the hair fiber together (14). Recent changes by the keratin nomenclature committee now refer to microfibrils or alpha keratins as keratin intermediate filaments (KIFs) and gamma or matrix keratins as keratin associated proteins (KAPs), (15).

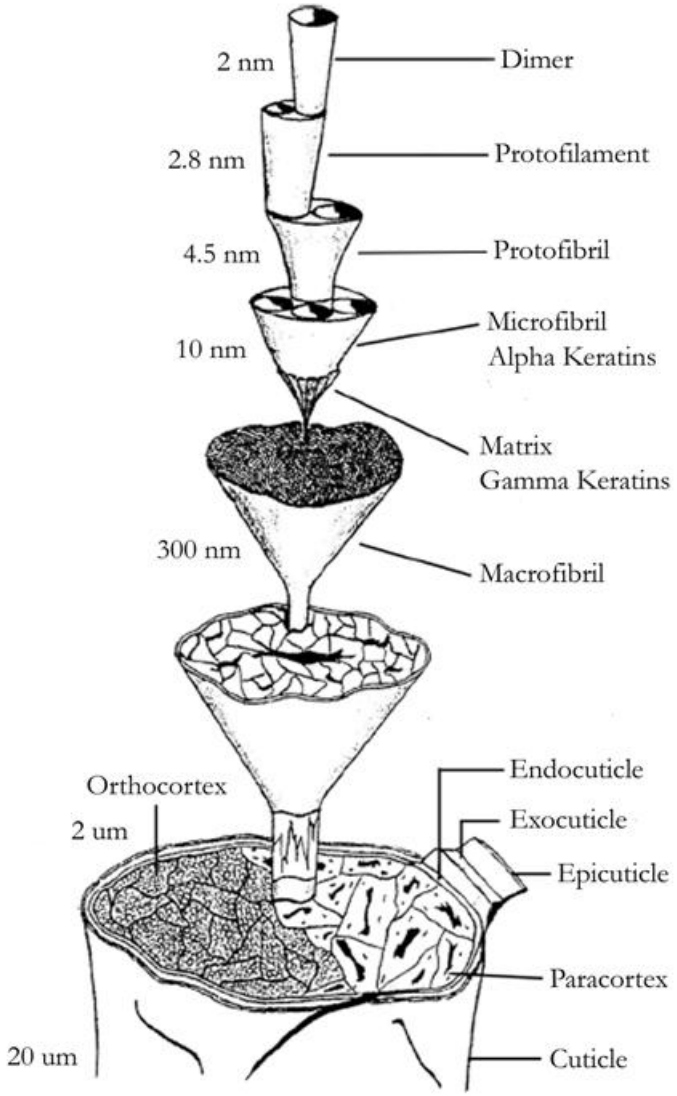

Figure 1. Cellular structure of a single hair fiber modified from Zahn, et al. (10). The cortex is surrounded by overlapping flattened cells of the cuticle. The cortex consists of alpha keratins that associate to form microfibrils. The microfibrils are held together by gamma keratins which serve as the glue that holds the complex structure of the cortex together.

Investigations aimed at characterizing human hair keratins have shown that the hair keratin family is more complex than previously assumed on the basis of protein studies. Over 75 distinct human hair protein structures have been proposed, and it is estimated that the total

number may exceed 100 (16). The alpha and gamma keratins can be further subdivided into Type I or acidic keratins and Type II or basic to neutral keratins, based on their overall charge at physiological pH (1). Recently, it has been suggested that there are ten Type I alpha and six Type II alpha keratins (17). Acidic and basic keratins are expressed in highly specific patterns within the regenerating hair follicle (18,19). Functional differences between acidic and basic keratins have not yet been identified, but based on their heavily regulated expression patterns in the hair follicle, epithelial and neuronal cells, it is theorized that specific functional differences likely exist (20).

THE HAIR FOLLICLE

The hair follicle is the point in the scalp from which the hair grows. It is a structure of actively migrating and differentiating stem cells, whose main function is to produce a hair follicle. The hair follicle is a cyclic regeneration system that exemplifies an active miniature organ (21). Hair morphogenesis is characterized by the recruitment of local stem cells, rapid proliferation, terminal differentiation, and cellular and matrix self-assembly (22). It is a highly controlled process that can be divided into four relatively distinct, successive periods: active growth phase (anagen), a short transition phase with regression (catagen), a resting phase (telogen) and a shedding stage (exogen) (23). These cyclical phases are turned on and off by over 30 growth factors, cytokines, and other signaling molecules (24,25). Many of the molecules that regulate hair morphogenesis have been characterized, and shown to be expressed in the hair

follicle (26-28), and the hair fiber itself (29). Expression of these factors, as well as other matrix and adhesion molecules, results in a hair fiber that is rich in regulatory molecules (30,31). Many of these same factors are essential in the numerous regenerative processes that maintain normal function in a variety of organs and tissues. Moreover, these same regulatory compounds have been found to be present in the regenerating amphibian limb (32), and play important roles in the regeneration of almost every tissue after injury (33,34), including nerve tissue (35,36).

EARLY USES OF KERATINS

The earliest use of keratins for therapeutic applications dates back to the 16th century in Chinese medicine. In 1596, a Chinese herbalist named Li Shi-Zhen published a collection of books that prescribed the use of a substance called Xue Yu Tan for accelerating wound healing and blood clotting. Xue Yu Tan, also called Crinis Carbonisatus, was the name given to ground ash from pyrolyzed human hair. The details of how Shi-Zhen discovered that human hair was biologically active are unknown. However, its uses in human medicine are clearly documented in a collection of over 800 books referred to as the Ben Cao Gang Mu (37).

The word "keratin" first appears in the literature in the early 1800's, where it is used to describe the material that makes up hard tissues such as animal horns and hooves. At that time, keratins were fascinating to scientists because they did not behave like other proteins. One of their unique characteristics was their resistance to solubility using the normal methods for dissolving proteins. In 1905, John Hoffmeier was issued the first keratin based US patent on

the use of lime for extracting keratins from animal horns. He used the extracts to make keratin-based gels using formaldehyde crosslinking to strengthen the gels. In the 30 years that followed, many methods were developed to extract keratins using oxidative and reductive chemistries (38-41). These processes were initially applied to the extraction of keratins from horns and hooves, but were also eventually used to extract keratins from wool and human hair. The development of novel extraction techniques led to increased interest in keratins and their biological properties, and the potential of using keratins for medical applications became apparent. Some of the first keratin-based inventions consisted of powders for cosmetics, composites, and coatings for drugs (42-44).

KERATIN BIOMATERIALS

By the late 1920's many techniques had been developed for breaking down the structure of hair, horns and hooves (45). Once scientists knew how to extract keratins from hair fibers, purify and characterize them, the number of derivative materials that could be produced with keratins grew exponentially. In the 1970's, methods to form extracted keratins into powders, films, gels coatings, fibers, and foams were being developed. All of these methods made use of the oxidative and reductive chemistries developed decades earlier.

The prospect of using keratins as a biomaterial in medical applications was an obvious one. During the late 1980's, collagen became a commonly used biomolecule in many medical applications. Other naturally derived molecules soon followed such as alginates from seaweed,

chitosan from shrimp shells, and hyaluronic acid from animal tissues. The potential uses of keratins in similar applications began to be explored by a number of scientists. In 1982, a Japanese scientist published the first study describing the use and biocompatibility of a keratin coating on vascular grafts as a way to eliminate blood clotting (46,47). Soon thereafter in 1985, two researchers from the UK published a review article speculating the prospect of using keratin as the building block for new biomaterials development (48,49). In 1992, the development and testing of a host of keratin-based biomaterials was the subject of a doctoral thesis for a French graduate student (49). Soon thereafter, Japanese scientists published a commentary in 1993 on the prominent position keratins could take at the forefront of biomaterials development.

KERATIN BIOMATERIALS FOR NEURAL TISSUE ENGINEERING

Due to the fundamental research of scientists all over the world, and more importantly the publication of their experimental results, the field of keratin research has continued to grow with wound healing, drug delivery, tissue engineering, cosmetics and medical devices as popular subjects for keratin-based research in the past decade. One application of keratin biomaterials that our lab has been extensively exploring is their use as a potentially neuroinductive conduit filler matrix for regeneration of peripheral nerves. The use of keratin biomaterials for neural tissue engineering applications is promising for multiple reasons.

First, keratin biomaterials have an intrinsic ability to self-assemble into porous, fibrous scaffolds that may provide a good provisional matrix for regenerating nerves. The ability of extracted keratin solutions to spontaneously self-assemble at the micron scale was first published by Thomas et al. in 1986 and van de Locht in 1987 (50,51). Self-assembly results in a highly regular structure with reproducible architectures, dimensionality and porosity. This phenomenon is not surprising given the highly organized superstructure of the hair fiber. When processed correctly, this ability to self-assemble can be preserved and used to create regular architectures on a size scale conducive to cellular infiltration. This is a useful characteristic for tissue engineering scaffolds in general, and nerve conduit filler matrices in particular, since Schwann cell infiltration into the defect site is critical to the regeneration process (52).

The second reason that keratins are promising as a nerve conduit filler matrix is due to their ability to mimic the ECM of native nerve. Cellular recognition is an important characteristic of biomaterial fillers that seek to mimic the ECM. Such recognition is facilitated by the binding of cell surface integrins to specific amino acid motifs presented by constituent ECM proteins. Predominant proteins include collagen, fibronectin and laminin, all of which have been found to promote Schwann cell adhesion and axonal guidance in regenerating nerves (53,54). These proteins contain several regions that support attachment by a wide variety of cell types, including neuronal, glial and endothelial cells. It has been shown that in addition to the widely known arginine-glycine-aspartic acid (RGD) motif, the "X"-aspartic-"Y" motif on fibronectin is also recognized by the integrin $\alpha 4\beta 1$ where X equals glycine, leucine, or glutamic acid and Y equals serine or valine. Keratin biomaterials derived from human hair contain these

same binding motifs. The leucine-aspartic acid-valine (LDV) and glutamic acid-aspartic acid-serine binding residues are most prevalent in acidic alpha keratins. Taken together with its unique physical properties, this suggests that human hair keratins may support regeneration of peripheral nerves by providing a provisional matrix that mimic the nerve ECM and supports Schwann cell infiltration, attachment and growth.

In addition to providing a favorable three dimensional matrix and sites of cellular attachment, keratin biomaterials may be superior to previously used nerve conduit fillers due to their biological activity. Previously, it was assumed that keratins were just another group of intermediate filament proteins that provide structural support to the cell, and have little, if any, regulatory functions. However, recent evidence suggests that this is not the case, and supports the notion that intermediate filament proteins, including keratins themselves, mediate cell behavior. Soft keratins have been shown to participate in the control of epithelial cell and tissue growth by regulating protein synthesis and proliferation (55). They have been shown to contribute to the tissue response to injury and aid in recovery from environmental insult. Furthermore, keratins, along with other IF proteins, have been shown to be upregulated in the differentiation of embryoid bodies to a neuronal fate (56). A recent study documented the use of a chimeric keratin protein for formation of a keratin based hydrogel to serve as a cell delivery matrix for Parkinson's disease. This group reported that neural stem/progenitor cells specifically adhered to the keratin based composite and proliferated at a high survival rate (57).

Keratins are further advantageous as scaffolds for nerve regeneration because they are not susceptible to degradation by proteolysis. This allows a keratin matrix to degrade by

hydrolysis, which is somewhat independent of metabolic activity and relatively consistent across species. Since damage to the peripheral nervous system triggers a series of events that result in a protease-rich environment at the site of injury, this is an important feature of keratin biomaterials that many other naturally derived materials like collagens, fibronectins and laminins do not possess (58). As such, a keratin matrix would provide a predictable degradation rate that can be further optimized and controlled. This characteristic may be particularly important over longer defects, or in cases where nerve regeneration is impaired, as in the elderly or in patients with underlying diseases that affect nerve growth. For such individuals, one may envision engineering a slower degrading keratin hydrogel filler that is capable of maximizing the diminished regenerative capacity seen in these patients.

Keratin extracts may also be biologically active due to the presence of residual regulatory molecules within the hair fiber. It is theorized that when the hair follicle keratinizes, the resident growth factors and cytokines become entrained in this crosslinked matrix. Since the hair shaft is a very tough structure which is resistant to environmental damage, it is presumed that these growth factors are permanently 'locked in' to the hair fiber and stabilized by this environment. This suggests that growth factors involved in the normal hair morphogenesis process can become incorporated into the hair fiber upon keratinization, and may be extracted from the hair fiber along with the keratins. As such, keratin biomaterials may have the capacity to act both as neuroconductive and neuroinductive biomaterials, and may facilitate nerve repair beyond current clinical limits without the use of exogenous cells.

The main objective of this dissertation work was to develop novel, scaffold-based bridging strategies for nerve regeneration. Toward this goal, we first investigated a more traditional, non-keratin based tissue engineering approach that employed decellularized nerve tissue. Acellular nerve grafts have been extensively studied, and have been found to repair small defects in rodent models. However, the use of acellular grafts to bridge large defects has been unsuccessful. The first aim of this thesis work was to investigate whether *in vitro* structural modification of acellular grafts could produce a more favorable architecture for regeneration, and whether such a scaffold could be used to regenerate large segmental nerve defects *in vivo*.

The second scaffold-based bridging strategy was developed using human hair derived keratins as a candidate filler material for nerve conduits. Due to the unique physical and biochemical properties of keratins, we hypothesized that keratin biomaterials could serve as a neuroinductive scaffold for bridging peripheral nerve defects. We hypothesized that keratins could do this by acting directly on regenerative cells and actively stimulating nerve growth. Prior to testing keratins on nervous tissue, we first needed to assess the biocompatibility of human hair derived keratin preparations. Because keratins are naturally derived, they are believed to be non-antigenic and highly biocompatible regardless of the source. However, the basic biocompatibility of keratin biomaterials has not been established. To test this, we performed basic *in vitro* and *in vivo* biocompatibility experiments to assess the cellular and host response to keratin biomaterials.

To evaluate the neuroinductive properties of keratin biomaterials, we performed a series of studies using cellular and animal models of nerve regeneration. *In vitro* assessment consisted of testing the ability of keratins to activate Schwann cells. *In vivo* experiments were designed to test the effectiveness of a keratin hydrogel in repairing small gaps in a mouse model. The ability of a keratin hydrogel to act at the early stages of regeneration was investigated, and a follow up study was performed to characterize long-term motor function recovery. After establishing efficacy in a rodent model, we developed a more clinically relevant animal model to assess keratin's performance over longer gaps. Specifically, we developed a critical size defect model of nerve injury and repair using clinically approved bioabsorbable nerve guides. We used this model to assess the ability of a keratin hydrogel filler to promote regeneration across a critical size defect in a rabbit.

Lastly, we sought to elucidate the mechanisms by which keratin biomaterials act on regenerative cells to promote nerve growth. To accomplish this, we developed fractionation schemes to separate out the different families of keratins contained within whole human hair extracts and analyzed these purified keratins using a combination of cellular and molecular assays.

In summary, this dissertation demonstrates the development of two novel guidance strategies for bridging peripheral nerve defects, the first of which is based on a traditional tissue engineering approach, and the second of which introduces keratin as a promising, neuroinductive biomaterial for use in neural regeneration.

References

(1) Plowman JE. The proteomics of keratin proteins. *J Chromatogr B Analyt Technol Biomed Life Sci.* 2007;849(1-2):181-189.

(2) Parry DAD, Steinhert P. Intermediate Filament Structure. New York: Springer-Verlag, 1995.

(3) Bradbury JH. The Structure and Chemistry of Keratin Fibers. In: Anfinsen CB, Edsall JT, Richards FM, editors. New York: Academic Press, 1973: 111-211.

(4) Breinl F, Baudisch O. The oxidative breaking up of keratin through treatment with hydrogen peroxide. *Z Physiol Chem.* 2009;52:158-169.

(5) Alibardi L. Structural and immunocytochemical characterization of keratinization in vertebrate epidermis and epidermal derivatives. *Int Rev Cytol.* 2006;253:177-259.

(6) Yu J, Yu DW, Checkla DM et al. Human hair keratins. *J Invest Dermatol.* 1993;101(1 Suppl):56S-59S.

(7) Stenn KS, Paus R. Controls of hair follicle cycling. *Physiological Reviews.* 2001;81(1):449-494.

(8) Crewther WG, Fraser RDB, Lennox FG, Lindley H. The Chemistry of Keratins. Anfinsen CB, Anson ML, Edsall JT, Richards FM, editors. New York: Academic Press, 1965: 191-343.

(9) Baran R, Dawber RP, Haneke E. Hair and nail relationship. *Skinmed.* 2005;4(1):18-23.

(10) Zahn H. Progress report on hair keratin research. *Int J Cosmet Sci.* 2002;24(3):163-169.

(11) Huggins ML. The structure of alpha-keratin. *Macromolecules.* 1977;10(5):893-898.

(12) Jones LN, Simon M, Watts NR et al. Intermediate filament structure: hard alpha-keratin. *Biophys Chem.* 1997;68(1-3):83-93.

(13) Marshall RC. Characterization of the proteins of human hair and nail by electrophoresis. *J Invest Dermatol.* 1983;80(6):519-524.

(14) Ward WH, Lundgren HP. The Formation, Composition, and Properties of the Keratins. In: Anson ML, Bailey KB, Edsall JT, editors. New York: Academic Press Inc., 1954: 244-97.

(15) Porter RM. The new keratin nomenclature. *J Invest Dermatol.* 2006;126(11):2366-2368.

(16) Marshall RC, Orwin DF, Gillespie JM. Structure and biochemistry of mammalian hard keratin. *Electron Microsc Rev.* 1991;4(1):47-83.

(17) Schweizer J, Bowden PE, Coulombe PA et al. New consensus nomenclature for mammalian keratins. *J Cell Biol.* 2006;174(2):169-174.

(18) Langbein L, Rogers MA, Winter H et al. The catalog of human hair keratins. II. Expression of the six type II members in the hair follicle and the combined catalog of human type I and II keratins. *J Biol Chem.* 2001;276(37):35123-35132.

(19) Langbein L, Rogers MA, Winter H et al. The catalog of human hair keratins. I. Expression of the nine type I members in the hair follicle. *J Biol Chem.* 1999;274(28):19874-19884.

(20) Izawa I, Inagaki M. Regulatory mechanisms and functions of intermediate filaments: a study using site- and phosphorylation state-specific antibodies. *Cancer Sci.* 2006;97(3):167-174.

(21) Hoffman RM. The pluripotency of hair follicle stem cells. *Cell Cycle.* 2006;5(3):232-233.

(22) Alonso L, Fuchs E. The hair cycle. *J Cell Sci.* 2006;119(Pt 3):391-393.

(23) Stenn KS, Paus R. What controls hair follicle cycling? *Exp Dermatol.* 1999;8(4):229-233.

(24) Stenn KS, Prouty SM, Seiberg M. Molecules of the cycling hair follicle--a tabulated review. *J Dermatol Sci.* 1994;7 Suppl:S109-S124.

(25) Stenn KS, Combates NJ, Eilertsen KJ et al. Hair follicle growth controls. *Dermatol Clin.* 1996;14(4):543-558.

(26) Blessings M, Nanney LB, King LE et al. Transgenic mice as a model to study the role of TGF-beta related molecules in hair follicles. *Genes and Development.* 1993;7:204-215.

(27) Jones CM, Lyons KM, Hogan BLM. Involvement of Bone-Morphogenetic Protein-4 (Bmp-4) and Vgr-1 in Morphogenesis and Neurogenesis in the Mouse. *Development.* 1991;111(2):531-541.

(28) Lyons KM, Pelton RW, Hogan BLM. Organogenesis and Pattern-Formation in the Mouse - Rna Distribution Patterns Suggest A Role for Bone Morphogenetic Protein-2A (Bmp-2A). *Development.* 1990;109(4):833-840.

(29) Sato T, Sato G, Shoji Y et al. Extraction and detection of mRNA from horsehair. *J Vet Med Sci.* 2006;68(5):503-506.

(30) Rogers GE. Hair follicle differentiation and regulation. *Int J Dev Biol.* 2004;48(2-3):163-170.

(31) Hardy MH. The secret life of the hair follicle. *Trends Genet.* 1992;8(2):55-61.

(32) Oro AE, Scott MP. Splitting hairs: dissecting roles of signaling systems in epidermal development. *Cell.* 1998;95(5):575-578.

(33) Ioannidou E. Therapeutic modulation of growth factors and cytokines in regenerative medicine. *Curr Pharm Des.* 2006;12(19):2397-2408.

(34) Chen MB, Zhang F, Lineaweaver WC. Luminal fillers in nerve conduits for peripheral nerve repair. *Annals of Plastic Surgery.* 2006;57(4):462-471.

(35) Frostick SP, Yin Q, Kemp GJ. Schwann cells, neurotrophic factors, and peripheral nerve regeneration. *Microsurgery.* 1998;18(7):397-405.

(36) Verge VM, Gratto KA, Karchewski LA, Richardson PM. Neurotrophins and nerve injury in the adult. *Philos Trans R Soc Lond B Biol Sci.* 1996;351(1338):423-430.

(37) Shi-Zhen L. Ben Cao Gang Mu. 2009.

(38) Neuberg C, inventor. Process of producing digestable substances from keratin. patent 926999. 2009 2009.

(39) Lissizin T. Behavior of keratin sulfur and cystin sulfur in the oxidation of these proteins by potassium permanganate I. *Biochem Bull.* 1915;(4):18-23.

(40) Lissizin T. The oxidation products of keratin by oxidation with permanganate II. *Z Physiol Chem.* 1928;(173):309-311.

(41) Goddard DR, Michaelis L. A study on keratin. *J Biol Chem.* 1934;106:605-614.

(42) Beyer C, inventor. The keratin or horny substance of the hair. patent Ger Pat no 22643. 1907 Oct 1907.

(43) Goldsmith BB, inventor. Thermoplastic composition containing keratin. patent 922692. 1909 May 1909.

(44) Dale HN. Keratin and other coatings for pills. *Pharm J.* 1932;129:494-495.

(45) Crewther WG, Fraser RDB, Lennox FG, Lindley H. The Chemistry of Keratins. In: Anfinsen CB, Anson ML, Edsall JT, Richards FM, editors. New York: Academic Press, 1965: 191-343.

(46) Noishiki Y, Ito H, Miyamoto T, Inagaki H. Application of denatured wool keratin derivatives to an antithrombogenic biomaterial: Vascularized graft coated with a heparinized derivative. *Kobunshi Ronbunshu.* 1982;39(4):221-227.

(47) Ito H, Miyamoto T, Inagaki H, Noishiki Y. Biocompatibility of denatured keratins from wool. *Kobunshi Ronbunshu.* 1982;39(4):249-256.

(48) Jarman T, Light J. Prospects for novel biomaterials development. *World Biotechnology Report.* 1985;505-512.

(49) Valherie I, Gagneiu C. Chemical modifications of keratins: Preparation of keratin biomaterials and study of their physical, physiochemical and biological properties. Inst Natl Sci Appl Lyon, 1992.

(50) van de Locht M. Reconstitution of microfibrils from wool and filaments from epidermis proteins. *Melliand Textilberichte.* 1987;(10):780-786.

(51) Thomas H, Conrads A, Phan KH et al. In vitro reconstitution of wool intermediate filaments. *Int J Biol Macromol.* 1986;(8):165-170.

(52) Hall S. The response to injury in the peripheral nervous system. *Journal of Bone and Joint Surgery-British Volume.* 2005;87B(10):1309-1319.

(53) LuckenbillEdds L. Laminin and the mechanism of neuronal outgrowth. *Brain Research Reviews.* 1997;23(1-2):1-27.

(54) Ide C. Nerve regeneration and Schwann cell basal lamina: observations of the long-term regeneration. *Arch Histol Jpn.* 1983;46(2):243-257.

(55) Magin TM, Vijayaraj P, Leube RE. Structural and regulatory functions of keratins. *Exp Cell Res.* 2007;313(10):2021-2032.

(56) Oh JE, Karlmark RK, Shin JH et al. Cytoskeleton changes following differentiation of N1E-115 neuroblastoma cell line. *Amino Acids.* 2006;31(3):289-298.

(57) Nakaji-Hirabayashi T, Kato K, Iwata H. Self-assembling chimeric protein for the construction of biodegradable hydrogels capable of interaction with integrins expressed on neural stem/progenitor cells. *Biomacromolecules.* 2008;9(5):1411-1416.

(58) Siebert H, Dippel N, Mader M et al. Matrix metalloproteinase expression and inhibition after sciatic nerve axotomy. *J Neuropathol Exp Neurol.* 2001;60(1):85-93.

CHAPTER III

Regeneration of Peripheral Nerves Using Structurally Modified Acellular Grafts

Paulina Sierpinski[1], Peter J. Apel[2], Tamer AbouShwareb[1], James Yoo[1], Anthony Atala[1], and Mark Van Dyke[1]

[1] Wake Forest Institute for Regenerative Medicine

[2] Department of Orthopaedic Surgery

Wake Forest University School of Medicine, Winston Salem, NC, 27157

This manuscript was submitted to Tissue Engineering. Stylistic variations are due to the requirements of the journal. Paulina Sierpinski prepared the manuscript. Dr. Mark Van Dyke acted in an advisory and editorial capacity.

ABSTRACT

Acellular nerve allografts support regeneration across small peripheral nerve defects less than 2 cm in length. However, over larger gaps, decellularized scaffolds typically do not promote regeneration past the mid-portion of the graft. One reason for this may be due to the dense architecture of nerve allografts. This study tested the hypothesis that structurally modified grafts with increased porosity could support axon regeneration across large segmental defects. Excised nerves from cadaveric rabbit donors were decellularized and graft porosity was modified by treatment with peracetic acid, a strong chemical oxidant, under optimized conditions. Acellular control and structurally modified grafts were used to bridge a 5 cm tibial nerve defect in a rabbit model. Scanning Electron Microscopy (SEM) analysis showed an increase in scaffold porosity and pore size following oxidation. Histological assessment of implanted grafts showed increased axon regeneration in structurally modified scaffolds. Oxidized grafts had the highest density of neurofilaments and Schwann cells that extended into the distal end. Cross-sectional histomorphometry revealed larger myelinated axons in grafts pre-treated with an oxidant than in the acellular group. The size and density of regenerated axons within oxidized grafts was statistically equivalent to that of autograft. These findings indicate that nerve allograft architecture is an important factor in regeneration across large defects and that modification of graft porosity may increase the effective length of acellular grafts.

INTRODUCTION

Traumatic injuries to the extremities often result in large peripheral nerve defects that require surgical intervention. While small defects can be bridged using a nerve guidance conduit, sensory nerve autografts are the only available treatment for segmental gaps exceeding 2-3 cm (1). Autografts are advantageous in that they provide a scaffold for regenerating nerves, do not elicit an immune response, and possess native Schwann cells that clear debris and promote regeneration. But implantation of an autograft is a technically demanding procedure associated with long surgical times, donor site morbidity and limited graft availability (2). In addition, studies have shown that regeneration of motor nerves through sensory nerve autografts is limited, resulting in poor functional recovery (3,4). These outcomes have been largely attributed to inherent structural differences between sensory and motor nerve tissues (5). Motor nerve allografts from cadaveric donors are capable of overcoming this problem, but require immunosuppression due to the presence of the donor cells.

Acellular nerve grafts have been identified as a promising alternative to the sensory nerve autograft. Acellular grafts can be derived from motor nerves and possess many of the necessary components specifically required for motor nerve regeneration. Because the cellular and myelin components are removed prior to implantation, acellular grafts have reduced immunogenicity while still providing a basal lamina for the regenerating nerve (6). Numerous studies have shown that acellular grafts are often able to promote regeneration over 1-2 cm defects in a rat sciatic model (7-12). However, few studies have achieved similar results over longer defects in large animal models. Evaluation of published studies utilizing a rat sciatic

nerve injury model shows that even over 1-2 cm, axons do not always reach the distal segment of the graft in all cases. Moreover, the use of decellularized grafts to regenerate nerve across gaps larger than 2 cm has been largely unsuccessful. (1,8). One reason for this is the absence of growth promoting cells within the scaffold and an inability of indigenous cells to migrate over large distances.

Autologous Schwann cells seeded onto acellular grafts have been shown to improve regeneration by as much as 60-70% in 1-2 cm gaps (13,14). But the use of autologous Schwann cells in nerve regeneration therapy is impractical. Primary Schwann cells are difficult to isolate and expand e*x vivo*, so cell culture rarely yields enough cells for implantation *in vivo*. Furthermore, harvest of autologous Schwann cells has many of the same disadvantages as the use of nerve autograft. The use of other autologous and non-autologous cell sources has been explored, but finding a plentiful, readily available stem cell source is also a challenge. An unseeded biological scaffold that is capable of stimulating host cell ingrowth could potentially overcome many of the challenges associated with cell-based approaches.

The inability of acellular grafts to promote regeneration across larger defects may be due to the dense architecture and requirement for extensive matrix remodeling (15,16). Scaffold porosity is particularly important in the case of nerve regeneration to allow for migration of Schwann cells and outgrowth of axons toward distal muscle targets. If these processes are delayed, the nerve regeneration cascade is severely impaired. Previous studies have shown that predegradation of extracellular matrix components by matrix metalloproteases (MMPs) prior

to graft implantation significantly improves axonal outgrowth (11). This suggests that partial degradation of an acellular graft prior to implantation may result in a more porous microarchitecture that is conducive to cell infiltration and perhaps regeneration over short and long distances. We hypothesize that modifications to acellular grafts that yield a more porous architecture can increase the effective length of regeneration across acellular grafts. The objectives of this study were to determine (1) if established decellularization protocols could be used for decellularization of large diameter nerves, (2) if chemical processing techniques could be used to increase the porosity of a scaffold and (3) if such a scaffold could be used without exogenous cell seeding to regenerate long segmental nerve defects *in vivo*.

METHODS

Nerve Graft Preparation. Sciatic nerves were harvested from New Zealand White rabbit cadaveric donors. The two branches of the sciatic nerve were split, the tibial nerve was isolated and the surrounding fat and connective tissue dissected away under a microscope. The isolated nerve segments were placed in deionized (DI) water on a shaker (Barnstead/Lab-line Max Q 4000, Artisian Scientific, Champaign, IL) at 180 rpm and 4°C. The water was replaced 3-4 times daily for 48 hours to promote cell lysis. For extraction of the cellular material, nerve segments were exposed to 0.5% (v/v) Triton X-100 (Sigma, St. Louis, MO) and 0.05% ammonium hydroxide (Sigma) for 72 hours (180 rpm, 4°C). Nerves were washed thoroughly

with DI water for 4 days at 37°C, with 3-4 water changes per day, and stored in DI water at 4°C until use.

Assessment of Decellularization. Decellularized nerve segments were fixed in 10% Neutral Buffered Formalin (NBF) for 24 hours and transferred to 30% sucrose for 24 hours. Decellularized nerve segments were frozen embedded in O.C.T. media (Sakura Finetek, Torrance, CA) for cryosectioning. Native rabbit nerves rinsed in Phosphate Buffered Saline (PBS) were used as a control. Sections 10 μm in thickness were cut longitudinally and stained with hematoxylin & eosin (H&E) and DAPI to analyze cellular content. Residual DNA in acellular grafts was quantified using QIAGEN DNeasy tissue kit according to the manufacturer's instructions (QIAGEN, Germantown, MD). Decellularized nerves were cut in half and a 25 mg piece of the middle and end portion were analyzed (n=6). Native nerve was used as a positive control.

Chemical Processing and Structural Analysis. Acellular grafts were treated with peracetic acid (PA), (Sigma, St. Louis, MO) at 1%, 5% and 10% (w/v) concentrations in DI water (n=6 per group) for 24 hours (180 rpm, 37°C). Oxidized nerve segments were rinsed in DI water for 4 days with 3-4 water changes per day, then lyophilized (Freeze-Dry Systems, Labconco, Kansas City, MO). The microarchitecture of the treated nerves was analyzed by Scanning Electron Microscopy (SEM) using a Hitachi S-2600N variable pressure instrument. Grafts were trimmed down to 5 cm in length and sterilized by γ-irradiation (850 krad) using a ^{60}Co source.

Animal Model. Sixteen New Zealand White female rabbits (3.5-4 kg, Robinson's Rabbitry) were randomized into 4 treatment groups: 1) Acellular graft, 2) Acellular graft treated with 1% PA, 3) Acellular graft treated with 5% PA or 4) Sural Nerve Autograft. All procedures were conducted under a protocol approved by the Wake Forest University Animal Care and Use Committee (ACUC) and performed in accordance with the National Institutes of Health (NIH) guidelines.

Surgical Procedure. Animals were placed under general anesthesia and the left limb was shaved and cleansed with betadine. A longitudinal incision was made along the posterior aspect of the left hind limb and the sciatic nerve exposed. The tibial nerve was separated from the peroneal and sural nerves by microsurgical dissection and transected 1 cm proximal to its insertion into the gastrocnemius. A 4 cm segment of nerve was excised and the nerve was allowed to retract to a gap length of 5 cm. A 5 cm segment of decellularized allograft tissue was interposed across the defect and anastomosed to the severed nerve ends. The proximal and distal nerve ends were secured to the graft with four simple interrupted sutures using 9-0 Vicryl. The muscle and skin layers were closed with 4-0 Vicryl. A Tefla pad was placed over the surgical site and secured with skin staples. The left foot was bandaged immediately following surgery and E-collars were placed around the necks of each rabbit to prevent self-mutilation. Bandages were changed every 7-10 days. Bandages and e-collars were permanently removed on a case-by-case basis, depending on whether self-mutilation of the injured foot was observed.

Electrophysiology. After 6 months of regeneration, each animal underwent elecrophysiological testing of the tibial nerve. Under general anesthesia, the nerve was exposed and the compound motor action potential (CMAP) of the tibial nerve-gastrocnemius complex was measured using a Sierra Wave system (Caldwell Laboratories, Kennewick, WA). The peroneal nerve was transected prior to testing to ensure that a detectable signal was due to regeneration of the injured nerve. A bipolar stimulating electrode was placed on the tibial nerve proximal to the defect at the distance of the obturator externus tendon. A reference needle electrode was placed on the calcaneous and a surface recording electrode on the gastrocnemius muscle belly. The nerve was stimulated with a constant current of 1.0 mAmp for 0.1 ms. The contralateral limb was tested first and served as an internal reference for each animal.

Histology & Histomorphometry. Following testing, nerve tissues were harvested for histological examination. A 6-0 Vicryl suture was inserted into the proximal end of the nerve at time of harvest to provide anatomical orientation during analysis. Nerves were fixed in 10% NBF for 48 hours, then placed in 30% sucrose for a minimum of 24 hours. The tissue sample was cut in half and the distal portion was frozen embedded for sectioning. Nerves were sectioned longitudinally (8 um thick sections) and stained with H&E to analyze the regenerated nerve structure**.** Nerves were stained for Neurofilament-200 (NF-200, polyclonal, Abcam, Cambridge, MA) and S100-β (polyclonal, DAKO, Denmark) to examine axonal regeneration and Schwann cell growth, respectively. Masson's trichrome was used to assess scar tissue formation in the implanted grafts. The distal most portions of the nerves were osmium

tetroxide treated, dehydrated in graded ethanol solutions and embedded in Epon resin. Nerves were cut in cross-section (1 um) using an LKB III Ultramicrotome (LKB-Produkter A.B., Broma, Sweden), stained with 1% toluidine blue and mounted on slides for analysis. Photomicrographs were captured on a microscope system fitted with a digital camera (Carl Zeiss, Jena, Germany). Axon digital image analysis was performed using Image J (NIH, Bethesda, MD) and SigmaScan Pro 5.0 (SYSTAT, Chicago, IL).

Statistical Analysis. Histomorphometric and DNA content data was analyzed and comparisons between treatment groups made using SigmaStat 3.1 (SYSTAT software, Chicago, IL). A single-factor analysis of variance (ANOVA) employing a Tukey's multiple comparison post-hoc test was used to determine statistical significance ($p<0.05$). All data are expressed as mean +/- standard error of the mean (SEM).

RESULTS

Decellularization of rabbit tibial nerves

Acellular nerve grafts were prepared by chemical removal of cellular components from rabbit sciatic nerve using a detergent at basic pH. This procedure was originally developed for decellularization of rat sciatic nerves, where the diameter of the nerve was significantly smaller (9). The first aim of this study was to confirm that this protocol was adequate for the removal of cellular components from larger sized nerves. Rabbit sciatic nerves were processed through

the decellularization protocol and assessed histologically. Analysis revealed that the native extracellular matrix (ECM) of processed nerves was largely intact and that cellular components had been removed. H&E and DAPI showed no evidence of intact cells, myelin or axons in decellularized grafts (Fig. 1B&D) in comparison to native nerve (Fig. 1A&C). In addition, the processing did not appear to alter the nerve microarchitecture. These findings suggest that the decellularization solution permeated the entire depth of the graft and thoroughly removed the native cells.

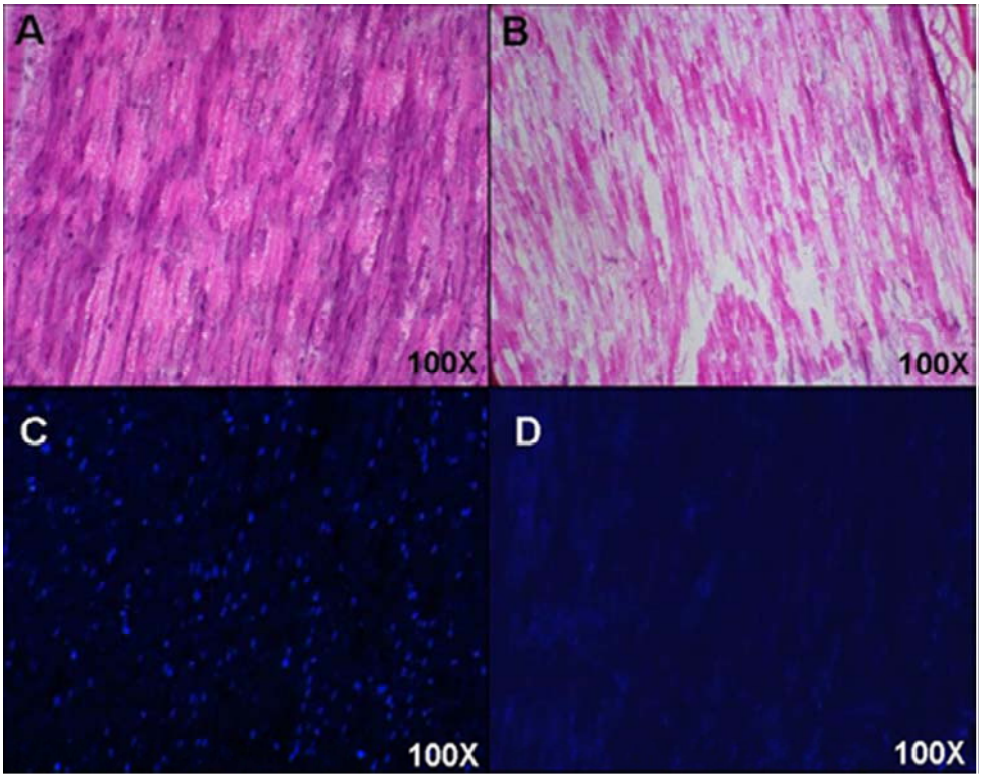

Figure 1. Histological analysis of rabbit nerves pre (A&C) and post decellularization (B&D). Staining by H&E and DAPI showed no evidence of intact cellular structures in decellularized grafts in comparison to native nerve. Processing did not alter the physical architecture of the grafts, and preserved the collagenous basal lamina matrix.

Residual DNA within acellular nerves

Although histological analysis showed the absence of intact cells and nuclei in decellularized grafts, this method has limited ability to assess cellular debris remaining within the graft. To confirm the effective removal of DNA, the percentage of DNA remaining in decellularized grafts was quantified. DNA analysis by QIAGEN DNAeasy showed a significant decrease ($p<0.05$) in cellular components following decellularization. Native nerves contained 35.64 (+/- 1.40) ng of DNA per mg of tissue whereas acellular middle and end segments contained 10.53 (+/- 2.04) and 8.88 (+/- 1.46) ng DNA/mg tissue, respectively. Approximately 75% of the native DNA was completely removed from grafts. There was no statistical difference in the DNA content of nerve segments taken from middle and end portions of the decellularized nerve, confirming that the decellularization process was effective in removing immunogenic components throughout the entire length of the graft.

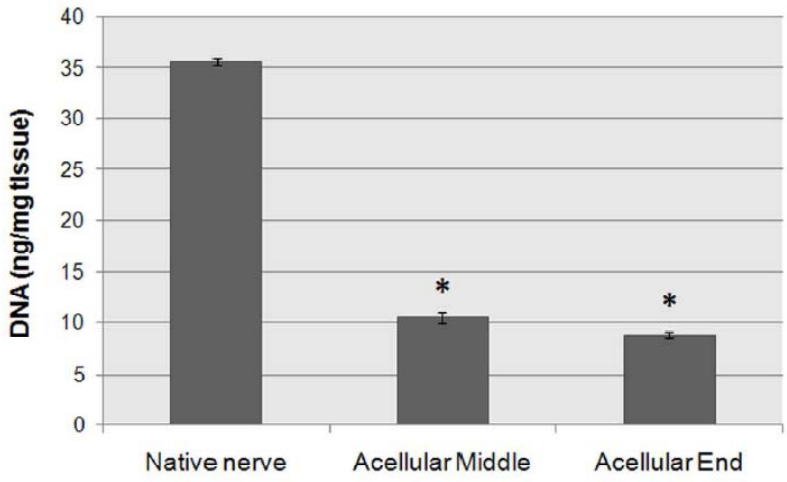

Figure 2. DNA content in native and decellularized rabbit sciatic nerves. Decellularization significantly decreased the amount of cellular DNA present within the nerve graft ($p<0.05$, $n=6$). No significant differences in DNA content were present between middle and end segments of the decellularized nerve.

Structural analysis

Analysis of scaffolds by SEM showed a network of aligned collagen fibrils in all groups, confirming the gross preservation of the nerve matrix structure. The acellular nerves were found to be devoid of intact cells, but had a very dense microarchitecture. Grafts that were decellularized and treated with increasing concentrations of peracetic acid were more porous in comparison to acellular untreated grafts (Fig. 3). The endoneurial tubes surrounding individual axons remained undamaged but appeared to be cleared of dense cellular debris. These basal lamina tubes serve as a scaffold for the regenerating neurites and must be porous enough to allow axonal outgrowth from the proximal end. We found that the porosity of the grafts could be fine-tuned by changing the concentration of oxidant used in the preparation process. As the

oxidant concentration was increased, more of the extracellular matrix was etched away and the scaffolds became more porous. There was no observable loss of mechanical integrity in 1% and 5% PA treated scaffolds, however 10% PA treated grafts were smaller and more brittle. Sutures inserted through these grafts did not hold well unlike in the rest of the groups. As a result, 10% PA treated grafts were eliminated from *in vivo* testing.

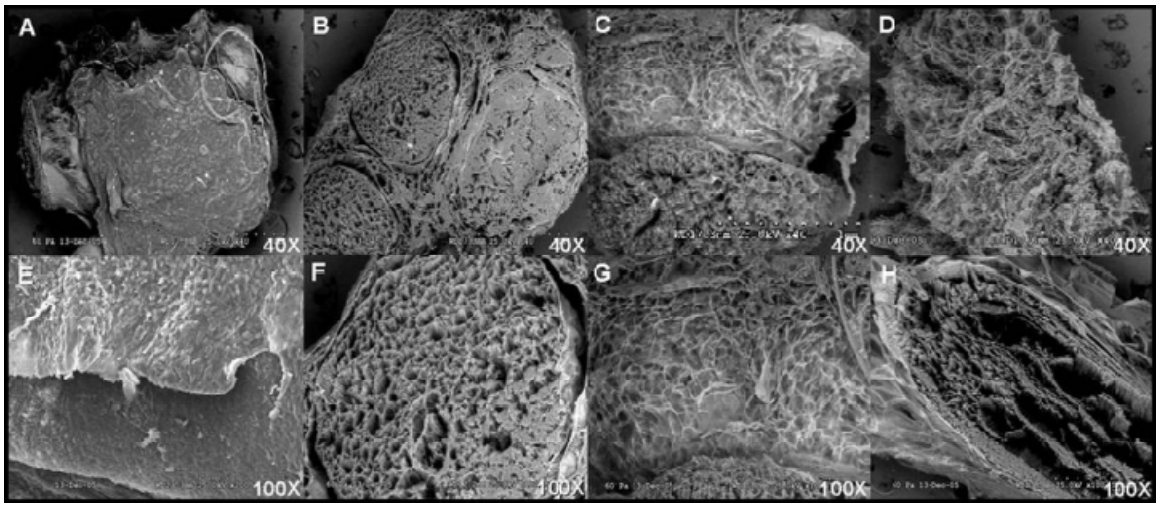

Figure 3. SEM images of decellularized and untreated nerves (A&E) with a dense physical architecture. A more porous morphology can be seen in nerves that were oxidized with peracetic acid. Treatment with 1% PA (B&F) and 5% PA (C&G) solubilized some of cellular debris present in dense acellular grafts, increasing the porosity and pore size of the scaffolds. Grafts treated with 10% (D&H) PA were very porous with only some preservation of the nerve basal lamina.

Graft remodeling and muscle tone

Incisional wounds were covered with a bandage and healed quickly with no signs of infection. Self-mutilation of the injured foot was observed in 8 of the 16 rabbits, starting as early as one week post-operatively and lasting for the duration of the study. This suggests that

50% of the animals had persistent hyperesthesia (loss of sensation) following repair with an acellular graft. Bandaging was done so as not to restrict movement of the injured leg. Self-mutilation was independent of treatment group. Four of the animals that did not self-mutilate developed foot ulcers. Flexion contracture was observed in ~60% of the rabbits with no repeating trend among groups. Four rabbits developed decubitous pressure ulcers on the heels of their feet due to lost sensation. Macroscopic observation at time of harvest at 6 months revealed an absence of inflammation and heavy scarring in all treatment groups. Small neuromas could be seen in some animals at sites of anastamosis in all groups, including autograft. Only one of the 16 grafts was not intact at the time of harvest and this animal was excluded from further analysis. All other grafts had a proper connection to the proximal end and were continuous along the length of the nerve down to the muscle. The gastrocnemius muscle tone was substantially decreased in all treatment groups in comparison to the contralateral side. Upon harvest, muscles appeared hypervascularized with numerous depositions of fatty tissue. Plantar fasciitis was evident in rabbits within all treatment groups, further indicating poor reinnervation of the tibial nerve into the gastrocnemius muscle.

Electrophysiology

Electrophysiology testing was performed to determine if functional reinnervation occurred through the nerve grafts. The contralateral side was tested first in all animals and served as an internal reference prior to testing of the experimental side. All 15 of the 16 rabbits with intact nerves were tested, however recordable CMAP was only detected in the autograft

group. Three of the four rabbits in the autograft group had measurable conduction delays and corresponding amplitudes. The mean CMAP in the autograft group was 23.4% +/- 4.4% compared to that of the contralateral reference. There was no detectable muscle function recovery in any of the animals that received acellular or oxidized grafts.

H&E staining and immunohistochemistry

The success of nerve regeneration is largely dependent on Schwann cell and axon growth within the endoneurial tubes. Histological analysis of H&E stained sections showed that regenerating axons reached the distal portions of the graft in all treatment groups (Fig 4). However, oxidized grafts had a higher density of neurofilaments and Schwann cells in the distal ends than the acellular group. In oxidized grafts, regeneration occurred mainly in organized, tightly packed fibers. The oxidized grafts also had more infiltrating host cells, which likely played a key role in remodeling of the graft following implantation. In general, grafts that were more porous prior to implantation had the highest density of regenerating fibers (Fig. 5) and Schwann cells (Fig. 6) after 6 months of regeneration. This suggests that graft remodeling may have been accelerated by the increased porosity of oxidized grafts. As expected, the autograft group showed denser axons and Schwann cells over all other treatment groups.

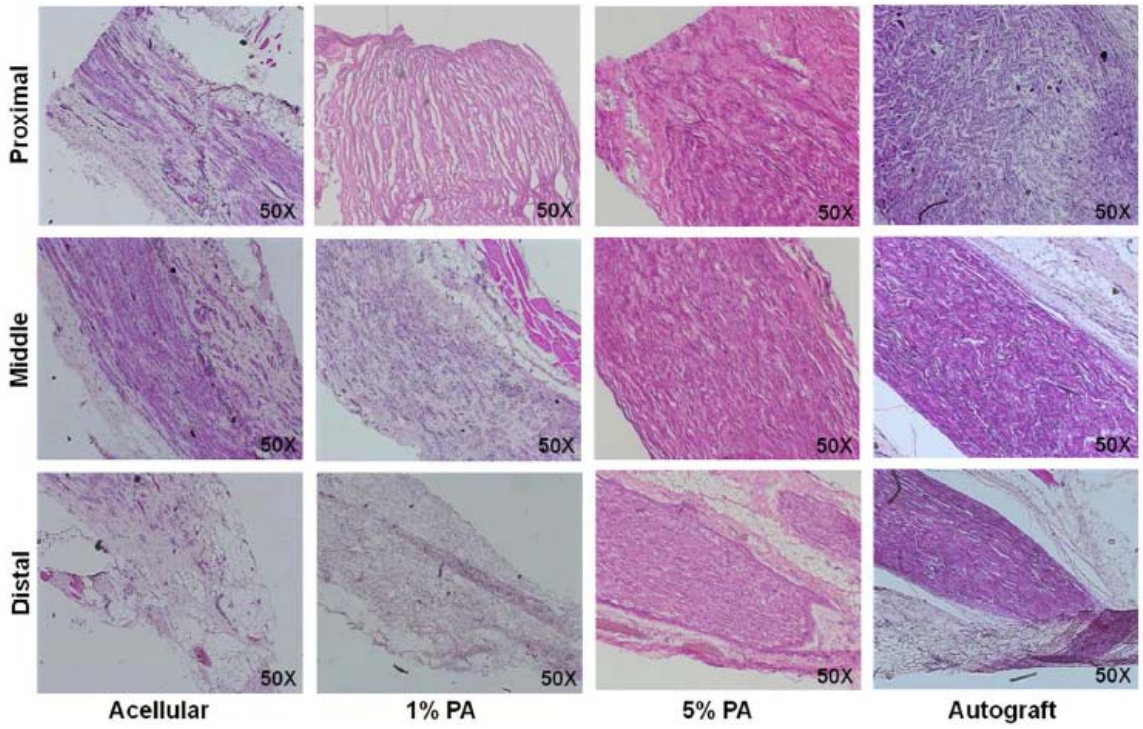

Figure 4. H&E staining of longitudinal sections of the distal portion of the regenerated nerve. The distal, middle & proximal portions represent the distal, middle and proximal portions of the distal half of the regenerated nerve. Oxidized grafts, especially those treated with 5% PA, were able to support neurite outgrowth better than acellular grafts that were not chemically treated.

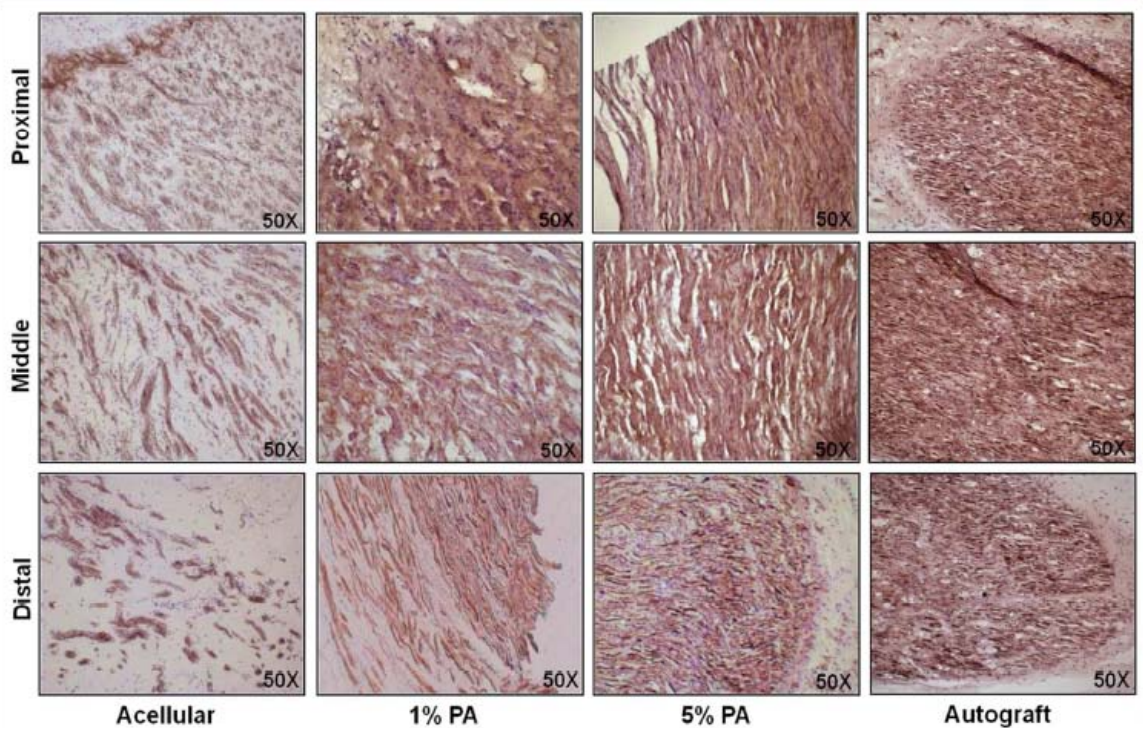

Figure 5. NF-200 immunostaining of neurofilaments within regenerated nerve fibers. The distal, middle & proximal portions represent the distal, middle and proximal portions of the distal half of the regenerated nerve. All grafts stained positive for NF-200, confirming the presence of sprouting axons in the distal nerve segments of all groups. Autografts & 5% PA treated grafts showed the highest nerve fiber density, whereas acellular grafts had considerably fewer regenerating axons.

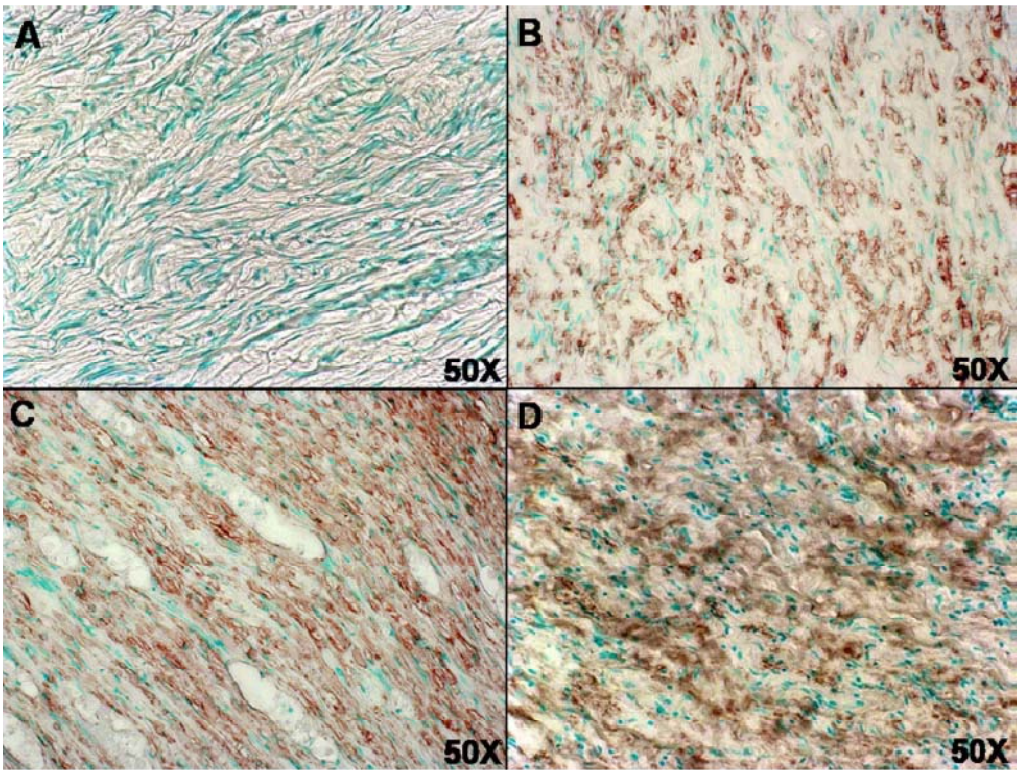

Figure 6. S100β immunostaining for Schwann cells in acellular (A), 1% PA (B), 5% PA(C) and autograft (D) groups. Nerves that regenerated through acellular grafts were repopulated with cells, but these were not positive for S100β. Oxidized scaffolds and autografts all contained myelinating Schwann cells positively expressing S100 β.

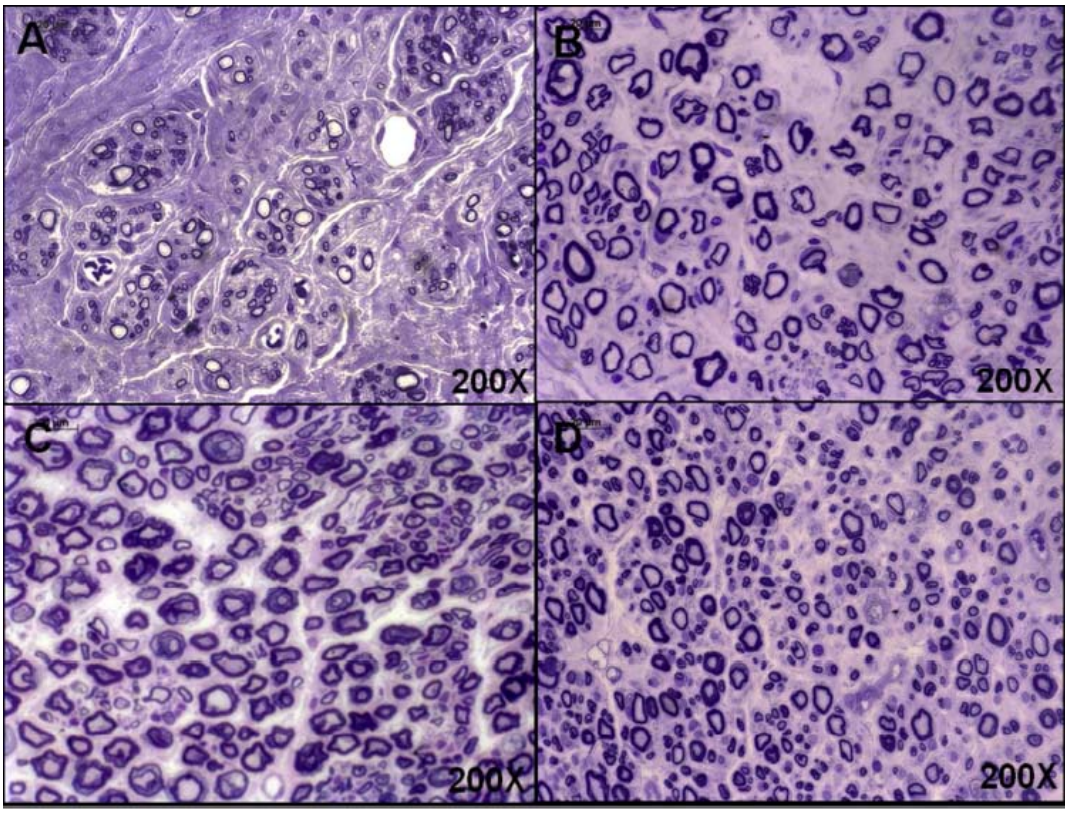

Figure 7. Toluidine blue cross-sections of the distal segments nerves that regenerated through acellular (A), 1% PA treated (B), 5% PA treated (C), Autograft (D). Sprouting axons reached the distal most portions of the regenerating nerve in all groups. Axons that regenerated through acellular grafts were smaller and only present in clusters surrounded by a collagenous matrix. Oxidized grafts had larger axons with developed myelination, particularly in the 5% PA group. Surprisingly, size and density of regenerating axons in the autograft group did not appear to be different than in oxidized grafts.

Histomorphometry

The degree of nerve regeneration was quantified by analyzing toluidine blue stained cross-sections using digital image analysis software. Myelinated axons were present in the distal segments of nerves harvested from all groups (Fig. 7). The total number and size of the regenerated axons was higher in oxidized grafts than in acellular grafts, although this data did

not reach statistical significance (Fig. 8, n=4, p=0.142, p=0.052, respectively). No statistical difference was observed between the 1% and 5% PA treated groups and autograft (p=0.259, p=0.508) with respect to axon size. Axons that regenerated through acellular grafts had significantly smaller axons than in the autograft group (p=0.015). Axons in the acellular graft group also appeared to have thinner myelin sheaths compared to that of structurally modified grafts.

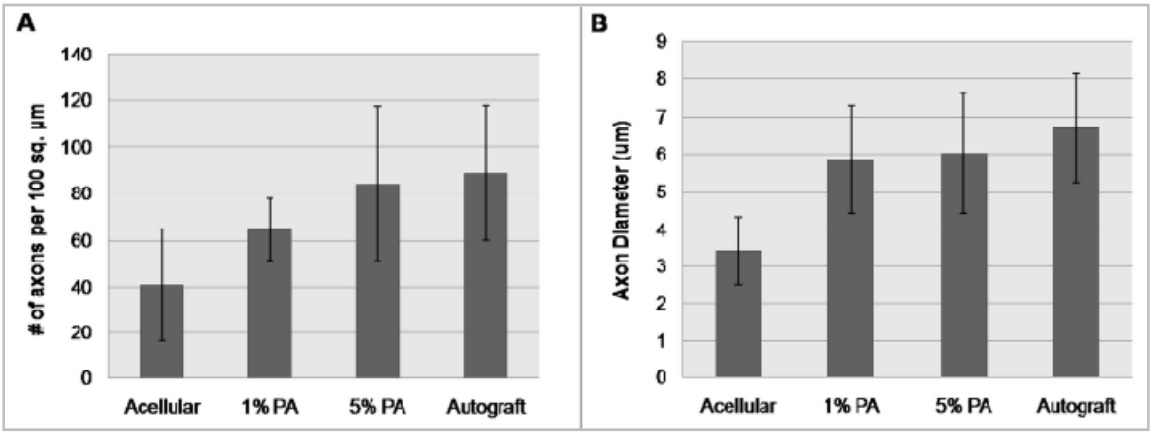

Figure 8. Histomorphometric analysis of distal nerve cross-sections. Quantification of regenerating axons showed that oxidized grafts had more regenerated axons in the distal nerve than acellular scaffolds (A). The sprouting axons were also larger in oxidized grafts and comparable to that of autograft (B).

DISCUSSION

Decellularized nerves have been widely investigated for their potential to serve as autograft substitutes. The extracellular matrix of native nerve possesses stimulatory signals critical for Schwann cell migration, proliferation and axonal sprouting. Minimally processed acellular grafts, in which the basal lamina remains intact, promote Schwann cell migration and

axonal outgrowth and are thought to retain many of these stimulatory properties (17). Thus, acellular scaffolds are considered to be superior to synthetic materials, which lack the biological components necessary to promote regeneration. The ability of acellular scaffolds to regenerate peripheral nerves has been assessed in rodent, canine and non-human primate models over gaps ranging from 5 mm to 5 cm (3,8,9,18,19). However, results with decellularized scaffolds have to date been disappointing. Rovak, et al. found that in a 1 cm rat peroneal gap, no axons were present in the distal portion of an acellular graft at 3.5 months (12). These grafts were chemically decellularized but not structurally modified in any way. In studies where functional testing was performed, nerves that regenerated through acellular grafts showed severely compromised functional recovery. Haase, et al. found a 60% decrease in functional regeneration, as measured by walking track analysis, in nerves that regenerated through an acellular grafts versus an autograft in a 1 cm rat defect model(8).

While it is generally accepted that the effective length of unseeded acellular grafts is 1-2 cm, and that longer gaps repaired with a detergent-based or thermally decellularized nerve graft do not result in functional recovery, many investigators have concluded that to the only way to overcome these limitations is by introducing cells and growth factors into the scaffolds. In one study, mesenchymal stem cells seeded onto 1 cm medial nerve grafts were found to improve conduction velocities by ~25% and compound motor action potential (CMAP) by ~50% in non-human primates (14). However, these approaches have limitations to clinical translation once the cellular component is added as cell sources are limited, manipulation of cells outside

the body is logistically complex, and the regulatory hurdles are more challenging than a simple scaffold.

Preservation of the basal lamina in acellular scaffolds may overcome some of these limitations by preserving matrix components that are instructive to infiltrating cells, but these grafts may require further modifications to yield a favorable environment for host cell remodeling (1,10,11,20). One consideration that has been omitted from these earlier studies has been graft architecture. While most investigators have strived to retain the original architecture of the native ECM, no other studies have examined how the physical geometry of acellular grafts might counteract the presence of biological cues. This study tested the hypothesis that the effective length of acellular grafts could be increased by structural modification of nerve scaffolds.

The majority of acellular graft studies have been carried out in a rat model. Thus, protocols for cellular removal were developed using rat sciatic nerves. Since decellularization methods are largely dependent on diffusion limitations, we first investigated whether these protocols could be used for larger diameter nerves. Our data shows that rabbit tibial nerves with an approximate diameter of 1.5 mm can be decellularized using methods commonly used for removal of cells from small rodent nerves. The decellularization efficiencies of larger nerves have been poorly characterization and have been limited to qualitative assessment of representative histological images. Pre and post decellularization histology is useful for assessing cell removal and structural changes in the nerve matrix but does not provide a quantitative assessment of

cellular removal. Here we quantify the degree of decellularization by measuring the percentage of DNA removed from the scaffold. We found that treatment with Triton X and ammonium hydroxide is effective in removing over 75% of immunogenic DNA from rabbit nerves.

The novel aspect of this study is the use of peracetic acid, a strong chemical oxidant, to non-specifically modify the structure of a decellularized scaffold. Until now, peracetic acid has only been used on acellular grafts at low concentrations as a means of sterilization. Our findings show that at higher concentrations and longer incubation times, peracetic acid can be used to modify the microarchitecture of acellular grafts. We show that the porosity of acellular grafts can be tailored by increasing the concentration of oxidant. As the concentration of peracetic acid is increased, more of the cellular debris and ECM is solubilized. This results in a highly porous scaffold architecture that is devoid of cells and nucleic acids but still retains its inherent organization and strength.

Implantation of such a graft is thought to promote nerve growth by facilitating migration of host cells during the early stages of regeneration. The infiltration of host Schwann and inflammatory cells into acellular grafts is critical to the regeneration process.(21). Over short defects, acellular grafts become repopulated with Schwann, macrophage and endothelial cells that migrate in from the periphery. But over longer gaps, migration of host cells into the mid-section of a scaffold is poor, with few cells penetrating the dense microarchitecture of the graft. In fact, some studies have shown that the use of an artificial scaffold that persists too long is actually detrimental to the regeneration process (22). Failure of host cells to repopulate the

scaffold leads to slow and incomplete remodeling, ultimately resulting in scar tissue formation (23). Excessive scarring impedes axonal outgrowth, inhibiting regeneration past the mid-portion of acellular grafts. Here we show that implantation of decellularized, oxidized grafts is able to promote axon regeneration into the distal segments of a 5 cm defect. This is a significant finding since acellular and further unmodified grafts have not been shown to support regeneration past the midpoint of grafts larger than 2 cm. (1,10).

Similar results have been obtained over smaller defects by pre-treatment of acellular grafts with MMPs. MMP-2 and MMP-9 expression is upregulated in the regenerating nerve, especially within the first 72 hours of regeneration (24,25). Pre-treatment of acellular grafts with MMP-2 and MMP-9 has been shown to significantly increase axon penetration into the proximal end of a 1 cm gap (11). However, the gap size in this study was small and regeneration in the distal segment was not assessed, making it difficult to assess the effect of protease pre-treatment on functional outcome. Other investigators have likewise shown that pre-degeneration of injured nerve *in vivo* prior to harvest and decellularization decreases the initial delay of axonal sprouting from the proximal end and promotes penetration into the graft (26). These studies serve as a proof of concept that pre-degradation of acellular grafts stimulates axon growth within the scaffold.

An oxidant such as peracetic acid is likely acting to non-specifically degrade the nerve ECM. This not only can potentially create a more favorable microarchitecture for migrating cells and sprouting axons, but may also remove some of the components of the nerve ECM that

have been shown to be inhibitory (27,28). One class of inhibitory molecules present in both native an acellular nerve is Chondroitin Sulfate Proteoglycans (CSPG). CSPGs prevent axon growth by binding to laminin and masking its neurostimulatory effect (20). This effect can be reversed by treatment of nerve with a CSPG inhibitor such as Chondroitinase (ChABC). Acellular grafts treated with ChABC have been shown to support regeneration over a 4 cm defect in a rat model (1) It is therefore plausible that peracetic acid treatment of acellular grafts solubilizes CSPG along with some of the other matrix proteins and unmasks the stimulatory effect of the nerve ECM, in addition to creating a more porous microarchitecture.

The present study shows that chemically modified acellular grafts are able to support regeneration across a 5cm defect. However, even though axons reached the distal segments of the graft at a density similar to that of autograft, electrophysiological testing showed no measurable neuromuscular recovery. There are two possible explanations for this: 1) Some neuromuscular recovery took place, but it was not enough to meet the minimum threshold of detection by our electrophysiology system, or 2) regenerating fibers did not reestablish functional neuromuscular junctions with the target muscle. It is well known that when the nerve to muscle connection is impaired, the neuromuscular junction degenerates (29,30). Innervation within a relatively short period of time after injury causes the neuromuscular junction to re-form, but, chronic denervation of the muscle results in loss of restorative potential (31). To our knowledge, there is only one study that has shown functional regeneration across a 5 cm tibial nerve defect using acellular grafts. Zhong *et al*. reported detectable CMAP in a canine model following 6 months of regeneration (18). However, the

electrophysiology measurements were taken from the tibialis anterior muscle, which is not innervated by the tibial nerve. Thus, it cannot be concluded that functional regeneration over a 5 cm defect is possible using an acellular graft. A 5 cm gap may simply exceed the critical size defect over which neuromuscular regeneration can take place following repair without the presence of exogenous Schwann cells. Our study shows that structural modification of allograft can improve the remodeling process and result in the formation of normal nerve tissue across large defects, but it does not guarantee the restoration of functional recovery. Although this data is encouraging, additional approaches are probably needed to accelerate regeneration and promote functional reinnervation of target muscle.

ACKNOWLEDGEMENTS

The authors would like to thank Sergio Rodriguez and Hazem Osman for assistance with the rabbit surgeries and Jacquie Burnell for assistance with histology.

References

(1) Neubauer D, Graham JB, Muir D. Chondroitinase treatment increases the effective length of acellular nerve grafts. *Exp Neurol.* 2007;207(1):163-170.

(2) Johnson EO, Zoubos AB, Soucacos PN. Regeneration and repair of peripheral nerves. *Injury-International Journal of the Care of the Injured.* 2005;36:S24-S29.

(3) Brenner MJ, Hess JR, Myckatyn TM et al. Repair of motor nerve gaps with sensory nerve inhibits regeneration in rats. *Laryngoscope.* 2006;116(9):1685-1692.

(4) Nichols CM, Brenner MJ, Fox IK et al. Effects of motor versus sensory nerve grafts on peripheral nerve regeneration. *Exp Neurol.* 2004;190(2):347-355.

(5) Moradzadeh A, Borschel GH, Luciano JP et al. The impact of motor and sensory nerve architecture on nerve regeneration. *Exp Neurol.* 2008;212(2):370-376.

(6) Rovak JM, Bishop DK, Boxer LK et al. Peripheral nerve transplantation: the role of chemical acellularization in eliminating allograft antigenicity. *J Reconstr Microsurg.* 2005;21(3):207-213.

(7) Frerichs O, Fansa H, Schicht C et al. Reconstruction of peripheral nerves using acellular nerve grafts with implanted cultured Schwann cells. *Microsurgery.* 2002;22(7):311-315.

(8) Haase SC, Rovak JM, Dennis RG et al. Recovery of muscle contractile function following nerve gap repair with chemically acellularized peripheral nerve grafts. *J Reconstr Microsurg.* 2003;19(4):241-248.

(9) Kim BS, Yoo JJ, Atala A. Peripheral nerve regeneration using acellular nerve grafts. *J Biomed Mater Res A.* 2004;68(2):201-209.

(10) Krekoski CA, Neubauer D, Zuo J, Muir D. Axonal regeneration into acellular nerve grafts is enhanced by degradation of chondroitin sulfate proteoglycan. *J Neurosci.* 2001;21(16):6206-6213.

(11) Krekoski CA, Neubauer D, Graham JB, Muir D. Metalloproteinase-dependent predegeneration in vitro enhances axonal regeneration within acellular peripheral nerve grafts. *J Neurosci.* 2002;22(23):10408-10415.

(12) Rovak JM, Mungara AK, Aydin MA, Cederna PS. Effects of vascular endothelial growth factor on nerve regeneration in acellular nerve grafts. *J Reconstr Microsurg.* 2004;20(1):53-58.

(13) Hu J, Zhu QT, Liu XL et al. Repair of extended peripheral nerve lesions in rhesus monkeys using acellular allogenic nerve grafts implanted with autologous mesenchymal stem cells. *Experimental Neurology.* 2007;204(2):658-666.

(14) Wang D, Liu XL, Zhu JK et al. Bridging small-gap peripheral nerve defects using acellular nerve allograft implanted with autologous bone marrow stromal cells in primates. *Brain Res.* 2008;1188:44-53.

(15) Zantop T, Gilbert TW, Yoder MC, Badylak SF. Extracellular matrix scaffolds are repopulated by bone marrow-derived cells in a mouse model of achilles tendon reconstruction. *J Orthop Res.* 2006;24(6):1299-1309.

(16) Derwin KA, Baker AR, Spragg RK et al. Commercial extracellular matrix scaffolds for rotator cuff tendon repair. Biomechanical, biochemical, and cellular properties. *J Bone Joint Surg Am.* 2006;88(12):2665-2672.

(17) Dubovy P, Svizenska I, Klusakova I et al. Laminin molecules in freeze-treated nerve segments are associated with migrating Schwann cells that display the corresponding alpha6beta1 integrin receptor. *Glia.* 2001;33(1):36-44.

(18) Zhong H, Chen B, Lu S et al. Nerve Regeneration and Functional Recovery after a Sciatic Nerve Gap Is Repaired by an Acellular Nerve Allograft Made through Chemical Extraction in Canines. *J Reconstr Microsurg.* 2007.

(19) Sondell M, Lundborg G, Kanje M. Regeneration of the rat sciatic nerve into allografts made acellular through chemical extraction. *Brain Res.* 1998;795(1-2):44-54.

(20) Zuo J, Ferguson TA, Hernandez YJ et al. Neuronal matrix metalloproteinase-2 degrades and inactivates a neurite-inhibiting chondroitin sulfate proteoglycan. *J Neurosci.* 1998;18(14):5203-5211.

(21) Sorensen J, Fugleholm K, Moldovan M et al. Axonal elongation through long acellular nerve segments depends on recruitment of phagocytic cells from the near-nerve environment. Electrophysiological and morphological studies in the cat. *Brain Res.* 2001;903(1-2):185-197.

(22) Valentini RF, Aebischer P, Winn SR, Galletti PM. Collagen- and laminin-containing gels impede peripheral nerve regeneration through semipermeable nerve guidance channels. *Exp Neurol.* 1987;98(2):350-356.

(23) Hodde J, Hiles M. Constructive soft tissue remodelling with a biologic extracellular matrix graft: overview and review of the clinical literature. *Acta Chir Belg.* 2007;107(6):641-647.

(24) Ferguson TA, Muir D. MMP-2 and MMP-9 increase the neurite-promoting potential of schwann cell basal laminae and are upregulated in degenerated nerve. *Mol Cell Neurosci.* 2000;16(2):157-167.

(25) Siebert H, Dippel N, Mader M et al. Matrix metalloproteinase expression and inhibition after sciatic nerve axotomy. *J Neuropathol Exp Neurol.* 2001;60(1):85-93.

(26) Ochi M, Wakasa M, Ikuta Y, Kwong WH. Nerve regeneration in predegenerated basal lamina graft: the effect of duration of predegeneration on axonal extension. *Exp Neurol.* 1994;128(2):216-225.

(27) Snow DM, Mullins N, Hynds DL. Nervous system-derived chondroitin sulfate proteoglycans regulate growth cone morphology and inhibit neurite outgrowth: a light, epifluorescence, and electron microscopy study. *Microsc Res Tech.* 2001;54(5):273-286.

(28) Oohira A, Matsui F, Katoh-Semba R. Inhibitory effects of brain chondroitin sulfate proteoglycans on neurite outgrowth from PC12D cells. *J Neurosci.* 1991;11(3):822-827.

(29) Carlson BM. Denervation, reinnervation, and regeneration of skeletal muscle. *Otolaryngol Head Neck Surg.* 1981;89(2):192-196.

(30) Carlson BM, Borisov AB, Dedkov EI et al. Effects of long-term denervation on skeletal muscle in old rats. *J Gerontol A Biol Sci Med Sci.* 2002;57(10):B366-B374.

(31) Carlson B, Borisov AB, Dedkov EI et al. The biology and restorative capacity of long-term denervated skeletal muscle. *Basic and Applied Myology.* 2008;12(6):247-254.

CHAPTER IV

Properties and Biocompatibility of Keratin Biomaterials Derived From Human Hair PArt I: Kerateine

Paulina Sierpinski Hill, Helen Brantley, Mark Van Dyke

Wake Forest Institute for Regenerative Medicine

Wake Forest University School of Medicine

Medical Center Boulevard

Winston Salem, NC 27157

The following manuscript has not been submitted. Paulina Sierpinski prepared the manuscript.

Dr. Mark Van Dyke acted in an advisory and editorial capacity.

ABSTRACT

Keratins are a family of structural proteins that can be isolated from a variety of tissues. "Soft" keratins are cytoskeletal elements found in epithelial tissues while protective tissues such as nails, hooves, and hair are composed of "hard" keratins. Hard keratins have been the subject of biomaterials investigations for more than three decades. Numerous methods exist for denaturing these proteins which are characterized by a high sulfur content and extensive disulfide bonding, extracting them from tissue, and processing them into various physical states such as gels, films, coatings, and fibers. These types of keratin biomaterials, alone or in combination with other biomaterials, have been tested in a small number of systems to demonstrate feasibility for medical applications such as wound healing, bone regeneration, hemostasis, and peripheral nerve repair. These investigations have shown generally good compatibility with cells and tissues, but the focus has been fairly narrow, and as a result there is relatively little published data on the general behavior of keratin biomaterials in biological systems. The goal of this study was to produce a reduced form of keratin biomaterial, kerateine, using a typical and well-published technique, and characterize several aspects of its behavior that may have implications to its general use as a biomaterial. Keratins were extracted from human hair, fabricated into gels and porous scaffolds, characterized, and placed into biological systems to determine their interactions with cells and tissue. The proteins were analyzed for purity, molecular weight and amino acid content, as well as their ability to facilitate cell adhesion and proliferation. Crosslinked hydrogels were investigated for their hydrolytic stability in vitro; the microarchitecture and in vivo tissue response of lyophilized gels was also

studied. These experiments both confirmed and expanded earlier findings that keratins demonstrate excellent compatibility in biological systems.

INTRODUCTION

Hair keratins are a family of structural proteins found abundantly in hair and fingernails and are often referred to as "hard" keratins (as opposed to soft keratins that are found in epithelial tissues). Keratin proteins are self-assembled into a hair fiber in the follicle by a highly proliferative process controlled by more than 30 growth factors and cytokines (1-7). After extrusion through the skin, the hair fiber is formed into a highly stable structure that is relatively impervious to environmental insult. This system is strikingly similar to synthetic polymers in that it contains structural macromolecules, crosslinkers, plasticizers, and UV stabilizers. The keratin proteins extracted from hair can be classified into three broad groups: alpha-, beta-, and gamma-keratins. The alpha-keratins are structural, have an alpha-helical tertiary structure, are low in sulfur content, and have an average molar mass in the range of 60–80 KDa; they reside in the hair fiber cortex. The beta-keratins are primarily protective and form the majority of the cuticle. Beta keratins are difficult to extract and do not form especially useful reconstituted structures. Gamma-keratins are globular, high in sulfur content, and lower in molecular weight (approximately 15 KDa) than the other types of keratins. They function as disulfide crosslinkers, holding the cortical superstructure together. A schematic of a wool fiber, which is similar to a human hair, is shown in Figure 1.

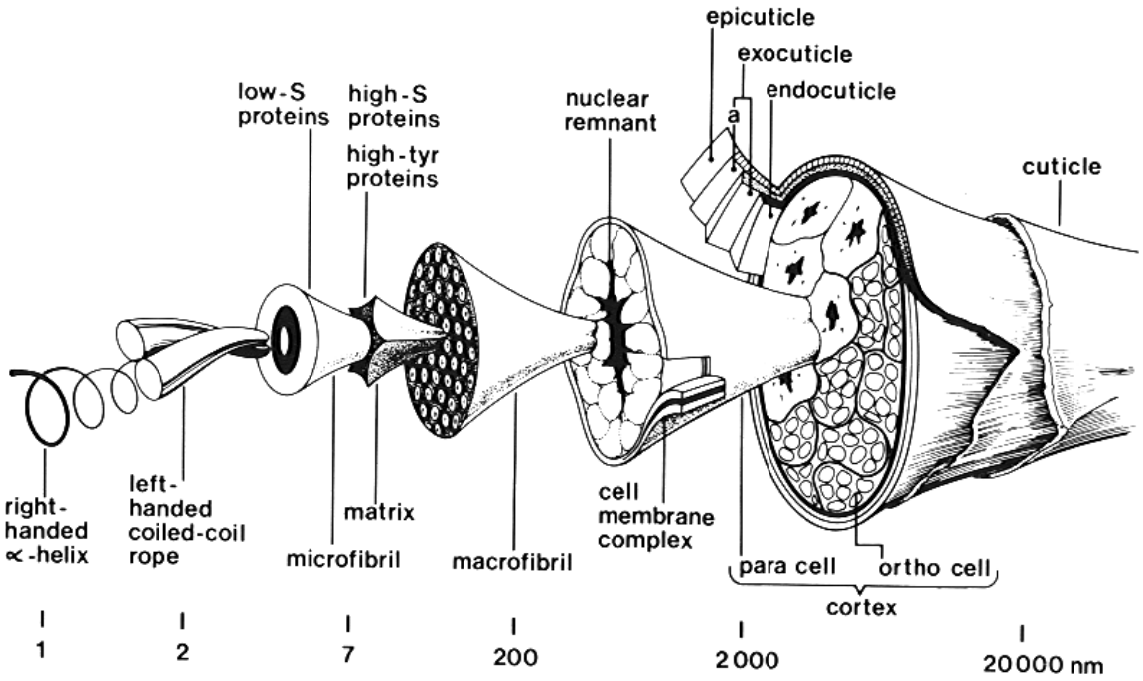

Figure 1. Schematic of a wool fiber drawn by Bruce Fraser and Tom MacRae [Copyright CSIRO Australia 1996. Reproduced with permission from The Lennox Legacy (Rivett DE, Ward SW, Belkin LM, Ramshaw JAM and Wilshire JFK). Published by CSIRO PUBLISHING, Melbourne Australia]. Human hair has a similar superstructure but varies in the ratio of alpha- to gamma-keratin. Alpha-keratin is composed of the right-handed, alpha-helical proteins that are low sulfur and have a molecular weight of approximately 60 kDa. Gamma-keratin is globular in nature and forms the matrix that holds the microfibrils together and is high in sulfur with a molecular weight of approximately 15 kDa. Oxidative and reductive chemistries can be used to break this structure down and extract both types of keratins from hair fiber.

Keratins are removed from the cortex first by using chemicals to break the disulfide bonds that are prevalent in keratinized tissues. The alpha and gamma-keratins are converted to their non-crosslinked forms by oxidation or reduction, during which cystine is converted to either cysteic acid or cysteine, respectively, and the free proteins extracted with denaturing solvents to produce a solution that can be purified by filtration and dialysis. If the extraction is

carried out using an oxidant, the cysteic acid derivatives are referred to as “keratoses”; if a reductant is used, the cysteine-containing proteins are call “kerateines”. While essentially homologous, the nature of sulfur-containing groups imparts some differences to keratoses and kerateines. Keratoses are hygroscopic, non-crosslinkable, water soluble, and susceptible to hydrolytic degradation at extremes of pH due to polarization of the backbone caused by the electron withdrawing properties of cysteic acid. These characteristics cause keratoses to degrade relatively quickly in vivo (i.e. on the order of days to weeks). Kerateines on the other hand, are less polar and therefore slightly less soluble in water. They are more stable at extremes of pH and can be re-crosslinked through oxidative coupling of cysteine groups. This results in biomaterials that can persist in vivo for weeks to months.

Methods for oxidation (8-10) and reduction (11-13) have been in the published literature for more than 100 years, and have been summarized in several reviews, most notably by Crewther et al. in 1965 (14). Investigations of the structure and properties of soluble keratins has continued, but beginning in the 1970’s, the processing of these protein solutions into derivative physical states such as gels and films began appearing in the literature (15-17). Soon thereafter, the first keratin biomaterials paper appeared wherein a vascular graft coated with a keratin derivative was successfully implanted into a large animal model for 200 days (18). Since then, keratins have been used in several in vitro and preclinical models for wound healing (19,20), fluid resuscitation (21), bone regeneration (22), hemostasis (23), and peripheral nerve repair (24,25). Overall, the literature on keratin biomaterials is weighted toward patents, with medical applications taking precedence over fundamental studies of biological properties. Only

a handful of studies of the basic biological properties of keratin biomaterials have ever been published. While the potential for biomedical use of keratins is demonstrably high, it would be useful to better understand some of the basic biological characteristics of these unique materials.

The aim of this study was to produce a typical keratin biomaterial from human hair and investigate its general chemical, physical, and biological properties. We hypothesized that keratin would demonstrate excellent cell and tissue compatibility based on its ubiquitous presence in mammalian systems and highly conserved primary amino acid structure. Utilizing a common extraction method, we created hydrogels and lyophilized scaffolds and determined the composition, structure, in vitro degradation, and cell and tissue interactions.

METHODS

Preparation of Kerateine Biomaterial. The keratin used in this study was extracted from human hair according to long-established protocols (11). Briefly, hair from a local barber shop was washed in mild detergent and degreased with organic solvent. The clean, dry, degreased hair was reduced to break cystine bonds that would otherwise render the keratin proteins insoluble. After chemical reduction, a crude fraction of kerateines was extracted using 100 mM tris base solution, followed by a second extraction with deionized (DI) water. The extracts were combined, centrifuged, filtered, and dialyzed against DI water using a 1K Dalton nominal low molecular weight cutoff, tangential flow, spiral wound cartridge (Prep/Scale, Millipore)

connected to a gear pump operating at ca. 1.5 L/min flow rate and 10 psi backpressure. During the dialysis, the pH of the kerateine solution was not allowed to drop below 7.0 by periodically adding small amounts of 0.1M NaOH solution. After 5 days, the ending concentration of protein was determined by lyophilization of a 1.00 g aliquot and adjusted to a final pH of 7.4 and concentration of 5 weight % by dropwise addition of a 0.1M NaOH solution and ultrapure water, respectively. Kerateine samples used for the experiments detailed below were conducted using this solution as the starting material.

SDS-PAGE Analysis. Electrophoretic separation of keratin proteins was performed on a BioRad Mini-Protean II system. The 5 wt. % keratin stock solution was diluted to 2.5 mg/mL with ultrapure water. 100 L of this solution was mixed with 20 mL of 5X SDS loading buffer containing 0.6M -mercaptoethanol (Biorad). Keratin was denatured by boiling for 5 min in SDS/ -mercaptoethanol solution and immediately placed on ice. 4 L of this cold, denatured solution was loaded onto precast 8-16% gradient Tris-HCl gels (Ready Gel, Biorad). Protein loading into the gel well was 8 μg. Separation was performed at 60 V for 30 min, followed by 120 V for 100 min. After separation, gels were rinsed with ultrapure water for 5 min twice before staining with Bio-Safe Comassie stain (G250, Biorad) for 30 min. Destaining was done overnight in ultrapure water with gentle rotation. Samples were compared to a standard ladder (Benchmark Prestained Protein Ladder, Invitrogen) and the gel imaged in DIA mode with a Fuji Film LAS-300 imaging system.

Amino Acid Analysis. Quantitative amino acid analyses were performed using the Pico-Tag method as described previously with slight modification (26). Briefly, kerateine samples were diluted from 5 wt. % to 1 wt. % using ultrapure water. Samples (n=4) were hydrolyzed using 6 N HCl in 6 x 50 mm borosilicate glass tubes using a vapor-phase hydrolysis method. Samples were dried in the glass tubes which were then placed in a sealed glass vial with glass beads and 500 L 6 N HCl. The vials were evacuated and flushed with nitrogen gas, then incubated at 110°C for 24 hours. Hydrolyzed amino acids were treated with phenylisothiocyanate to produce phenylthiocarbamyl-amino acid (PTC-AA) derivatives. The PTC-AA were separated and quantified by reverse phase high performance liquid chromatography using a Waters HPLC system. The total amount of each identifiable amino acid was determined and expressed as the mole % +/- standard deviation (n=4).

Structural Analysis. Kerateine disks were formed by pipetting 100 μL of a 5% kerateine solution into a 96 well plate and lyophilizing. The resulting disks were retrieved from plate wells and sterilized by γ-irradiation (850 krad) using a ^{60}Co source. The disks were mounted on stubs with colloidal graphite and analyzed using a Hitachi S-2600N variable pressure scanning electron microscope (SEM, Hitachi High Technologies Corp., Schaumburg, IL).

In vitro Hydrolytic Stability. A 10% kerateine gel was prepared by removing water using a rotary evaporation system (Buchi; 10 mm Hg, 50°C water bath). 500 l of kerateine was pipetted into a 15 mL tube, sterilized by γ-irradiation (850 krad) and centrifuged. 10 mL of sterilize PBS was carefully added to each tube and the sample placed at 37°C. At each time

point (n=6), 1 mL of PBS was removed from each tube and assayed by a Lowry assay to determine the amount of kerateine released into solution. Protein concentration was determined by measuring the absorbance at 750 nm. The liquid volume in each tube was replenished with 1 mL of fresh PBS to maintain constant volume.

Cytotoxicity. Cell viability in the presence of kerateine was assessed using an MTS cell viability assay NIH-3T3 cells were seeded at a density of 4,200 cells/cm^2 and allowed to grow for 24 hrs at 37° C in 5% CO_2. After 24 hrs, the media was replaced with media containing kerateine (0.0001-1%) with FBS and allowed to grow for 3 days. The negative control consisted of cells with serum free media. After 3 days, cell viability was determined with the Cell Titer 96 Aqueous Non-Radioactive MTS Cell Proliferation Assay (Promega, Madison, WI). Absorbance readings were taken at 490 nm using an ELX-500 UV plate reader (Bio-Tek, Winooski, VT) to determine viability of cells in reference to positive (serum containing) and negative (serum free) controls.

Adhesion. Cell adhesion to keratin biomaterials was examined with phase contrast microscopy and quantified using the fluorescent dye Calcein AM **.** Tissue culture treated 48 well plates were coated overnight with either keratin (100 μg/mL), fibronectin (5 μg/mL) or left uncoated. NIH 3T3 mouse fibroblasts were seeded onto plates at a density of 30,000 cells per well and allowed to adhere for 5 hours. Each well was gently rinsed with 500 μL of PBS to remove non-adherent cells. Attached cells were labeled with 5 μM Calcein AM (Molecular Probes, Invitrogen, CA) in PBS, by incubation at 37°C for 1 hr. The relative fluorescence emission was

determined using an FLX-500 fluorescent plate reader (Bio-Tek). Background Calcein AM levels in PBS only were measured and subtracted from all readings.

Proliferation. Cell proliferation on kerateine coatings was assessed using an MTS assay as described above. 3T3 fibroblasts were plated onto keratin, fibronectin or uncoated 48 well plates at 4,000 cells per cm^2. Seeded cells were cultured for 48 hours in serum-containing media. An MTS assay was performed to determine relative cell numbers on each substrate. The absorbance at 490 nm was measured using an ELX-500 UV plate reader. Cell proliferation on a keratin substrate was compared to an uncoated tissue culture treated plate (negative control) and fibronectin (positive control).

In vivo Degradation and Tissue Response. All animal procedures were performed under a protocol approved by the Institutional Animal Care and Use Committee. To assess the in vivo biocompatibility of kerateine biomaterials, small disks were implanted subcutaneously into mice. Adult male CD1 Swiss-Webster mice (Charles River Laboratories, approximately 30-35 g in weight, were placed under general anesthesia with isoflurane. The operative site on the back was shaved and cleansed with betadine. A 2 cm lateral skin incision was made on the mid-portion of the back and tissue pockets were created by gross dissection laterally using blunt scissors. Sterilized kerateine disks were implanted into the subcutaneous pocket of each mouse. Skin closures were performed with 5-0 absorbable Vicryl sutures. At 7 days, 1, 2, 3, and 6 months, animals were euthanized and an incision was made on the back of each mouse. Kerateine disks were imaged in situ and observed grossly for inflammation and capsule

formation. The entire implant site, including the disk was excised. Images of representative explants were taken at each time point to determine the relative in vivo degradation rate.

Histology. Tissue explants were fixed in 10% Neutral Buffered Formalin (NBF) for 24 hours, dehydrated in increasing concentrations of ethanol and embedded in paraffin. Cross-sections (5 mm thick) were cut on a microtome (Leica Ultramicrotome RM2265), mounted on StarFrost® glass slides (Engelbrecht), and air dried. Sections were stained with hematoxylin & eosin (H&E) and Masson's Trichrome to assess the presence and thickness of fibrous tissue, cellular response, collagen deposition and vascularization.

Statistical Analysis. All in vitro assays were analyzed by a single factor Analysis of Variance (ANOVA) using SigmaStat 3.1 to determine statistically significant differences. Post-hoc testing was performed using Student-Newman-Keuls method. Values of $p \leq 0.05$ were considered to be significant.

RESULTS

SDS-PAGE Analysis. Analysis of the purity and molecular weight of kerateine samples prior to crosslinking showed a characteristic banding pattern as described by other investigators (27). The gel image shows a large, broad band of keratins at the head of the lane that typically do not disassociate, even under strongly reducing, denaturing conditions. Characteristic bands for -keratins at 64 and 43 KDa represent the distinctly different acidic and basic families (28). Low molecular weight gamma-keratins can be seen in lesser abundance at 10 and 16 KDa (Figure 2).

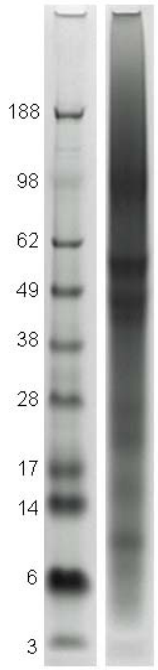

Figure 2. SDS-PAGE of a dilute keratin solution (1%) prior to gelation. The keratin stock solution was run under reducing conditions and gave the characteristic bands noted in other studies. The complexity of human hair extracts is evident in the number and breadth of bands present.

Amino Acid Analysis. The amino acid makeup of keratin samples was consistent with earlier reports in the literature for wool and human hair keratins (Table 1), with the exception of arginine (29,30). A total of 17 amino acids were identified in kerateine extracts. Tryptophan is irreversibly destroyed in the hydrolysis step and cannot be quantified. Asparagine and glutamine side chains are hydrolyzed to form Aspartic and Glutamic Acid, respectively. As expected, serine, glutamic acid and cysteine were the most abundant amino acids present in kerateine extracts.

Amino Acid	Mole % +/- SD
Cysteic Acid	9.97 +/- 0.55
Aspartic Acid	7.63 +/- 0.18
Glutamic Acid	11.56 +/- 0.12
Serine	11.66 +/- 0.26
Glycine	6.56 +/- 0.05
Histidine	1.10 +/- 0.03
Arginine	4.92 +/- 0.05
Threonine	6.87 +/- 0.32
Alanine	5.22 +/- 0.09
Proline	9.55 +/- 0.25
Tyrosine	1.20 +/- 0.31
Valine	6.18 +/- 0.21
Methionine	2.49 +/- 0.10
Isoleucine	3.12 +/- 0.07
Leucine	7.09 +/- 0.06
Phenylalanine	1.91 +/- 0.03
Lysine	2.96 +/- 0.05

Table 1. Amino acid composition of kerateine biomaterials derived from human hair. Values are expressed as the mol % of the total identifiable amino acids +/- standard deviation (n=4).

Structural Analysis. The microarchitecture of lyophilized kerateine biomaterial disks was examined by Scanning Electron Microscopy (SEM). Cross sectional images of a 5% kerateine

extract (Figure 3) show a continuous porous microstructure. Upon drying, kerateines were found to form a homogenous network of interconnected pores ranging in size from 30-70 μm. This ability for molecular self-assembly, where the keratin proteins spontaneously associate to form a porous network, is consistent with previously reported keratins derived from human hair (59) and wool (60).

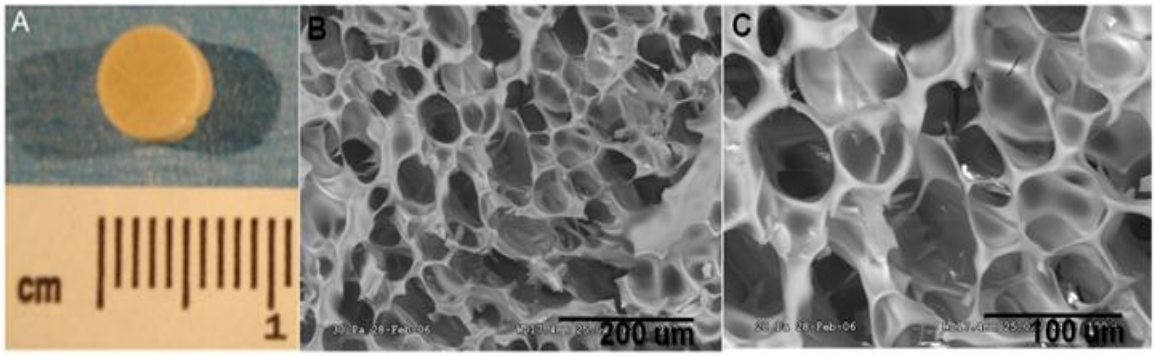

Figure 3. Images of kerateine disks prior to subcutaneous implantation. A digital photo shows a macroscopic view of a 6mm disk created by lyophilization of a kerateine solution (A). SEM of lyophilized kerateine disks at (B) 100X and (C) 300X. This homogenous porous network was formed by spontaneous re-crosslinking of the keratin proteins upon exposure to air.

In Vitro Hydrolytic Stability. A 10% kerateine gel was exposed to PBS at 37°C and the in hydrolytic stability of the gel was determined over time. At each time point, the total amount of keratin that was released into solution was quantified and expressed as a percentage of the total protein content within the gel. Initially, the amount of protein released into solution was high. Approximately 25% of the kerateine gel degraded within the first 7 days and over 50% degraded by 4 weeks. By 3 months, the amount of protein released began to stabilize at about 65%. At 6 months, the total kerateine released into solution was 66.1% (Figure 4).

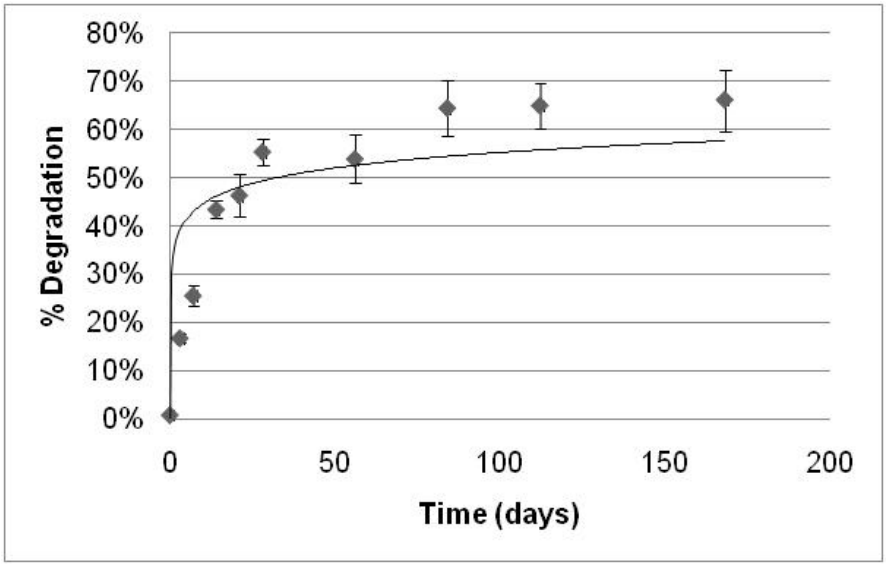

Figure 4. *In vitro* hydrolytic stability of kerateine biomaterials at 37°C. A 10% kerateine gel was placed in the bottom of a 15 mL falcon tube and exposed to PBS. The amount of kerateine released into solution was quantified at each time point (n=6). The degradation rate was rapid within the first month then gradually leveled off. Values are expressed as an average of the % degradation +/ standard deviation.

In Vitro Cytotoxicity. To determine whether kerateine biomaterial extracts were cytotoxic in soluble form, 3T3 fibroblasts were exposed to kerateine diluted in media at concentrations ranging from $1.0x10^{-6}$ mg/mL to 0.1 mg/mL. The MTS assay is an established method for quantifying relative cell numbers by measuring the mitochondrial activity in living cells. Kerateine biomaterial extracts diluted in media were not cytotoxic to 3T3 fibroblasts when exposed to cells for 48 hours at 0.1 mg/mL or less (Figure 5). At concentrations of 0.000001-0.1 mg/mL, cell viability was statistically equivalent when compared to serum-containing

media. Kerateine was found to be cytotoxic to 3T3 fibroblasts at concentrations above 1 mg/mL.

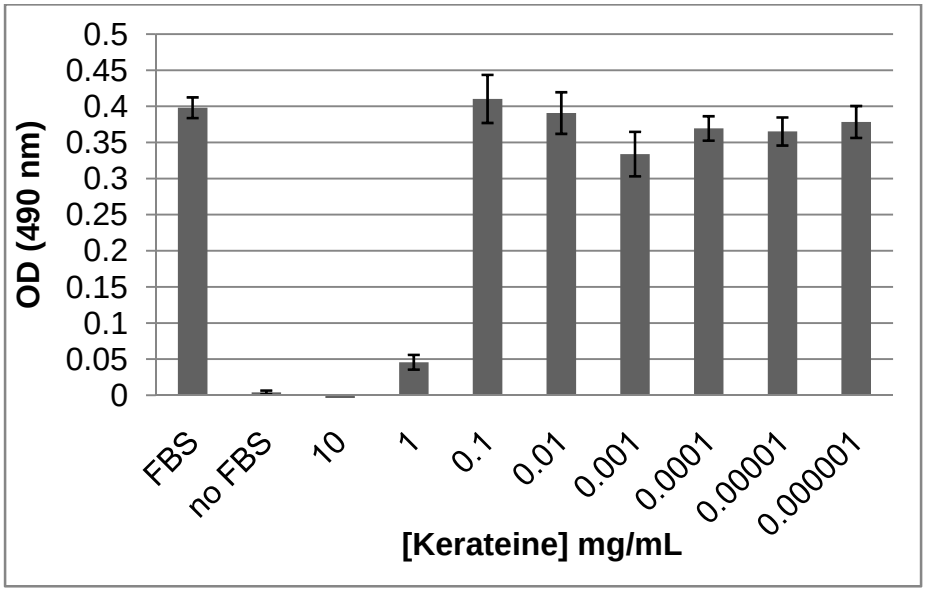

Figure 5. Cytotoxicity of kerateine biomaterials in serum containing media. Cells were exposed to kerateine solutions in the presence of fetal bovine serum (FBS) for 48 hrs except for the negative control, which has no serum (no FBS). Relative cell numbers were determined using an MTS assay. Kerateine is biocompatible at concentrations ranging from 0.000001-0.1 mg/mL and only inhibits cell proliferation at high concentrations of 1 mg/mL or higher. Error bars represent standard error of the mean with an $n \geq 10$.

Adhesion. Fibroblast cell adhesion to a kerateine substrate was evaluated *in vitro.* Cells were seeded onto kerateine coated plates and compared to tissue culture treated plates (uncoated) and fibronectin coated plates (n=6 per group). Cell morphology was observed with phase contrast microscopy. Relative adhesion was quantified by measuring the fluorescence emission of Calcein AM stained cells that remained attached on each substrate. Within a few hours after plating, fibroblasts seeded onto kerateine and fibronectin substrates were spread out and had a

characteristic polygonal morphology. Fibroblasts seeded on uncoated plates had a more spherical, less elongated morphology. Fibroblast adhesion to kerateine and fibronectin was significantly better than on an uncoated plate, $p=0.044$ and $p<0.001$ respectively (Figure 6). Adhesion on fibronectin coatings was significantly better than on kerateine coated dishes ($p=0.02$).

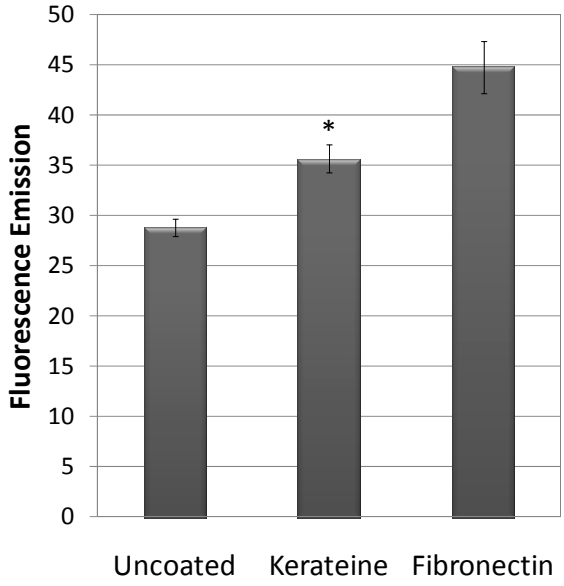

Figure 6. A kerateine biomaterial coating promotes 3T3 fibroblast adhesion. Cells were seeded onto pre-coated dishes and allowed to adhere for 5 hours. Unattached cells were washed off and adherent cells were labeled with Calcein AM. The fluorescence emission was measured to determine the relative number of adherent cells on each coating. Keratin was found to significantly promote fibroblast cell adhesion over an uncoated dish. Adhesion on fibronectin coatings was significantly better than on both uncoated and kerateine coated dishes.

Proliferation. Biocompatible biomaterials are not only non-cytotoxic and supportive of cell adhesion, but in some cases may promote cell proliferation. To assess the ability of a kerateine

substrate to promote cell proliferation, fibroblasts were seeded onto kerateine coated plates and cultured for 48 hours in serum-containing media. Cells seeded on a kerateine substrate stimulate 3T3 fibroblast proliferation. Cells were seeded onto pre-coated dishes and allowed to proliferate for 48 hours. Relative cell numbers were determined using the MTS proliferation assay. 3T3 growth on a kerateine substrate was significantly higher than on an uncoated dish and not statistically different than fibronectin (Figure 7).

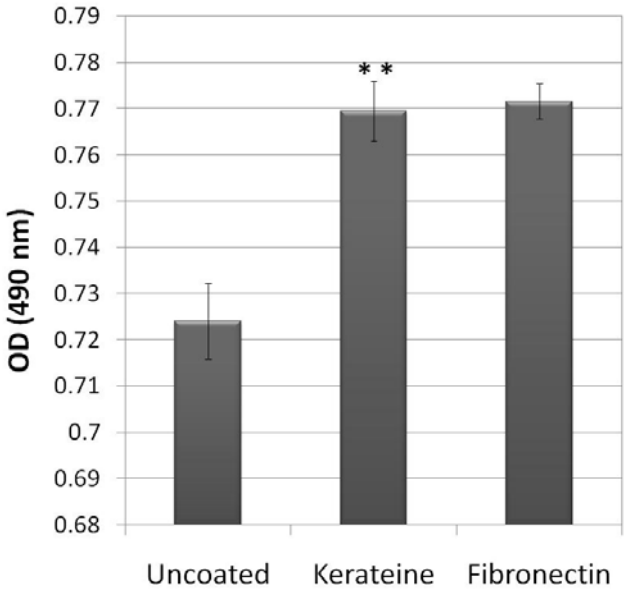

Figure 7. A kerateine substrate stimulates 3T3 fibroblast proliferation. Cells were seeded onto pre-coated dishes and allowed to proliferate for 48 hours. Relative cell numbers were determined using the MTS proliferation assay. 3T3 growth on a kerateine substrate was significantly higher than on an uncoated dish and not statistically different than fibronectin.

In Vivo Tissue Response. Lyophilized kerateine disks approximately 8 mm in diameter (Figure 3A) were implanted onto the backs of immunocompetent mice. Disks were harvested at 7 days, 1, 2, 3 and 6 months after implantation. Examination of the biomaterial tissue interface showed no gross inflammation or fibrosis at early or late time points (Figure 8). The in vivo degradation rate of kerateine implants was assessed by measuring the size of disks at time of harvest. Explanted disks did not appear to decrease in size within the first 3 months. At 4 months, kerateine explants were approximately 6 mm in diameter and by 6 months disks, they had degraded to 5 mm or approximately 60% of their original size.

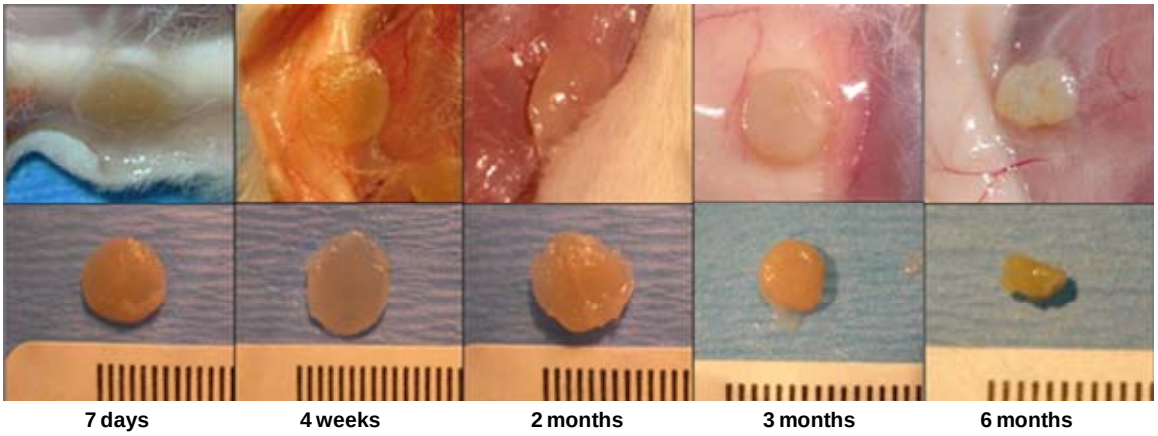

Figure 8. Kerateine disks harvested at 1 week to 6 months following subcutaneous implantation. Gross examination of the implant area did not show any observable inflammation or capsule formation. Implanted kerateine disks did not visibly decrease in size until 3 months. By 6 months the implants could still be easily identified upon harvest, but were considerably smaller in size.

Histological analysis by H&E and Masson's trichrome confirmed the absence of fibrous capsule formation (Figure 9 and 10). Fibroblast accumulation on the periphery of the kerateine implants was highest at 1-2 months and was a few cell layers thick (Figure 9). The formation of supportive vasculature could be seen as early as 2 weeks post implantation (Figure 9D). By 1 month, many small vessels were present throughout the inner portion of the scaffolds. At later time points, vascular in-growth decreased, particularly in the center of the implants. Host cell migration, consisting of fibroblasts, endothelial cells and inflammatory cells, into kerateine scaffolds could be seen as early as 3 days following implantation (data not shown), with cells migrating to the center of the scaffold by day 7 (Figure 9A). Cell infiltration was high during the first 4 weeks then gradually dropped off. Cell density throughout the scaffolds peaked at 1 month. By 6 months, only a few cells could be seen within the middle portion of the disks. Foreign body giant cells, a classic sign of a chronic inflammatory response, were absent at all time points indicating that kerateine biomaterials are highly tissue compatible. Masson's trichrome staining showed an increase in collagen deposition as cell infiltration increased. Collagen deposition was highest at 1 month and appeared to stabilize at later time points.

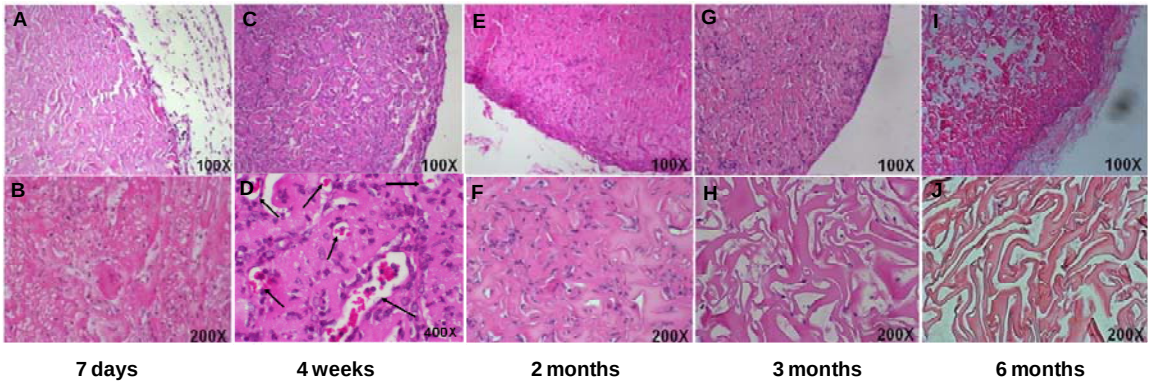

Figure 9. Hematoxylin & Eosin (H&E) staining of kerateine biomaterial implants. At 7 days, host inflammatory cells have begun to infiltrate the scaffold from the surrounding tissue. By 1 month, host cells have migrated to the middle of the scaffold and there is formation of supporting vasculature. By 2 months, there is a high density of cells homogenously dispersed throughout the scaffold. At 3 months, the cell density within the scaffold has started to decrease and by 6 months, the scaffold appears to be more degraded with relatively few cells scattered throughout.

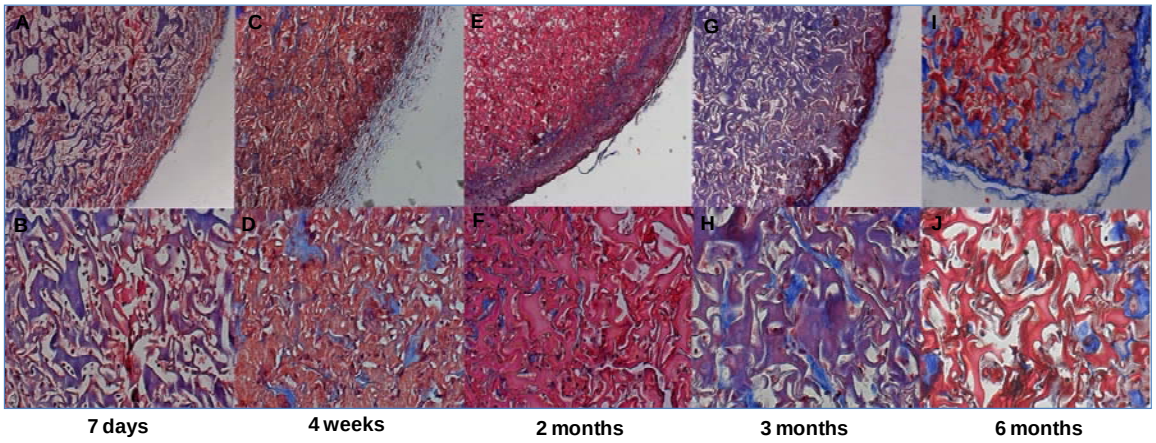

Figure 10. Masson's Trichrome staining of kerateine biomaterials implants for collagen deposition. No fibrotic capsule was present around the implants at any time point. Collagen deposition within the scaffold was high by 4 weeks but and did not appear to increase considerably over time.

DISCUSSION

The first study using a keratin biomaterial was published in 1982. Noishiki and colleagues coated a heparinized keratin derivative onto a polymer stent and implanted it into a dog for more than 200 days without thrombosis (28). It was logical to assume that keratins would be biocompatible, though no studies had been published at that time describing a systematic analysis of biocompatibility. Much of the keratin literature was not focused on the basic science, but on potential medical applications. However, a few isolated studies have consistently shown good cell compatibility despite the many differences in keratin source, extraction, processing methods, fabrication of keratin derivatives, and assay protocols.

Using the method of O'Donnell and Thompson for the production of kerateines (13), and the method of Thompson and O'Donnell for the production of keratoses, (31). Ito et al. generated samples from sheep wool and determined isoelectric point, amino acid composition, and biological responses to keratin-coated materials implanted into animal models (32). Polyester meshes were coated with keratin and implanted into the dorsal muscle of rabbits and dogs. Polyester filaments were also coated and implanted into the femoral and jugular veins of dogs. Results showed what the authors characterized as a "mild" foreign body response to the intra-muscular implantation with no foreign body giant cells at 2, 4, and 6 weeks in both models using either type of keratin coating. Implantation into the vasculature showed little to no thrombus formation at 2 hours or 2 weeks, respectively, in the keratose-treated group, while a kerateine derivative showed mild thrombus at 2 hours and none at 2 weeks.

In another study of the general biocompatibility of keratins, the physical, chemical, and biological properties of an *s*-aminoethylkeratin derivative made from extracted rat hair was investigated (33). The authors processed the keratin into films and performed standard cell assays with fibroblasts and keratinocytes, as well as immunogenicity studies in rabbits. Cells (species not specified) were tested in direct and indirect contact modes and quantified using an MTT assay. Results showed no cytotoxicity at 5 mg/mL of keratin film and slight toxicity at 20 mg/mL in direct contact with fibroblasts after three days of incubation. In the indirect contact experiment, keratin films were washed in water for three weeks at 37°C to remove processing chemicals, incubated for 48 hours in sterile water at 37°C at 50 mg/mL, and the water used to prepare media. After incubation with fibroblasts for 48 hours, no evidence of cytotoxicity was observed. Keratinocytes were also seeded onto keratin films and showed delayed proliferation, but eventually caught up to the control (cells grown on tissue culture plastic) after a few days. For the immunogenicity study, keratin films were implanted into rabbits. The films degraded after two weeks and elicited what the authors characterized as a "weak immunological reaction" (i.e. serum was positive at a 1/10 dilution but not at higher dilutions) which they considered normal for a rat protein implanted in a rabbit model.

Many scientists have assessed general cell compatibility by investigating the attachment and growth of cells on keratin biomaterials. Keratin-chitosan films (34), compression molded keratin films (35), keratin-hydroxyapatite sponges (36), modified keratin sponges containing growth factors (37), pure keratin scaffolds (38), and keratin-coated hydroxyapatite (39) have all been investigated. Cell types in these studies have included NIH 3T3 fibroblasts, L929

fibroblasts, MC3T3-E1 pre-osteoblasts, and human fetal osteoblasts. In general, all have shown good attachment and growth of cells on keratin substrates compared to standard controls such as tissue culture plastic or other biomaterials such as collagen. Presently there are no reports in the literature of cells that do not grow well on keratin substrates, although only a limited number have been tested.

In the present study we obtained soluble keratins from human hair that was collected from a local salon. Dialyzed protein samples showed characteristic bands in the SDS-PAGE for alpha- and gamma-keratins and good agreement with published values for amino acid composition (15). General cell compatibility of these samples was demonstrated by marked cell adhesion and proliferation. This was likely due to the amino acid binding motifs expressed by keratins that are specific to the integrin receptors on many cell types. Tachibana et al. were the first to make this observation in a study that demonstrated excellent cell attachment to keratin scaffolds (40).

Structural analysis by SEM showed a highly porous architecture with pore sizes that are conducive to cell infiltration as demonstrated by implantation experiments. These interconnected, microporous structures likely form spontaneously due to the intrinsic ability of keratins to self-assemble (41,42). Subcutaneous implantation of similar scaffolds showed gradual degradation over a 6 month period in vivo, which was in general agreement with our in vitro degradation curve. Subcutaneous implant studies published by other investigators demonstrated faster degradation rates (35), but these keratin biomaterials were not disulfide

crosslinked as was the case in our experiments. Our crosslinking method results in keratins that are degraded slowly by hydrolysis rather than enzymatic activity. Robust host cell infiltration was observed within the entire thickness of the 6mm x 4mm implants at 1 and 4 weeks, thus confirming the interconnectivity observed in SEM analysis, with substantially reduced cell numbers at 2 to 6 months. Interestingly, the infiltrating cells did not mediate a foreign body response that is prevalent with most biomaterials, particularly synthetics (43). This process typically ensues after coating of the biomaterial with serum proteins. It may not occur with keratin biomaterials to any appreciable level due to their highly hydrated state. The keratin implants used in this study also did not become encapsulated, another typical response to biomaterial implants, or filled with cell-secreted collagen, even after 6 months.

Overall our study demonstrates some general properties of keratin biomaterials and supports their use as biomaterials. As the number of different cells, tissues, and medical applications that make use of keratin biomaterials widens, the intrinsic compatibility of this novel class of compounds will provide investigators with an excellent platform for many medical applications. As the interactions of keratin biomaterials with specific cell and tissue types become more completely elucidated, enhanced performance may be possible.

ACKNOWLEDGEMENTS

The authors gratefully acknowledge the funding support provided by the Errett Fisher Foundation and the US Army. The authors would also like to thank Jacquie Burnell for assistance with Masson's trichrome staining.

REFERENCES

1. Jones CM, Lyons KM, and Hogan BLM. Involvement of bone morphogenetic protein-4 (BMP-4) and Vgr-1 in morphogenesis and neurogenesis in the mouse. Development 1991;111:531-42

2. Lyons KM, Pelton RW, and Hogan BLM. Organogenesis and pattern formation in the mouse: RNA distribution patterns suggest a role for bone morphogenetic protein-2A (BMP-2A). Development 1990;109:833-44

3. Blessings M, Nanney LB, King, LE, Jones CM, and Hogan BLM. Transgenic mice as a model to study the role of TGF-ß related molecules in hair follicles. Genes and Develop 1993;7:204-15.

4. Hardy MH. The secret life of the hair follicle. Trends Genet 1992;8(2):55-61

5. Stenn KS, Prouty M, and Seiberg. Molecules of the cycling hair follicle – a tabulated review. J Dermato Sci 1994;7S:S109-24

6. Rogers GE. Hair follicle differentiation and regulation. Int J Dev Biol 2004;48(2-3):163-70.

7. Panteleyev AA, Jahoda CAB, and Christiano AM. Hair follicle predetermination., J Cell Sci 2001;114:3419-31

8. Breinl F and Baudisch O. The oxidative breaking up of keratin through treatment with hydrogen peroxide 1907. Z physiol Chem;52:158-69

9. Earland C and Knight CS. Structure of keratin II: Amino acid content of fractions isolated from oxidized wool. Biochem et Biophys Acta 1956;22:405-11

10. Buchanan JH. A cystine-rich protein fraction from oxidized alpha-keratin. Biochem J 1977;167(2):489-91

11. Goddard DR and Michaelis L. A study on keratin. J Biol Chem 1934;106:605-14

12. MacLaren JA. The extent of reduction of wool proteins by thiols. Australian J Chem 1962;15:824-31

13. O'Donnell IJ, Thompson EOP. Studies on reduced wool IV: The isolation of a major component. Aust J Biol Sci 1964;17:973–89

14. Crewther WG, Fraser RDB, Lennox FG, and Lindley H. in The chemistry of keratins. Anfinsen CB Jr., Anson ML, Edsall JT, Richards FM (editors). Advances in protein chemistry. Academic Press, New York. pp 191-346 (1965)

15. Anker CA. Method of preparing keratin-containing films and coatings. US pat no 3642498. February 15, 1972

16. Kawano Y and Okamoto S. Film and gel of keratins. Kagaku To Seibutsu 1975;13(5):291-2

17. Okamoto S. Formation of films from some proteins. Nippon Shokuhin Kogyo Gakkaishi 1977;24(1):40-50

18. Noishiki Y, Ito H, Miyamoto T, and Inagaki H. Application of denatured wool keratin derivatives to an antithrombogenic biomaterial: Vascular graft coated with a heparinized keratin derivative. Kobunshi Ronbunshu 1982;39(4):221-7

19. Rothman J, Band P, and Oceta J. Wound healing promoting compositions containing film-forming proteins. PCT pat no 9102538. March 7, 1991

20. Van Dyke ME, Nanney LB. Elastomeric biomaterials from human hair keratins as bioactive wound dressings. Abst Papers Amer Chem Soc 2002;224(1):U36

21. Widra A. Alpha-keratose as a blood plasma expander and use thereof. US pat no 6746836. June 8, 2004

22. Tachibana A, Kaneko S, Tanabe T, Yamauchi K. Rapid fabrication of keratin-hydroxyapatite hybrid sponges toward osteoblast cultivation and differentiation. Biomaterials 2005;26(3):297-302

23. Aboushwareb T, Eberli D, Ward C, Broda C, Holcomb J, Atala A, Van Dyke M. A keratin biomaterial gel hemostat derived from human hair: Evaluation in a rabbit model of lethal liver injury. J Biomed Mat Res (in press)

24. Sierpinski P, Garrett J, Ma J, Apel P, Klorig D, Smith T, Koman LA, Atala A, Van Dyke M. The use of keratin biomaterials derived from human hair for the promotion of rapid regeneration of peripheral nerves. Biomaterials 2008;29(1):118-28

25. Apel PJ, Garrett JP, Sierpinski P, Ma J, Atala A, Smith TL, Koman LA, Van Dyke M. Peripheral nerve regeneration using a keratin-based scaffold: Long-term functional and histological outcomes in a mouse model. J Hand Surg 2008;33(9):1541-7
26. Bennett HP, Solomon S. Use of Pico-Tag methodology in the chemical analysis of peptides with carboxyl-terminal amides. J Chromatogr 1986;359:221-30

27. Mies HH, Zahn H. Chromatographic and electrophoretic investigations of the properties of unprotected low-sulphur wool kerateins. J Chromatogr 1987;405:365-70

28. Crewther WG, Fraser RDB, Lennox FG, Lindley H. The chemistry of keratins. Anfinsen CB Jr., Anson ML, Edsall JT, and Richards FM (editors). Advances in protein chemistry. New York: Academic Press;1965: 191-346

29. Aluigi A, Zoccola M, Vineis C, Tonin C, Ferrero F, Canetti M. Study on the structure and properties of wool keratin regenerated from formic acid. Int J Biol Macromol 2007;41(3):266-73

30. Simmonds DH. The Amino Acid Composition of Keratins: Part V: A Comparison of the Chemical Composition of Merino Wools of Differing Crimp with that of Other Animal Fibers. Textile Res J 1958;28:314

31. Thompson EOP, O'Donnel IJ. Studies on oxidized wool I: A comparison of the completeness of oxidation with peracetic and performic acids. Aust J Biol Sci 1959;12(3):282-93

32. Ito H, Miyamoto T, Inagaki H, Noishiki Y. Biocompatibility of denatured wool keratin. Kobunshi Ronbunshu 1982;39(4):249-56

33. Valherie I and Gagnieu C. Chemical modifications of keratins: Preparation of biomaterials and study of their physical, physiochemical and biological properties. Doctoral thesis. Inst Natl Sci Appl Lyon, France 1992

34. Tanabe T, Okitsu N, Tachibana A, Yamauchi. Preparation and characterization of keratin-chitosan composite film. Biomaterials 2002;23(3):817-25

35. Katoh K, Shibayama M, Tanabe T, Yamauchi K. Preparation and physiochemical properties of compression-molded keratin films. Biomaterials 2004;25(12):2265-72

36. Tachibana A, Kaneko S, Tanabe T, Yamauchi K. Rapid fabrication of keratin-hydroxyapatite hybrid sponges toward osteoblast cultivation and differentiation. Biomaterials 2005;26(3):297-302

37. Tachibana A, Nishikawa Y, Nishino M, Kaneko S, Tanabe T, Yamauchi K. Modified keratin sponge: Binding of bone morphogenetic protein-2 and osteoblast differentiation. J Biosci Bioeng 2006;102(5):425-9

38. Verma V, Verma P, Ray P, Ray AR. Preparation of scaffolds from human hair proteins for tissue-engineering applications. Biomed Mater 2008;3(2):25007 (Epub April 15, 2008)

39. Belcarz A, Ginalska G, Zalewska J, Rzenski W, Slosarczyk A, Kowalczuk D, Godlweski P, Niedzwiadek J. Covalent coating of hydroxyapatite by keratin stabilizes gentamicin release. J Biomed Mat Res B: Appl Biomat 2009;89(1):102-13

40. Tachibana A, Furuta Y, Takeshima H, Tanabe T, Yamauchi K. Fabrication of wool keratin sponge scaffolds for long-term cell cultivation. J Biotech 2002;93(2):165-70

41. Thomas H, Conrads A, Phan KH, van de Löcht M, and Zahn H. In vitro reconstitution of wool intermediate filaments. Int J Biol Macromol 1986;8:258-64

42. van de Löcht M. Reconstitution of microfibrils from wool and filaments from epidermis proteins. Melliand Textilberichte 1987;10:780-6

43. Anderson JM, Rodriguez A, Chang DT. Foreign body reaction to biomaterials. Semin Immunol 2008;20(2):86-100

CHAPTER V

THE USE OF KERATIN BIOMATERIALS DERIVED FROM HUMAN HAIR FOR THE PROMOTION OF RAPID REGENERATION OF PERIPHERAL NERVES

Paulina Sierpinski[1], Jeffrey Garrett[2], Jianjun Ma[2], Peter J. Apel[2], Klorig David[1], Tom Smith, L. Andrew Koman[2], Anthony Atala[1], and Mark Van Dyke[1]

[1] Wake Forest Institute for Regenerative Medicine

[2] Department of Orthopaedic Surgery

Wake Forest University School of Medicine, Winston Salem, NC, 27157

This manuscript was published in Biomaterials 29: 118-128 (2008), and is reprinted with permission. Stylistic variations are due to the requirements of the journal. Paulina Sierpinski prepared the manuscript. Mark Van Dyke acted in an advisory and editorial capacity.

Abstract

The management of trauma-associated nerve defects is difficult because of the absence of autologous donor motor or sensory nerves. Pre-clinical development and clinical experience has shown that damaged nerves can be surgically repaired using a tubular conduit interposed across the defect. Acceptable patient outcomes are achieved so long as the gap distance does not exceed a few centimeters. Although research in animals has demonstrated that nerve repair can be facilitated across slightly larger gaps by introducing a biomaterial filler into the conduit lumen, these biomaterials are not typically "neuroinductive" (i.e. capable of acting directly on regenerative cells to enhance nerve tissue formation beyond clinical limits). Moreover, their use does not often result in functional recovery equivalent to nerve autograft, the clinical gold standard. Here we show that a biomaterial gel made from the proteins found in human hair can mediate a robust nerve regeneration response, in part through activation of Schwann cells. In vitro, keratins extracted from human hair enhance the activity of Schwann cells by a chemotactic mechanism, increase their attachment and proliferation, and up-regulate expression of important genes. Moreover, these characteristics translate to improved functional nerve recovery in an animal model. These results suggest that a biomaterial derived from human hair keratins is neuroinductive and can facilitate an outcome comparable to autograft in a nerve injury model.

Introduction

The surgical management of nerve defects or gaps greater than 2 cm is a significant clinical challenge. Options include mobilization, nerve or joint positioning, end-to-end repair, autologous grafts, and tubular conduits. Many investigators have demonstrated that peripheral nerve regeneration through a conduit can be improved with a biomaterial filler. Included among these fillers are extracellular matrix (ECM) proteins such as collagen, fibrin, and laminin, some naturally occurring polysaccharides such as alginate, chitosan and hyaluronic acid, and synthetic polymers [1]. Most of these biomaterials interact with invading cells by providing structural support. An optimal luminal filler provides a provisional matrix that is cell instructive, providing cues to help guide functional tissue regeneration.

The hair follicle is a remarkably proliferative organelle that exemplifies a highly orchestrated regenerative process. Hair morphogenesis is characterized by the recruitment of local stem cells, rapid proliferation, terminal differentiation, and cellular and matrix self-assembly [2]. It is a highly orchestrated process controlled by more than 30 growth factors, cytokines, and other signaling molecules as the cyclical phases of hair formation are continuously turned on and off [3] and [4]. Expression of these factors, as well as other matrix and adhesion molecules, results in a hair fiber that is rich in regulatory molecules [5] and [6]. Many of these same materials are essential in the numerous regenerative processes that maintain normal function in a variety of organs and tissues. Moreover, these same regulatory compounds

play important roles in the regeneration of almost every tissue after injury [7], including nerve tissue [8] and [9].

After extrusion through the skin, the hair fiber is formed into a highly stable and robust structural tissue that is relatively impervious to environmental insult. In a system that is intriguingly similar to synthetic polymers, hair fibers contain structural macromolecules, crosslinkers, plasticizers, and UV stabilizers. The hair fiber represents a stable materials-based system capable of protecting the regulatory molecules contained within it. The useful contents of a hair fiber can be extracted using established chemical methods that break down the constituent matrix proteins known as keratins. Numerous methods have been developed to chemically cleave the disulfide crosslinks found in wool keratin and solubilize the entire cortex [10]. These methods have been applied to both wool and human hair fibers, resulting in the development of keratin-based biomaterials [11], [12], [13] and [14].

Human hair keratins are a family of proteins that can be classified into three broad groups: alpha-, beta-, and gamma-keratins. The alpha-keratins are the main structural component and are the most abundant in human hair. They have an alpha-helical tertiary structure, are low in sulfur content, and have an average molar mass in the range of 60–80 KDa. The beta-keratins are primarily protective and form the majority of the cuticle. Beta-keratins are difficult to extract and do not form especially useful reconstituted structures. Gamma-keratins are globular, higher in sulfur content, and lower in molecular weight (approximately 15 KDa) than the other types of keratin. They function as a disulfide crosslinker, holding the

cortical superstructure together (Fig. 1). Soluble keratins are removed from this structure by breaking down the disulfide crosslinks prevalent in keratinous tissues. The cuticle is opened, although not dissolved, by an initial oxidation step. As the oxidant permeates the cortex of the fiber, gamma- and alpha-keratins are converted to their non-crosslinked, soluble form and can be extracted with denaturing solvents to produce a solution of keratins that can be purified by filtration and dialysis.

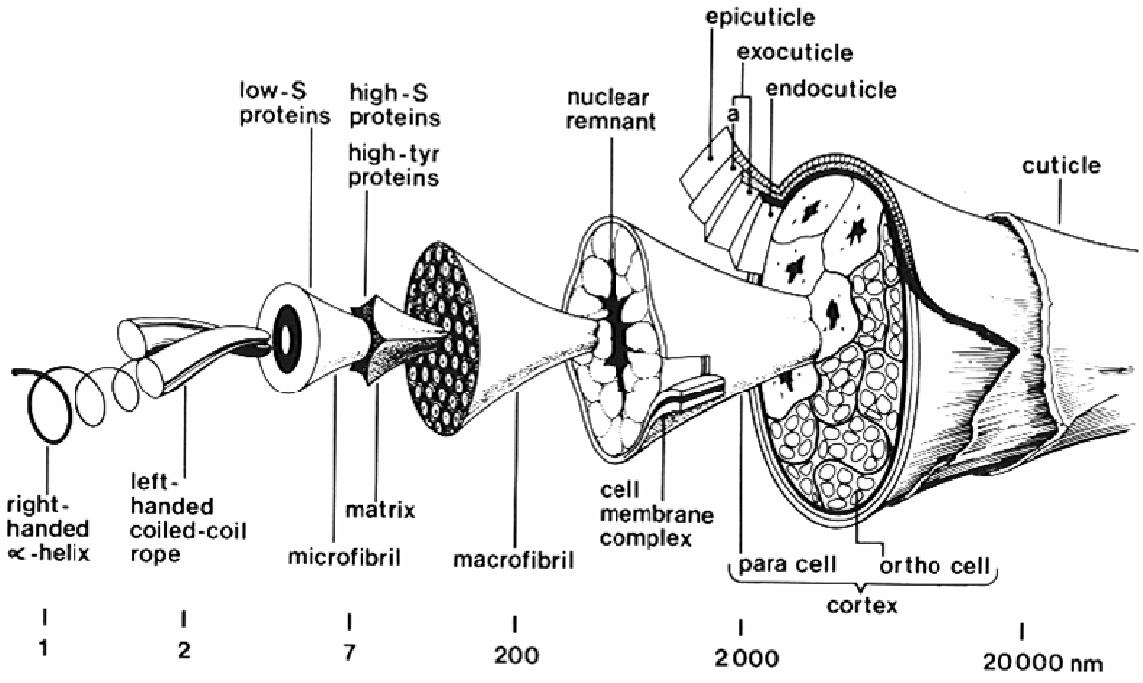

Figure 1. Schematic of a wool fiber. Human hair has a similar superstructure but varies in the ratio of alpha- to gamma-keratin (human hair is higher at about 80% alpha- and 20% gamma keratin). Alpha-keratin is composed of the right-handed, alpha-helical proteins that make up the low-sulfur proteins and have a molecular weight of approximately 60–85 KDa. Gamma-keratin is globular in nature and forms the matrix that holds the microfibrils together. It is high in sulfur proteins and therefore, it is more highly crosslinked. However, it is of lower molecular weight than alpha, at approximately 15 KDa. Oxidative chemistry can be used to break this structure down and extract both types of keratins from hair fiber.

In the present study a chemical process is applied to oxidize the keratin crosslinks within human hair fibers, extract the cortical contents, and used this keratin-based material to form hydrogels. Based on the premise that this keratin biomaterial contains minute amounts of molecules that regulate cell behavior, and larger amounts of matrix proteins that control self-assembly, cell attachment and migration, we tested its biological activity on cellular function by investigating the migration, proliferation, and gene expression of Schwann cells in the presence of keratin solutions, as well as the attachment of these cells to a keratin substrate. Moreover, the ability of a keratin gel filler to serve as a neuroinductive provisional matrix and mediate improved functional recovery compared to sensory nerve autograft in an animal model of peripheral nerve injury was investigated.

2. Materials and methods

2.1. Preparation of keratin biomaterial

Human hair was obtained from a local barber, chopped into small fibers and treated with a 2 wt%/vol% solution of peracetic acid (Sigma-Aldrich, St. Louis, MO) in deionized (DI) water for 12 h. The hair was removed from the liquid by passing the solution through a 500 μm sieve (W.S. Tyler, Mentor, OH) and rinsed thoroughly to remove residual oxidant. Free proteins were extracted into excess 100 mm Tris base for 1 h, followed by DI water for 1 h. All extractions were carried out on a shaker (Barnstead/Lab-line Max Q 4000, Artisian Scientific,

Champaign, IL) at 37 °C and 180 rpm. Extracts were retained by passage through a 500 μm sieve to remove the hair fibers, neutralized, centrifuged (Sorvall Evolution RC, Thermo Electron, Asheville, NC), and filtered. Extracts were combined, purified for 24 h by dialysis, and concentrated and isolated by lyophilization (Freeze-Dry Systems, Labconco, Kansas City, MO).

2.2. Structural analysis of keratin biomaterial hydrogel

A keratin hydrogel was formed by re-hydration of the lyophilized material with PBS at a 15 wt%/vol% concentration. The gel was sterilized by γ-irradiation (800 krad) using a ^{60}Co source. The hydrogel was lyophilized, mounted on stubs with colloidal graphite and examined using a Hitachi S-2600N variable pressure scanning electron microscope (SEM, Hitachi High Technologies Corp., Schaumburg, IL).

2.3. Cell culture

A rat Schwannoma cell line, RT4-D6P2T, was obtained from the American Type Culture Collection (ATCC, Manassas, VA) and cultured as previously described [15]. Low passage RT4-D6P2T cells were used for all *in vitro* assays.

2.4. In vitro cell proliferation

The ability of keratin to induce Schwann cell proliferation was assessed using an MTS assay [16]. Cells were plated on a 48-well tissue culture plate, grown to 50% confluency and

serum starved for 24 h. Lyophilized keratin powder was dissolved in media with fetal bovine serum (FBS, Invitrogen Corp., Carlsbad, CA) at concentrations of ranging from 10 mg/mL to 1 ng/mL and sterile filtered. Cultures were exposed to keratin-containing media solutions until they reached 90% confluency and assayed. Absorbance readings were taken using an ELX-500 UV plate reader (Bio-Tek, Winooski, VT) to determine relative cell numbers.

2.5. Migration

A modified Boyden chamber (Chemicon® QCM™ Chemotaxis Assay, Chemicon International Inc., Temecula, CA) was used to asses the chemotactic properties of keratin on Schwann cells. Cells were cultured to 80% confluency and serum starved in FBS-free media for 24 h. Cells were seeded on an 8-μm pore trans-well membrane at a density of 1.2×10^6 cells/mL. Solutions of keratin dissolved in media were placed at the bottom of each well at concentrations ranging from 10 mg/mL to 10 ng/mL. Cells were incubated for 24 h, during which stimulated cells migrated through the porous membrane and attached to the other side. Cells were detached from the bottom of the membrane only, lysed and fluorescently labeled according to the manufacturer's instructions. A fluorescent autoplate reader was used to obtain readings (FLx800, BioTek, Winooski, VT).

2.6. Adhesion

Schwann cell adhesion to keratin biomaterials was examined using a parallel flow chamber apparatus (Glycotech, Gaithersburg, MD). Glass slides were coated overnight with

either keratin (100 μg/mL), fibronectin (5 μg/mL), or left uncoated. Cells were seeded onto pre-coated slides, placed into a flow chamber, and subjected to flow-induced shear stress of 10 dyn/cm^2. Phase-contrast images were taken using a Zeiss Axiovert 100 microscope (Carl Zeiss, Thornwood, NY) and the percentage of adherent cells remaining over time was quantified using digital image analysis software (SigmaScan Pro 5.0, Systat, San Jose, CA).

2.7. Gene expression

The ability of keratin to induce expression of specific genes in Schwann cells was examined using quantitative reverse transcription polymerase chain reaction (qRT-PCR). Cells were cultured for 72 h in media without FBS (control group for solutions), or keratin dissolved in media (without FBS) at 1 mg/mL, 10 μg/mL, and 100 ng/mL. Total RNA was extracted from cell cultures using RNeasy spin columns (Qiagen, Hilden, Germany) according to the manufacturer's instructions. Extracted RNA was quantified using RiboGreen (Molecular Probes, Eugene, OR) and reverse-transcribed into cDNA using oligo(dT) primers and SuperScript II (Invitrogen). The QuantiTect SYBR Green RT-PCR kit (Qiagen) was used with 50 ng of RNA per sample. Reactions were run on the Applied Biosystems ABI 7300 Real-time PCR System (Applied Biosystems, Foster City, CA). Relative expression of the genes of interest was determined following normalization to the level of a housekeeping gene, GAPDH, and untreated controls according to the method of Livak and Schmittgen [17].

2.8. Animal model and surgical procedure

All animal procedures were conducted under a protocol approved by the Wake Forest University Animal Care and Use Committee. Adult male Swiss Webster mice were randomly placed into one of three groups: Empty conduit (n=10), keratin-filled conduit (n=5), or autograft (n=8). The tibial nerve was exposed under anesthesia and transected 5 mm proximal to its insertion into the gastrocnemius muscle. A 4 mm defect was generated and repaired under a double-headed operating microscope (Superlux 40; Carl Zeiss, Oberkochen, Germany) by securing the proximal and distal nerve ends inside Silastic® tubing (Dow Corning, MI, USA) using 9-0 non-absorbable nylon microsutures (Surgical Specialties, Reading, PA). In the keratin group, a pre-sterilized keratin gel was injected into the conduit upon fixation. In the autograft group, the sural nerve was harvested and a 4 mm three-cable interpositional graft was used to bridge the defect.

2.9. Functional testing (electrophysiology and muscle force generation)

At 6 weeks following nerve injury and repair, each animal underwent functional testing of the tibial nerve. A Nicolet Viking Ile electrodiagnostic system (Nicolet Instrument Corp, Madison, WI) was used to test nerve latency and action potential amplitude. A bipolar stimulating electrode was placed on the exposed tibial nerve 5 mm proximal to the defect and a recording electrode placed on the gastrocnemius muscle belly. The nerve was stimulated with a constant current (1.0 mAmp) for a duration of 0.1 ms.

For muscle force measurements, the limb was immobilized by driving K-wires through the femur and tibia. The Achilles tendon/gastrocnemius complex was isolated and a wire suture tied around the distal end of the Achilles tendon. The tendon was transected and the suture was attached to a force transducer (FT03 Grass, Quincy, MA) connected to an amplifier (Model 13-G4615-50, Gould, Cleveland, OH). The tibial nerve was stimulated 4 mm proximal to the conduit (Grass SD9 stimulator, Quincy, MA) with increasing voltage until the maximum isometric single twitch force was obtained. The frequency of stimulation at this voltage was increased until maximum tetanic contractile force was generated. Responses were recorded using a calibrated recording oscillograph (RS 3800, Cleveland, OH) connected to the force transducer.

2.10. Nerve harvest and histology

Following testing, the tibial nerve was harvested and fixed in 4% paraformaldehyde, washed with PBS and post-fixed in 1% osmium tetroxide. The nerve segments were dehydrated in increasing concentrations of ethanol and embedded using epoxy resin (Polysciences Inc., Warrington, PA). Semi-thin sections (1 μm) were cut using an LKB III Ultramicrotome (LKB-Produkter A.B., Broma, Sweden), stained with 1% toluidine blue and mounted on slides for analysis by light microscopy. Nerves were qualitatively assessed for the preservation of nerve architecture, quality and quantity of regenerated nerve fibers and extent of myelination.

2.11. Histomorphometry

Nerve area, axon density, axon size, and degree of vascularization were quantified from digital images using SigmaScan Pro 5.0. To determine the total nerve area, a low magnification image (100×) which encompassed the entire regenerated nerve area was used. The circumference of the nerve was outlined and the resulting area determined by Sigma Scan. Axon density was determined by randomly sampling four regions of the nerve at 200×, manually counting the number of axons in a given region and extrapolating to the entire nerve area. The average axon diameter was determined by randomly sampling an area of the nerve at 1000× and measuring a minimum of 50 axon diameters. The same process was used to determine the number and size of blood vessels within the regenerated nerve.

2.12. Statistical analysis

All graphical data are presented as means plus or minus standard error of the mean (SEM). Sigma Stat 3.1 software was used for all statistical analysis. A one-way analysis of variance (ANOVA) was used to determine differences between treatment groups in the proliferation and migration assays, as well as in all *in vivo* regeneration experiments. A two-way ANOVA was used to determine difference between treatment groups in the RT-PCR assays. A two-way repeated measures ANOVA was used to determine difference between treatment groups in the adhesion assay. Significant differences were established at $p<0.05$ with Tukey's *post hoc* method using the Studentized range statistic. Kruskal–Wallis ANOVA on ranks was performed on non-parametric data.

3. Results

3.1. Keratin hydrogels with interconnected pores

Keratins derived from wool fibers have been shown to have an intrinsic capacity for molecular self-assembly [18] and [19]. The microstructural architecture of the biomaterial hydrogels was investigated by SEM and found to have formed fibrous networks upon drying with morphologies ranging from ribbon-like to highly fibrous. Fiber diameters were on the order of 2–20 μm and pore sizes ranged from 20 to 50μm. Interconnectivity of the pores—an important consideration for cellular infiltration during tissue regeneration through the hydrogel—was evident from cross-sectional micrographs (Fig. 2).

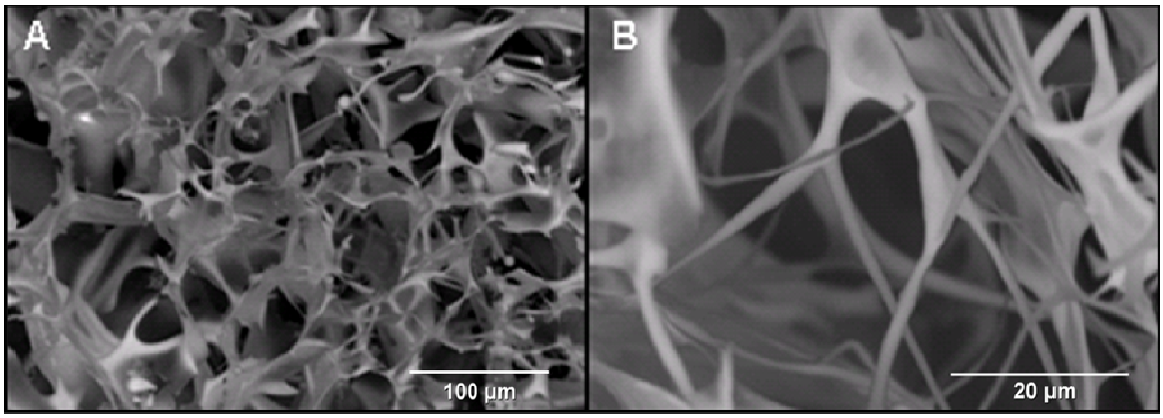

Figure 2. SEM of two different keratin hydrogels at 300× (A) and 2000× (B). These architectures were formed by a process of self-assembly wherein the keratin proteins arrange themselves into a porous, fibrous network.

3.2. Enhancement of Schwann cell function

Increasing the number of regenerative cells through enhanced proliferation improves functional healing in large tissue injuries. The ability of keratin to induce cell multiplication was tested with RT4-D6P2T Schwann cells using the MTS assay, a method that correlates metabolic reduction of a tetrazolium salt to cell number [20]. The cell line used in this assay has been shown to be similar to primary cultures of Schwann cells in previous studies [21]. Dilutions of keratin in basal media were added to cell cultures and incubated for 24 h. The growth response of the cells was measured and compared to basal media containing FBS as the positive control (Fig. 3). The proliferation data shows a normal distribution of dose response with inhibition at the highest dose tested (10 mg/mL). This is not unexpected because normal hair follicle cycling is controlled by both stimulatory and inhibitory molecules. At higher concentrations of keratin, it is reasonable to assume that inhibitory factors may dominate. When the keratin concentrations were reduced, even as low as 10 ng/mL, results showed statistically significant ($p<0.05$, $n=6$) increases in cell growth over media containing serum.

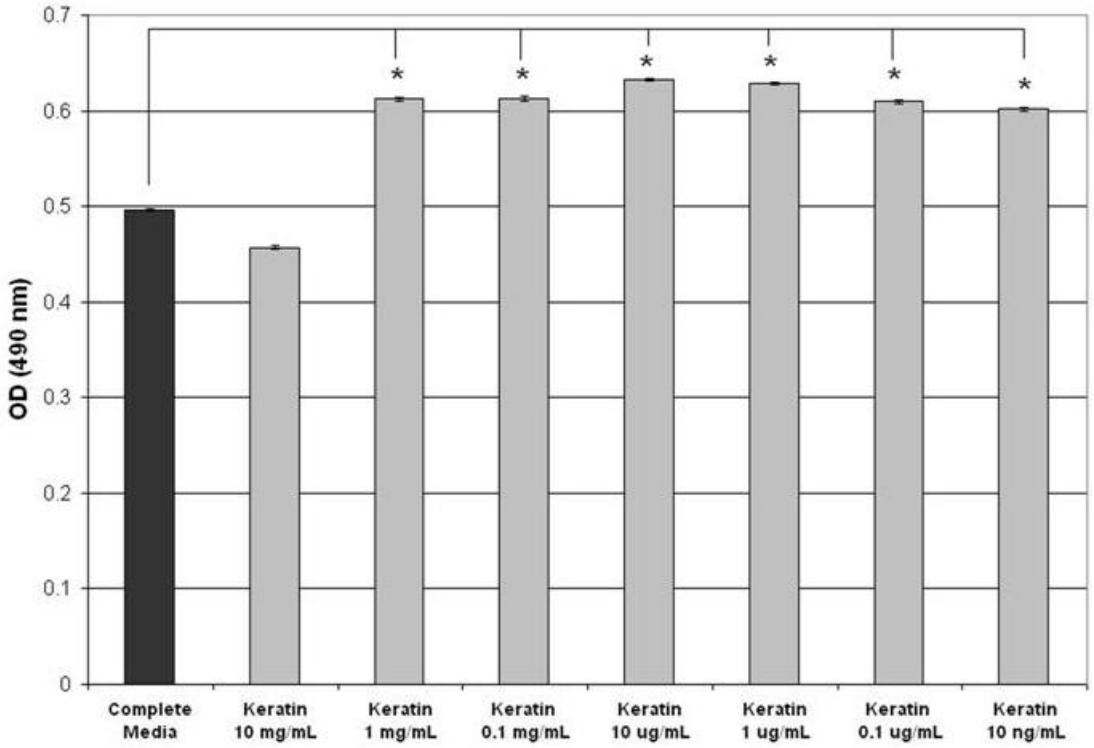

Figure 3. Assessment of *in vitro* keratin cytocompatibility with RT4-D6P2T Schwann cells by an MTS assay. Cells cultured in the presence of keratin dissolved in media showed significantly higher rates of proliferation at concentrations ranging from 10 mg/mL to 10 ng/mL in comparison to serum-containing media ($p<0.05$, $n=6$).

Enhancing the migration of regenerative cells into the site of injured tissue is essential for functional healing. Functional repair of tissues is often size limited, due primarily to the inability of regenerative cells to migrate over long distances. In the case of nerve regeneration, infiltrating Schwann cells are driven by chemotactic mechanisms to migrate into the damaged nerve's provisional matrix and initiate the repair process. Materials that have chemotactic properties can be tested using the modified Boyden method [22]. RT4-D6P2T Schwann cells were used to investigate this phenomenon in the presence of several dilutions of keratin in basal

media. Media with and without serum served as positive and negative controls, respectively. Media with serum plus nerve growth factor (NGF, 50 ng/mL), a known chemotactic agent for Schwann cells, was also included for comparison. Keratin enhanced Schwann cell migration at 1 and 0.1 mg/mL significantly ($p<0.05$, $n=8$) better than basal media alone (Fig. 4).

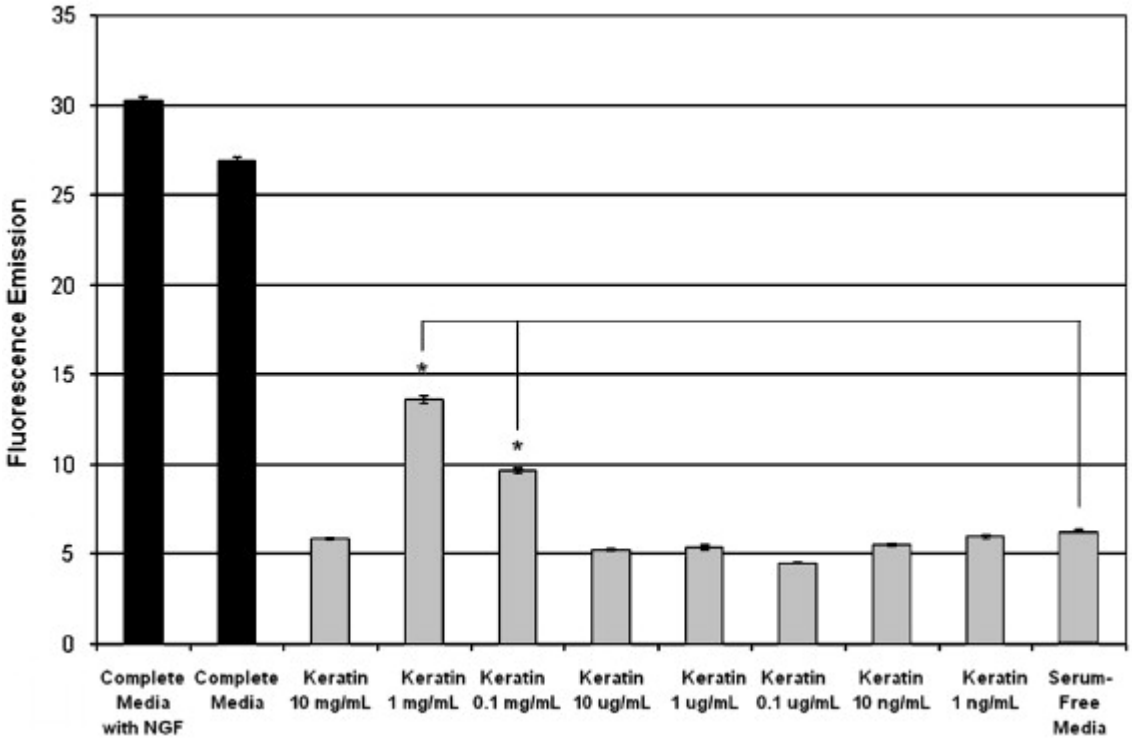

Figure 4. *In vitro* migration of Schwann cells in response to keratin in a modified Boyden chamber. Keratin in serum-free media is chemotactic for Schwann cells at 1 and 0.1 mg/mL concentrations compared to serum-free media alone ($p<0.05$, $n=8$).

One of the main purposes of using a biomaterial in tissue regeneration is to provide a surrogate ECM for cells to attach and grow. Specific interactions to ECM binding sites through cell receptors are important in maintaining proper cell function [23], [24], [25] and [26]. Cells

attach to the ECM through more than 20 known integrin receptors, more than half of which bind to the arginine–glycine–aspartic acid (RGD) peptide motif [26]. Inspection of the more than 70 known human hair keratin protein sequences reveals that 78% contain at least one binding domain specific to the integrins expressed on many cell types, and 23% contain two or more such domains [27].

Schwann cell adhesion to a keratin matrix was assessed *in vitro*. Keratin was coated onto glass microscope slides and RT4-D6P2T Schwann cells were cultured on this substrate. Uncoated slides served as a negative control. After allowing time for attachment, the slides were placed into a specially designed flow chamber that exposed the cells to a high shear environment. Light microscopy was used to monitor the number of cells remaining attached under constant shear at increasing time intervals. More than 80% of cells remained attached to the keratin substrate while less than 60% maintained adhesion to fibronectin, a common matrix molecule containing RGD binding domains and previously shown to promote Schwann cell adhesion [28]. Only 30% of cells remained attached to the uncoated slides (Fig. 5). The results showed that a keratin substrate significantly ($p<0.05$) improves Schwann cell adhesion over both untreated and fibronectin-coated slides.

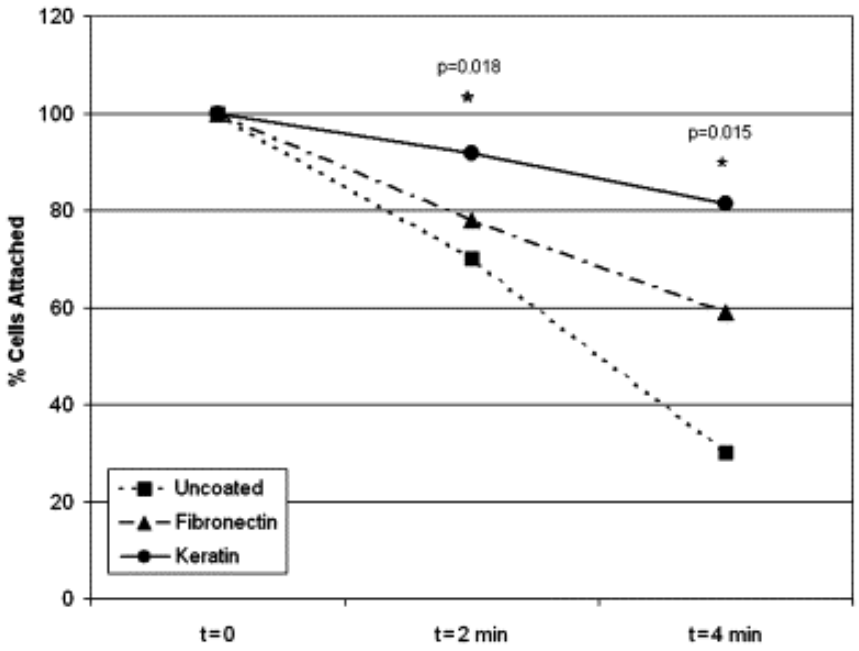

Figure 5. Biomaterial coated slides seeded with Schwann cells were placed into a chamber system and exposed to a constant flow rate (10 dyn/cm^2) at 37 °C under a microscope. Phase contrast images were captured at different time points and the percentage of cells remaining attached over time was quantified. After 4 min, it was found that an average of 81.3% of the cells remained attached on the keratin biomaterial compared to 59% on fibronectin and 30% on uncoated slides. Keratin was found to significantly improve Schwann cell adhesion in comparison to uncoated and fibronectin-coated slides (p<0.05).

The effect of keratin on transcriptional regulation of RT4-D6P2T Schwann cells was assessed using qRT-PCR to determine the levels of transcription of several important proteins. S100β is a binding protein responsible for calcium homeostasis and normal glial cell function [28]; GFAP is an intermediate filament protein important for Schwann cell proliferation [29]; NGF and p75 (LNGFR) are NGF and low-affinity NGF receptor [30], respectively; L1CAM is a neuroglial cell adhesion molecule expressed in both myelinating and non-myelinating Schwann cells [31] and [32]; CD104 is the beta-4 integrin subunit and is important for

Schwann cell to axon interaction [33]; and VEGF is an important growth factor that enhances angiogenesis [34].

The keratin was exposed to the cells as an additive dissolved in the media at 1 mg/mL, 10 μg/mL, and 100 ng/mL. Increases in expression were considered significant at $p<0.05$ when compared to maintenance media. qRT-PCR data showed an up-regulation of S100β when the keratin was exposed to the cells in solution at 1 mg/mL. CD104 was also up-regulated by more than 50% when keratin was added to the media at 1 mg/mL. These data were statistically significant ($p<0.05$, $n=4$). P75 and NGF were slightly up-regulated at the 1 mg/mL and 10 μg/mL keratin concentrations, respectively, but these data did not reach statistical significance ($p=0.07$ and 0.06, respectively, $n=4$, Fig. 6). Keratin did not induce significant down-regulation in any of the assayed genes.

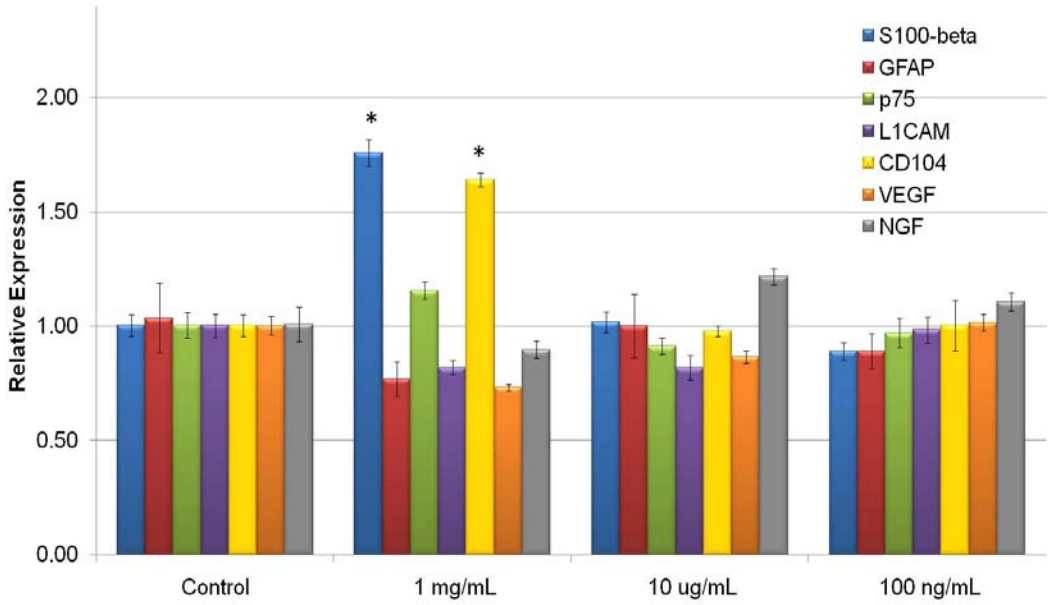

Figure 6. Gene expression changes in Schwann cells following 72 h of culture in keratin-containing media compared to standard culture conditions (growth media). Expression of S100β and CD104 at the 1 mg/mL concentration were significantly up-regulated (p<0.05, n=4).

3.3. Nerve regeneration *in vivo*

Isolated Schwann cells in culture can only approximate behavior *in vivo*. To directly test the effect of keratin biomaterial hydrogel on nerve regeneration, a nerve injury model in mice was employed. At 6 weeks, 100% of the animals in the keratin (5/5) and autograft (8/8) groups showed visible axon regeneration across the 4 mm nerve gap, whereas only 50% (5/10) of the animals in the empty conduit group displayed visible fiber regeneration (Fig. 7). Animals which did not display visible fiber regeneration did not undergo further testing (electrophysiology, muscle force generation, or histology).

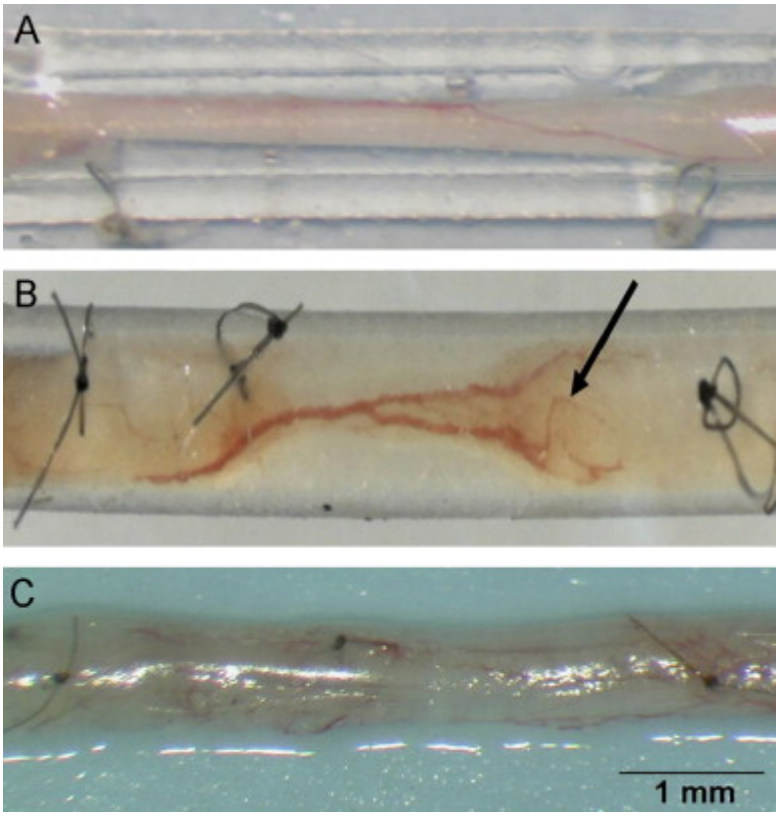

Figure 7. Nerve fiber regeneration 6 weeks after repair in empty (A), keratin- (B) and autograft- (C) treated animals. In the keratin and autograft groups, bridging of the nerve gap was observed in 100% of the animals, whereas only 50% of the animals in the empty group showed regeneration across the defect. Keratin-treated nerves also demonstrated a more developed and advancing growth cone (arrow) which was absent in the empty conduits. A robust angiogenic response was also noted in the keratin and autograft groups.

3.4. Electrophysiology

The latency (conduction delay; essentially the time required for an electrical impulse to travel down the nerve to the muscle) and amplitude of the compound motor action potential (CMAP; amplitude of the electrical impulse) was compared to the animal's contralateral control and expressed as a percentage. After 6 weeks of regeneration, latency measurements

revealed that the conduction delay was significantly (p<0.05) better in the keratin group (16.6%±3.52%) than either the empty conduit (72.7%±24.8%) or autograft (43.8%±3.98%) groups (Fig. 8A). The recovery of amplitude of the motor action potential was also statistically better (p<0.05) in the keratin group (34.5%±2.77%) than in the empty conduit (14.1%±5.27%) group (Fig. 8B).

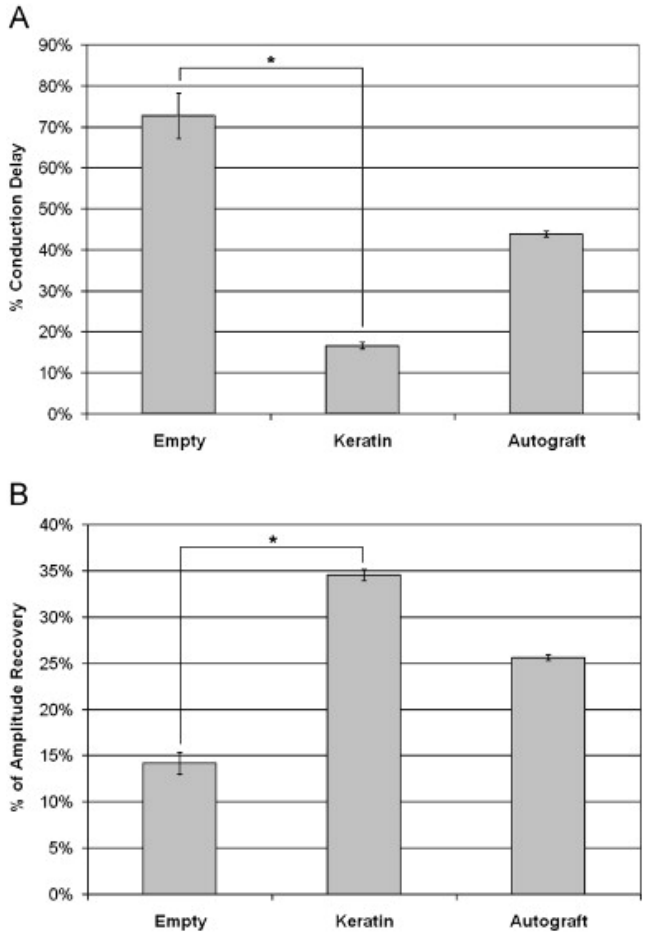

Figure 8. Electrophysiology testing following 6 weeks of regeneration showed an improvement in conduction delay (A) and amplitude of the nerve impulse (B) in keratin-filled tubes versus empty conduits and autograft. Values are expressed as mean±SEM normalized to the contralateral control (n=5 for keratin and empty groups; n=8 for autograft group).

3.5. Muscle force generation

Maximum single twitch and maximum tetanus of the muscle innervated by the repaired nerve were measured in grams and averaged for each experimental and control group. After 6 weeks, the maximum single twitch force was 25.3±4.8 g in the keratin group, 21.0±6.0 g in the empty conduit group, and 23.8±1.4 g in the autograft group (Fig. 9A). Recovery of maximum tetanus was 85.3±16.2 g in the keratin group, 65.0±47.0 g in the empty conduit group, and 89.0±8.0 g in the autograft group (Fig. 9B). These data were not statistically significant ($p>0.05$) between groups, but were significantly ($p<0.05$) lower than their contralateral controls.

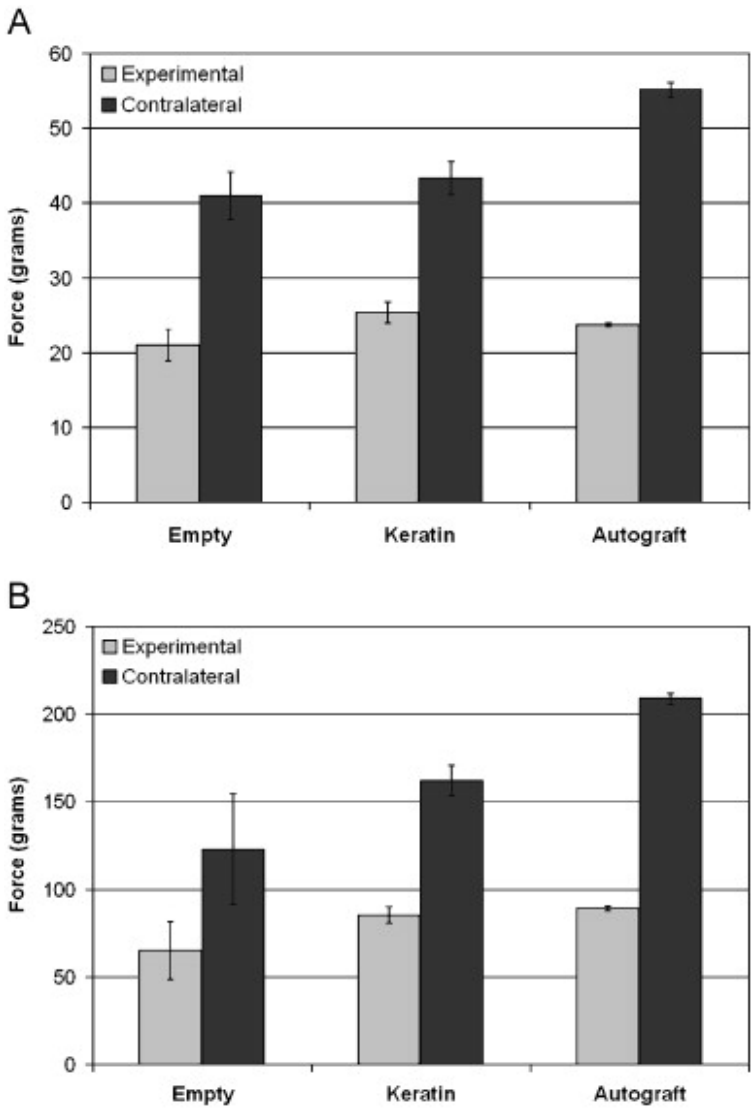

Figure 9. Muscle force testing at 6 weeks following regeneration showed a return of muscle single twitch (A) and muscle tetanus (B) in all treatment groups. There was no statistical difference between the groups and each was lower than its contralateral control.

3.6. Histology and histomorphometry

Histological investigation of toluidine blue-stained cross-sections showed myelinated axons in all treatment groups (Fig. 10). Quantitative analysis revealed a statistically significant

(p<0.05) increase in the overall nerve area and axon density in the keratin group compared to the empty conduit and autograft groups (Fig. 11A and B). The average axon diameter was higher in the keratin group than in the empty and comparable to the autograft group (Fig. 11C). Interestingly, nerve fibers that regenerated through keratin-filled conduits were more vascularized, with a significantly larger blood vessel area in comparison to all other groups (Fig. 12A and B).

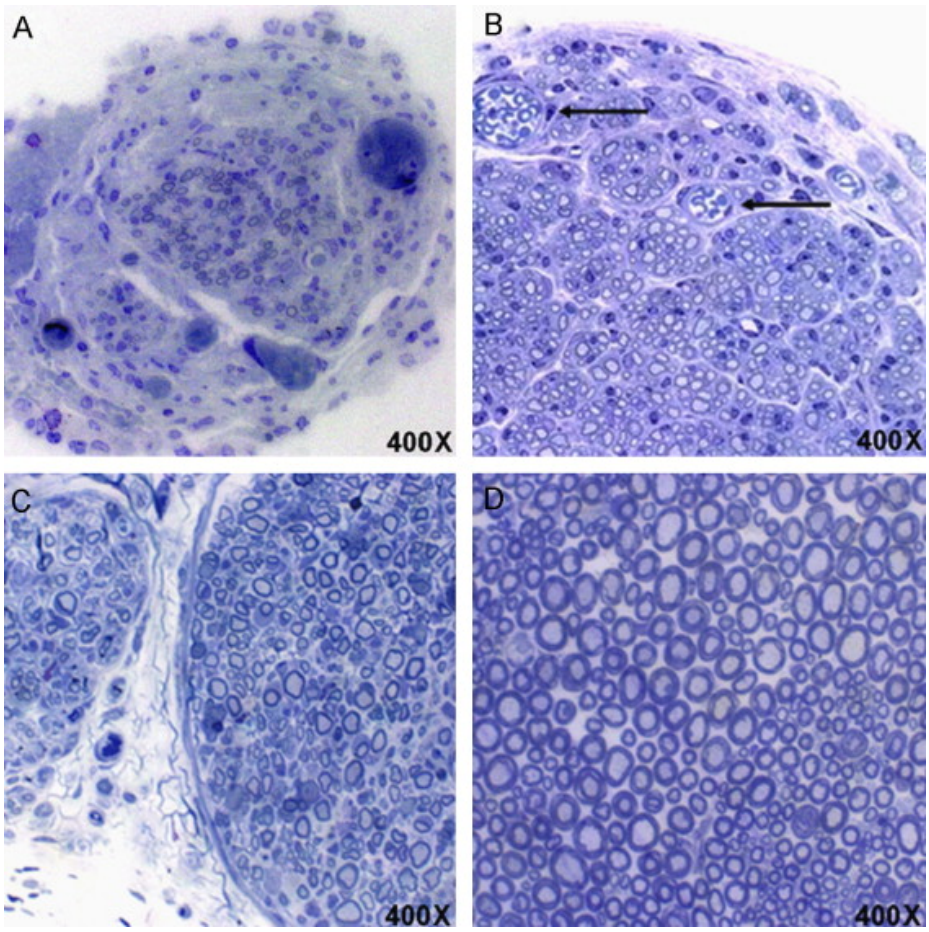

Figure 10. Toluidine blue staining of regenerated nerve cross-sections showing myelinated axons in (A) empty, (B) keratin, (C) autograft, and (D) native nerve groups. Increased vascularization (arrows) was observed in the keratin gel-filled conduit group in comparison to all other treatment groups and native nerve.

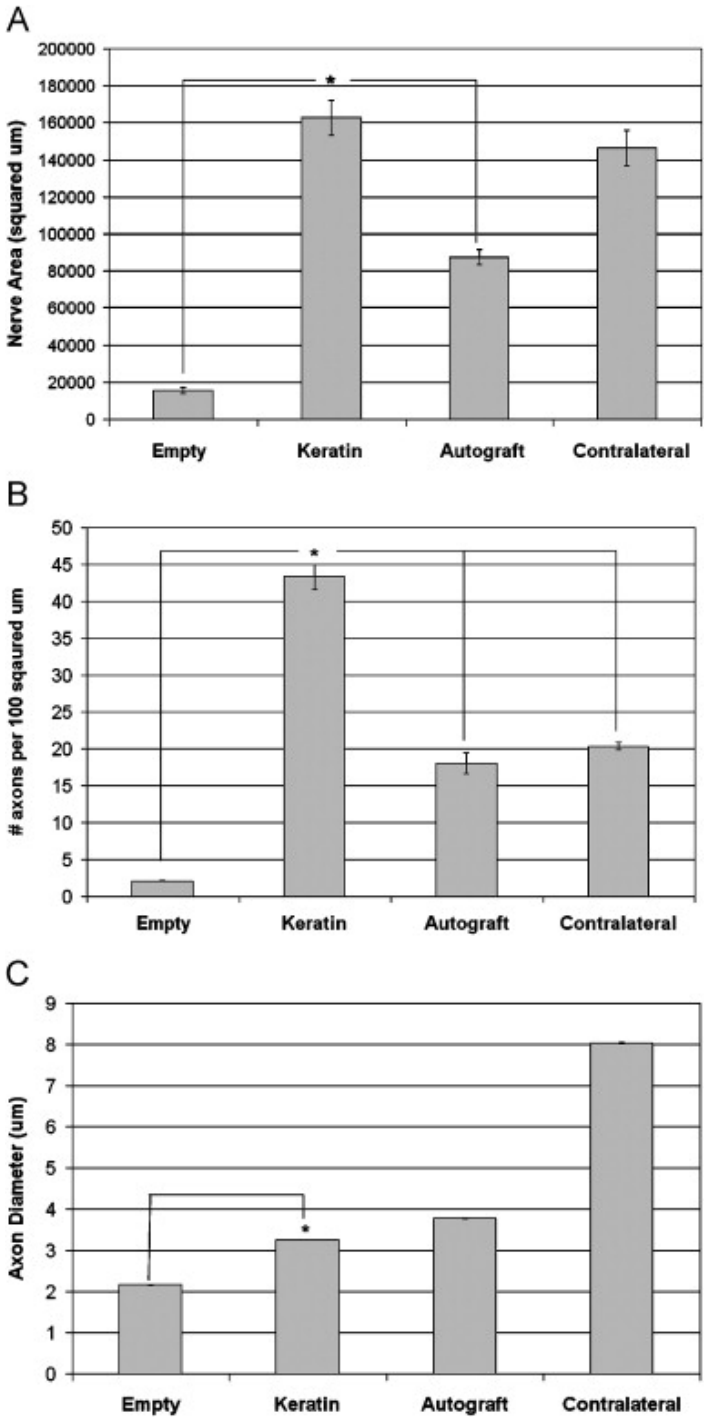

Figure 11. Histomorphometric analysis of regenerated nerve cross-sections. Overall nerve area and axon density were greatest in the keratin-treated group (A, B). Regenerated axons in the keratin-treated group were larger than in the empty group and comparable to autograft (C) (n=5, 5, 8, and 5, respectively, for empty, keratin, autograft, and native nerve groups).

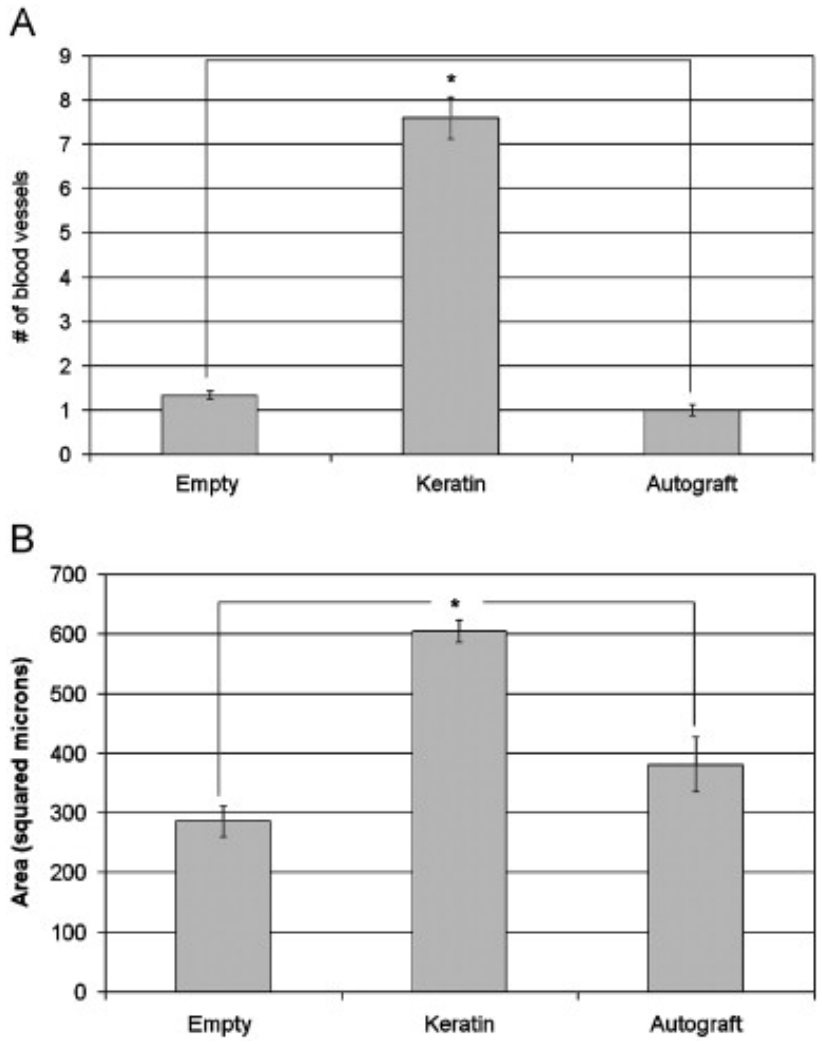

Figure 12. The robust angiogenic response noted upon gross observation was confirmed by the larger number and size of blood vessels present in the keratin-treated nerves (A, B).

4. Discussion

Owning to their capability for self-assembly, the formation of hydrogels occurs spontaneously upon addition of water to extracted, freeze-dried keratins. The samples used in the present study were a mixture of alpha- and gamma-keratins and formed the porous architectures shown in Fig. 2. As a scaffold for nerve regeneration, the fiber diameter, pore size,

and interconnectivity is permissive of cell penetration during the early phases of tissue remodeling. Since these hydrogels are not covalently crosslinked, they degrade slowly through disintegration of the gel structure and dissolution of the protein constituents over the course of several days when immersed in a large excess of saline at 37 °C (data not shown). It is thought that this process is likely extended to a few weeks *in vivo* due to the lower liquid ratio and absence of any natural proteinases specifically against hair keratins. As such, early invading cells are thought to be the most affected by the keratin hydrogel. Inside the nerve conduit, invading Schwann cells are exposed to both the underlying fibrous structure of the hydrogel and soluble molecules as the keratin slowly disintegrates and dissolves. The *in vitro* experiments were intended to simulate these conditions and showed that when Schwann cells were exposed to solutions of keratins, proliferation, migration, and gene expression increased (Fig. 3, Fig. 4 and Fig. 6, respectively). This may not be exclusively a consequence of an intrinsic characteristic of keratin biomaterials, but rather the presence of co-purifying compounds in the hair fiber extract. Many of the molecules that regulate hair morphogenesis have been characterized [3] and several of these growth factors have been shown to be expressed in the hair follicle [35], [36] and [37]. We postulate that regulatory molecules such as growth factors are retained in the hair fiber and extracted during processing in a form that provides some measurable level of biological activity. It is this latent activity that is thought to be responsible for the mitogenic, chemotactic, and gene regulation characteristics shown in Fig. 3, Fig. 4 and Fig. 6, respectively.

Another contributing factor to Schwann cell behavior is the degree and specificity to which these cells interact with the keratin substrate. As was shown in Fig. 5, Schwann cells

readily attach to a keratin substrate. The majority of keratins express either the widely know RGD motif, or the "*X*"-aspartic acid–"*Y*" motif where *X* equals glycine, leucine, or glutamic acid and *Y* equals serine or valine. The prevalence of these binding domains in keratin biomaterials may be responsible for at least some of the activity demonstrated in the present study as adhesion of integrins to these sites promotes intracellular signaling pathways.

The provisional matrix that forms inside of a nerve guidance tube is an essential element in the cascade of peripheral nerve regeneration [38]. If a provisional matrix fails to form, regeneration across an entubulated gap will not ensue. In the 4 mm gap used in the present study, half of the animals failed to regenerate nerve tissue when an empty conduit was used. In contrast, 100% of the keratin-filled tubes regenerated. Whether by itself or in combination with blood from the severed nerve ends, the keratin gel was likely able to act as a better provisional matrix than blood alone to support the infiltration of early invading regenerative cells. Since the keratin matrix was expected to be resorbed within the first few weeks, remodeling of this matrix by infiltrating Schwann cells was likely a key factor in the axonal regeneration evident in histological sections (Fig. 10). Although all treatment groups showed myelinated axons, keratin-treated nerves were larger in diameter, and had greater axon density with an average axon diameter equal to that of autograft (Fig. 11). Moreover, the robustness of the regenerative response was further demonstrated by the degree of angiogenesis observed in the keratin-treated nerves (Fig. 7 and Fig. 12). As a consequence, the keratin-treated groups tested significantly better for conduction delay and amplitude of the nerve-motor unit (Fig. 8). However, these results did not translate to muscle function recovery.

Muscle force had not fully reconstituted in any of the treatment groups by the 6-week time point (Fig. 9). This may have been due to the early timing of the test, but could also be related to permanent changes to denervated muscle that even autograft repair cannot reverse [39]. Our data supports this notion in that despite excellent histological findings, muscle single twitch and tetanus was statistically indistinguishable in all treatment groups and significantly lower than the contralateral controls.

5. Conclusions

Nerve autografting constitutes a method whereby living tissue is interposed into the repair site. Despite the obvious advantages this approach provides, nerve autograft tissue is tough and dense and may actually impede some of the early stages of regeneration. The use of a provisional matrix that is more permissive of regenerative cell infiltration may be capable of mediating nerve repair beyond current clinical barriers if it can recruit beneficial cells and direct their behavior toward restoration of functional tissue. Keratin biomaterials appear to be neuroconductive, and the evidence we present here suggests that they contain regulatory molecules capable of enhancing nerve tissue regeneration by inductive mechanisms as well. Further work in our laboratory is aimed at the identification and characterization of specific neurotrophic factors present in keratin biomaterials, as well as studies to investigate the ability of keratins to support regeneration across large nerve gaps.

Acknowledgments

The authors would like to thank Casey Northam, Eileen Martin, Vamsy Bobba, Weldon Whitener, Ken Grant and Cathy Mathis for their assistance with this study. The authors gratefully acknowledge the funding support provided by the Wake Forest Institute for Regenerative Medicine and the Department of Orthopaedic Surgery.

References

[1] J.S. Belkas, M.S. Shoichet and R. Midha, Peripheral nerve regeneration through guidance tubes, *Neurol Res* **26** (2) (2004), pp. 151–160.

[2] L. Alonso and E. Fuchs, The hair cycle, *J Cell Sci* **119** (3) (2006), pp. 391–393.

[3] K.S. Stenn, S.M. Prouty and M. Seiberg, Molecules of the cycling hair follicle-a tabulated review, *J Dermatol Sci* **7** (Suppl) (1994), pp. S109–S124.

[4] K.S. Stenn, N.J. Combates, K.J. Eilertsen, J.S. Gordon, J.R. Pardinas and S. Parimoo *et al.*, Hair follicle growth controls, *Dermatol Clin* **14** (4) (1996), pp. 543–548.

[5] M.H. Hardy, The secret life of the hair follicle, *Trends Genet* **8** (2) (1992), pp. 55–61.

[6] G.E. Rogers, Hair follicle differentiation and regulation, *Int J Dev Biol* **48** (2-3) (2004), pp. 163–170.

[7] E. Ioannidou, Therapeutic modulation of growth factors and cytokines in regenerative medicine, *Curr Pharm Des* **12** (19) (2006), pp. 2397–2408.

[8] V.M. Verge, K.A. Gratto, L.A. Karchewski and P.M. Richardson, Neurotrophins and nerve injury in the adult, *Phil Trans R Soc London B Biol Sci* **351** (1338) (1996), pp. 423–430.

[9] S.P. Frostick, Q. Yin and G.J. Kemp, Schwann cells, neurotrophic factors and peripheral nerve regeneration, *Microsurgery* **18** (7) (1998), pp. 397–405.

[10] W.G. Crewther, R.D.B. Fraser, F.G. Lennox and H. Lindley, The chemistry of keratins. In: C.B. Anfinsen Jr, M.L. Anson, J.T. Edsall and F.M. Richards, Editors, *Advances in protein chemistry*, Academic Press, New York (1965), pp. 191–346.

[11] Y. Noishiki, H. Ito, T. Miyamoto and H. Inagaki, Application of denatured wool keratin derivatives to an antithrombogenic biomaterial: vascular graft coated with a heparinized keratin derivative, *Kobunshi Ronbunshu* **39** (4) (1982), pp. 221–227.

[12] K. Katoh, T. Tanabe and K. Yamauchi, Novel approach to fabricate keratin sponge scaffolds with controlled pore size & porosity, *Biomaterials* **25** (18) (2004), pp. 4255–4262.

[13] A. Tachibana, Y. Furuta, H. Takeshima, T. Tanabe and K. Yamauchi, Fabrication of wool keratin sponge scaffolds for long-term cell cultivation, *J Biotechnol* **93** (2002), pp. 165–170.

[14] A. Tachibana, S. Kaneko, T. Tanabe and K. Yamauchi, Rapid fabrication of keratin-hydroxyapatite hybrid sponges toward osteoblast cultivation and differentiation, *Biomaterials* **26** (3) (2005), pp. 297–302.

[15] R. Bansal and S.E. Pfeiffer, Regulated galactolipid synthesis and cell surface expression in Schwann cell line D6P2T, *J. Neurochem* **49** (6) (1987), pp. 1902–1911.

[16] T. Mosmann, Rapid colorimetric assay for cellular growth and survival: Application to proliferation and cytotoxicity assays, *J Immunol Meth* **65** (1-2) (1983), pp. 55–63.

[17] K.J. Livak and T.D. Schmittgen, Analysis of relative gene expression data using real-time quantitative PCR and the $2^{-\Delta\Delta C}{}_{T}$ method, *Methods* **25** (4) (2001), pp. 402–408.

[18] H. Thomas, A. Conrads, K.H. Phan, M. van de Löcht and H. Zahn, *In vitro* reconstitution of wool intermediate filaments, *Int J Biol Macromol* **8** (1986), pp. 258–264.

[19] M. van de Löcht, Reconstitution of microfibrils from wool & filaments from epidermis proteins, *Melli Textil* **10** (1987), pp. 780–786.

[20] A.H. Cory, T.C. Owen, J.A. Barltrop and J.G. Cory, Use of an aqueous soluble tetrazolium/formazan assay for cell growth assays in culture, *Cancer Commun* **3** (7) (1991), pp. 207–212.

[21] M. Hai, N. Muja, G.H. DeVries, R.H. Quarles and P.I. Patel, Comparative analysis of Schwann cell lines as model systems for myelin gene transcription studies, *J Neurosci Res* **69** (4) (2002), pp. 497–508.

[22] S. Boyden, The chemotactic effect of mixtures of antibody and antigen on polymorphonuclear leucocytes, *J Exp Med* **115** (1962), pp. 453–466.

[23] D. Ingber, Integrins as mechanochemical transducers, *Curr Opin Cell Biol* **3** (5) (1991), pp. 841–848.

[24] P.A. Tooney, M.V. Agrez and G.F. Burns, A re-examination of the molecular basis of cell movement, *Immunol Cell Biol* **71** (2) (1993), pp. 131–139.

[25] B.M. Jockusch *et al.*, The molecular architecture of focal adhesions, *Annu Rev Cell Dev Biol* **11** (1995), pp. 379–416. View Record in Scopus | Cited By in Scopus (356)

[26] E. Ruoslahti, RGD and other recognition sequences for integrins, *Annu Rev Cell Dev Biol* **12** (1996), pp. 697–715.

[27] Entrez Protein Database. National Center for Biotechnology Information (NCBI). ⟨http://www.ncbi.nlm.nih.gov.go.libproxy.wfubmc.edu⟩.

[28] Z. Xiong, D. O'Hanlon, L.E. Becker, J. Roder, J.F. MacDonald and A. Marks, Enhanced calcium transients in glial cells in neonatal cerebellar cultures derived from S100B null mice, *Exp Cell Res* **257** (2) (2000), pp. 281–289.

[29] D. Triolo, G. Dina, I. Lorenzetti, M. Malaguti, P. Morana and U. Del Carro *et al.*, Loss of glial fibrillary acidic protein (GFAP) impairs Schwann cell proliferation and delays nerve regeneration after damage, *J Cell Sci* **119** (19) (2006), pp. 3981–3993.

[30] E.S. Anton, G. Weskamp, L.F. Reichardt and W.D. Matthew, Nerve growth factor and its low-affinity receptor promote Schwann cell migration, *Proc Natl Acad Sci USA* **91** (7) (1994), pp. 2795–2799.

[31] C. Ide, Peripheral nerve regeneration, *Neurosci Res* **25** (2) (1996), pp. 101–121.

[32] S.Y. Fu and T. Gordon, The cellular and molecular basis of peripheral nerve regeneration, *Mol Neurobiol* **14** (1-2) (1997), pp. 67–116.

[33] M.L. Feltri, S.S. Scherer, R. Nemni, J. Kamholz, H. Vogelbacker and M.O. Scott *et al.*, Beta 4 integrin expression in myelinating Schwann cells is polarized, developmentally regulated and axonally dependent, *Development* **120** (5) (1994), pp. 1287–1301.

[34] M. Sondell, G. Lundborg and M. Kanje, Vascular endothelial growth factor stimulates Schwann cell invasion and neovascularization of acellular nerve grafts, *Brain Res* **846** (2) (1999), pp. 219–228.

[35] C.M. Jones, K.M. Lyons and B.L.M. Hogan, Involvement of bone morphogenetic protein-4 (BMP-4) and Vgr-1 in morphogenesis and neurogenesis in the mouse, *Development* **111** (1991), pp. 531–542.

[36] K.M. Lyons, R.W. Pelton and B.L.M. Hogan, Organogenesis and pattern formation in the mouse: RNA distribution patterns suggest a role for bone morphogenetic protein-2A (BMP-2A), *Development* **109** (1990), pp. 833–844.

[37] M. Blessings, L.B. Nanney, L.E. King, C.M. Jones and B.L.M. Hogan, Transgenic mice as a model to study the role of TGF-ß related molecules in hair follicles, *Genes Dev* **7** (1993), pp. 204–215.

[38] H.M. Liu, The role of extracellular matrix in peripheral nerve regeneration: a wound chamber study, *Acta Neuropathol (Berlin)* **83** (5) (1992), pp. 469–474.

[39] Ma J, Shen J, Garrett JP, Lee CA, Li Z, Elsaidi GA et al. Gene expression of myogenic regulatory factors, nicotinic acetylcholine receptor subunits, and GAP-43 in skeletal muscle following denervation in a rat model. J Orthop Res 2007, in press.

CHAPTER VI

Peripheral Nerve regeneration using a Keratin-based Scaffold: Long-term Functional and Histological Outcomes in a Mouse Model

Peter J. Apel[2], Jeffrey Garrett[2], Paulina Sierpinski[1], Jianju Ma[2], Anthony Atala[1], Tom Smith, L[2].

Andrew Koman[2], and Mark Van Dyke[1]

[1] Wake Forest Institute for Regenerative Medicine

[2] Department of Orthopaedic Surgery

Wake Forest University School of Medicine, Winston Salem, NC, 27157

This manuscript was published in Journal of Hand Surgery 33(9):1541-1547 (2008), and is reprinted with permission Stylistic variations are due to the requirements of the journal. Paulina Sierpinski assisted with manuscript preparation and was responsible for keratin biomaterial preparation, histology and histomorphometric analysis.

Abstract

Purpose

The management of peripheral nerve injuries with segmental defects is a challenge to both patient and surgeon. Repairs under tension have a poor prognosis; sensory nerve allografts have donor site morbidity and suboptimal motor recovery, but remain the gold standard. The development of conduit-based repair strategies has evolved and these are promising for sensory nerves and short defects; however, no conduit filler is clinically available that improves motor recovery equivalent to sensory autografts. In this study, motor recovery using keratin-based hydrogel filler was compared with that for sensory nerve autografts and empty conduits.

Methods

Fifty-four mice were randomized into 3 treatment groups: empty conduit, sural nerve autograft, and keratin hydrogel-filled conduit. Animals were followed for 6 weeks, 3 months, and 6 months. Outcomes included compound motor action potential (CMAP), nerve area, myelinated axon number and density, and myelinated axon diameter.

Results

Neuromuscular recovery with keratin was greater than with empty conduits in most outcome measures. Nerves that regenerated through the keratin hydrogel had lower conduction delays, greater amplitudes, more myelinated axons, and larger axons than nerves that regenerated through empty conduits. Sensory nerve autografts and keratin hydrogel were statistically

equivalent in CMAP measurements at 6 months. Moreover, keratin-filled conduits demonstrated greater axon density and larger average axon diameter than both empty conduits and autograft at 6 months.

Conclusions

In a mouse tibial nerve model, keratin hydrogels significantly improved electrophysiological recovery, compared with empty conduits and sensory nerve autografts, at an early time point of regeneration. Keratin hydrogels also produce long-term electrical and histological results superior to empty conduits and equivalent to sensory nerve autografts.

Key words: Hydrogel; keratin; mouse model; nerve regeneration; scaffold; tibia

Introduction

Peripheral nerve injury is a challenging clinical problem. In a 10-year study, Noble et al.[1] found that 2.8% of patients treated in a level I trauma center sustained an injury to the radial, median, ulnar, sciatic, femoral, peroneal, or tibial nerve—half of whom required surgical intervention. Midha[2] found that 1.2% of patients brought to a regional trauma center had sustained a brachial plexus injury, 38% of whom required surgical exploration and reconstruction. Peripheral nerve injury accounts for more than $150 billion annually in health care costs in the United States.[3] Surgical treatment of peripheral nerve injuries is challenging and often requires the bridging of a gap between the proximal and distal nerve stumps when end-to-end repair is not possible.

Keratins are a family of large structural proteins found abundantly in hair and fingernails. Keratins can self-assemble into nanofilaments when placed in solution.[4] These nanofilaments can further self-assemble into a porous, fibrous microarchitecture upon gelation. Moreover, keratins contain several peptide binding motifs that support attachment of a wide variety of cell types, similar to other well-known proteins of the extracellular matrix, including fibronectin and collagen.[5] A keratin-based hydrogel that self-assembles into a fibrous matrix capable of promoting cell adhesion is a promising scaffold for peripheral nerve regeneration for multiple reasons. First, it is known that establishment of a provisional matrix is the first step in nerve regeneration within conduits,[6] and that for long nerve gaps a matrix does not reliably form.[7] Surgical implantation of a keratin-based scaffold ensures that a matrix is present. Second,

keratin-based scaffolds have fibronectin-like binding domains that facilitate Schwann cell adhesion to the provisional matrix.[8]

We hypothesized that a keratin-based hydrogel would facilitate early nerve regeneration and lead to better long-term histological and electrical outcomes. This study was designed to evaluate the time course of peripheral nerve regeneration with respect to neuromuscular recovery and nerve histomorphometry comparing keratin-filled conduits to empty conduits and sensory nerve autografts.

Materials and methods

Scaffold preparation

Details of the keratin hydrogel scaffold preparation have been previously described.[8] Briefly, human hair was cut, washed, and degreased. Soluble keratins were obtained by treatment with peracetic acid, followed by extraction with Tris base and deionized water. Extracts were combined and dialyzed. The dialysate was concentrated, neutralized, and freeze-dried. The resulting solid was ground into a fine powder and sterilized with gamma irradiation. Fifteen percent keratin hydrogels (w/v) were then prepared by addition of 0.9% normal saline.

Animal model

Fifty-four CD1 Swiss–Webster (Charles River Laboratories, Wilmington, MA) mice were randomized into 3 treatment groups (empty conduit, keratin-filled conduit, and sural nerve autograft) with 3 time points each (6 weeks, 3 months, and 6 months). All experiments were conducted under a protocol approved by the Institutional Animal Care and Use Committee and animals were housed in an appropriate facility in accordance with National Institutes of Health guidelines. Animals were group-housed and allowed food and water ad libitum.

Surgical procedure

General anesthesia was obtained with isoflurane, and the operative site was shaved and cleansed. A 1.5-cm incision was made on the dorsal aspect of the left thigh. Using an operating microscope, soft tissues were dissected to expose and then separate the tibial nerve from the common peroneal and sural nerves. The tibial nerve was then transected 5 mm proximal to its insertion into the gastrocnemius. The proximal and distal nerve ends were secured inside a 7-mm nerve conduit made of sterile silicone rubber laboratory tubing (0.64 ± 0.13 mm inside diameter, 1.19 ± 0.13 mm outside diameter, 0.28 mm wall diameter) (Silastic; Dow Corning, Midland, MI) using 10-0 nylon. The nerve was pulled into the conduit with a single horizontal mattress suture. After visual confirmation of the nerve gap using a ruler, an additional epineurial suture was used to secure the nerve on each end. A final suture was placed transversely through both the conduit and nerve to provide additional fixation. The keratin

hydrogel was introduced into the gap space via a 28 gauge needle. The needle was gently slid between the proximal nerve stump and the conduit wall and the hydrogel injected as the needle was retracted. Because of the contrast of the hydrogel and the silicone rubber tubing, direct visualization of the hydrogel placement was easily confirmed (Figs. 1A–C). The final nerve gap was measured and confirmed to be 4.0 mm in all animals. The contralateral limb of each animal served as an internal reference. A deep muscle closure was performed around the conduit using 8-0 nylon, followed by superficial muscle and skin closure with 5-0 absorbable suture (Vicryl; Ethicon, Somerville, NJ).

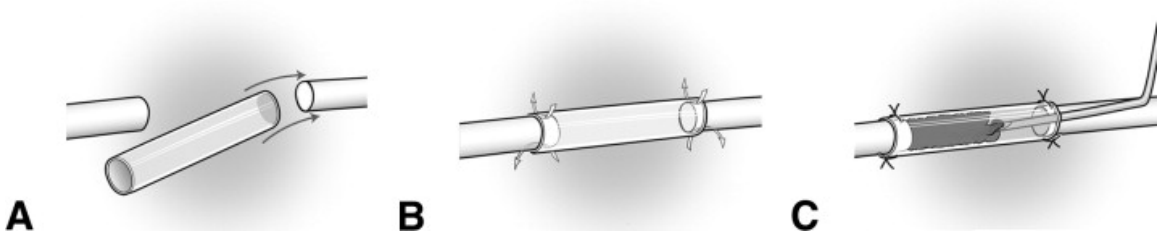

FIGURE 1. Placement of the keratin hydrogel in the conduit. **A** The tibial nerve is cut and the silicone tube is interposed. **B** The nerve is sutured in place with 10-0 nylon after visually verifying the gap distance using a ruler. **C** The hydrogel is slowly injected as the modified 28-gauge needle is retracted, thereby filling the luminal space.

Compound motor action potential (CMAP)

At study termination, each animal was anesthetized with isoflurane and motor conduction of the tibial nerve was tested. The tibial nerve was exposed and the peroneal nerve was transected in order to eliminate artifact. Care was taken to keep the nerve moist and warm. The compound motor action potential (CMAP) of the tibial nerve and gastrocnemius complex

was measured with either a Sierra Wave (Caldwell Laboratories, Kennewick, WA) or a Nicolet Viking IIe (Nicolet Instrument, Madison, WI) electrodiagnostic system. The stimulation and recording protocol was identical for both instruments. Parameters measured included latency and amplitude of the action potential. A bipolar stimulating electrode was placed on the tibial nerve at the level of the obturator externus tendon. A surface recording electrode was placed on the gastrocnemius muscle and a reference electrode on the calcaneus (Fig. 2). The stimulating–recording electrode distance was verified visually using a ruler. The nerve was then stimulated with a constant current of 0.4 to 0.5 mA for 0.1 ms. The testing protocol was repeated 3 times. The single result with the highest amplitude was recorded and used for further analysis. The contralateral limb was similarly tested and served as an internal reference. Parameters were expressed as a percentage of the value obtained for the contralateral limb.

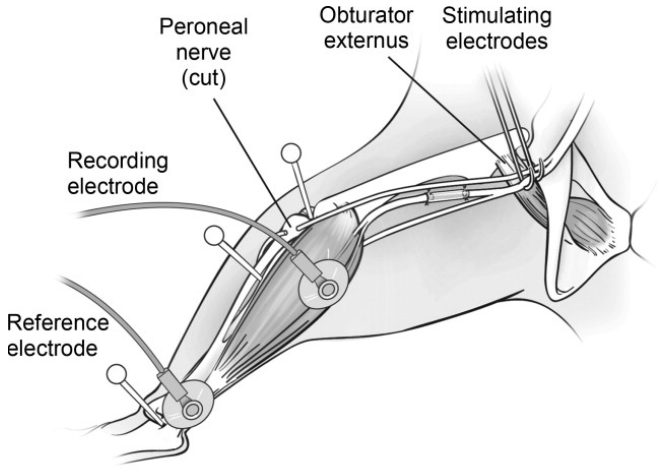

FIGURE 2. Diagram of electrode placement and setup for CMAP recording. The peroneal nerve is cut at the head of the fibula to reduce electrical artifact. The stimulating electrodes are placed on the sciatic nerve at the level of the obturator externus tendon. The reference electrode is placed on the calcaneus and the recording electrode on the gastrocnemius and the stimulating-recording electrode distance verified using a ruler.

Histomorphometry

Following electrical testing, the regenerated nerve within the conduit was harvested and fixed in glutaraldehyde. After embedding, 1-μm semi-thin cross-sections from the midpoint of the nerve were sectioned and stained with toluidine blue. Digital photomicrographs were acquired on a Zeiss microscope (Carl Zeiss, Jena, Germany) and imported into ImageJ image processing software (National Institutes of Health, Bethesda, MD) for blinded analysis. Nerve area was measured for each nerve on low-power magnification. The nerve cross-section was divided into 4 quadrants, and 2 to 3 high-power fields (1000×) of equal area from each quadrant (ie, 8 to 12 total high-power fields) were evaluated for myelinated axon number and average axon diameter. Myelinated axons less than 1 μm and unmyelinated axons were not

counted. Depending on the diameter of the nerve being examined, this counting method encompassed 30% to 100% of the total nerve area. Axon number was divided by the area sampled to calculate average myelinated axon density.

Statistical analysis

Data were imported for analysis into SigmaStat 3.11 (Systat, San Jose, CA) and SAS 9.1 with Enterprise Guide 4 (SAS Institute, Cary, NC). Multiple linear regression models and a 2-factor analysis of variance were used to examine the effects of time and treatment. Transformations to nonparametric methods were performed as appropriate. Direct pairwise comparisons were performed where appropriate with the Student–Newman–Keuls post hoc test or with 95% confidence intervals. In order to more closely examine the effect of treatment, the differences due to time were controlled through the multiple linear regression models. The differences due to treatment were isolated and quantified by the use of indicator variables and calculating the coefficient of the slope for the linear regression model. This coefficient represents the difference due to treatment and is reported as the linear regression coefficient. Differences due to time were also calculated within the models, but are not reported. Differences between groups were considered significant if $\alpha \leq .05$ for all statistical tests. Data are expressed as mean ± standard error of the mean (SEM) with the number of animals and corresponding p values indicated.

Results

Compound motor action potential

Partial results from the 6-week time point have been previously reported.[8] For direct pairwise comparisons at 6 weeks, the keratin group showed significantly improved conduction delay, compared with autografts (n = 13, p = .001) and empty conduits (n = 10, p = .048) (Fig. 3). Amplitude recovery was also significantly higher in the keratin group, compared with the other 2 groups. This trend persisted at 3 months, with conduction delay maintaining statistical significance in the keratin group, compared with empty and autograft, and with amplitude recovery trending higher (although not reaching statistical significance). At 6 months, the keratin group showed significant improvement in amplitude recovery, compared with empty conduits (n = 13, p = .008), and was statistically equivalent to autograft in both conduction delay (95% CI: −14.0 to 29.1) and amplitude recovery (95% CI: −48.6% to 28.9%).

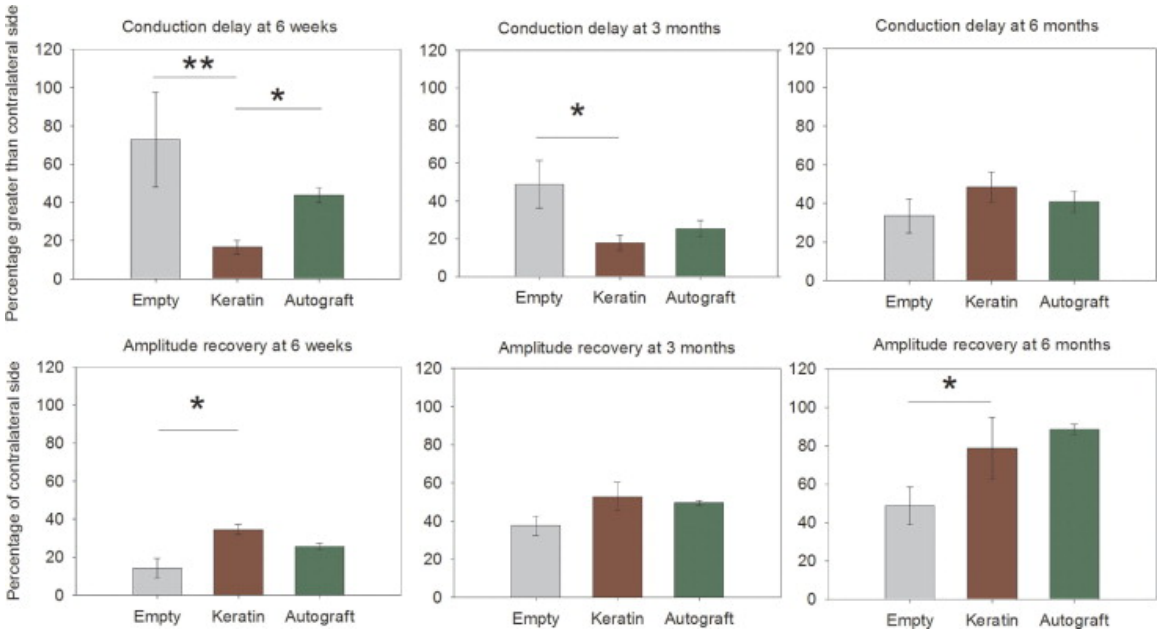

FIGURE 3. Summary of CMAP results. All results were normalized to the uninjured contralateral reference and reported as mean ± SEM. Significant pairwise comparisons are noted: *p < .05, **p < .01. Lower conduction delay is seen at 6 weeks in keratin-treated nerves, compared with both autograft and empty. Lower conduction delays were also seen in keratin versus empty at 3 months. For amplitude recovery, keratin was consistently greater than empty at 6 weeks and 6 months.

Overall results, as represented by the linear regression curves of conduction delay and amplitude over time, in the keratin group showed a reduction in conduction delay, compared with the empty group (linear regression coefficient = −21.1% ± 10.5%, n = 35, p = .054) and autograft group (linear regression coefficient = −10.1% ± 5.3%, n = 37, p = .067). For amplitude of the CMAP, the keratin group demonstrated significantly higher recovery, compared with the empty group (linear regression coefficient = +22.1% ± 7.9%, n = 35, p =

.009), and was statistically equivalent the autograft group (linear regression coefficient = −1.02% ± 6.7%, n = 37, p = 0.88, 95% CI: −1.46% to 1.25%).

Histomorphometry

Partial results from the 6-week time point have been previously reported.[8] Representative photomicrographs of regenerated nerve segments are shown in Figure 4. Analysis of nerve area showed that the keratin hydrogel-treated nerves had larger cross-sectional areas at 6 weeks and 3 months; however, this did not reach statistical significance (Table 1). Axon area at 6 months was statistically equivalent in all 3 groups. For axon density and average axon diameter, there was a significant effect of treatment, with keratin-treated nerves showing significantly higher axon densities and average myelinated axon diameter (Table 1). For direct pairwise comparisons, the keratin-treated nerves had significantly greater axon density than either the empty or the autograft group at 6 weeks and at 6 months (Fig. 5). In addition, the keratin-treated nerves had significantly greater average myelinated axon diameters, compared with the empty group at 6 weeks and compared with both the empty and autograft groups at 6 months (Fig. 6).

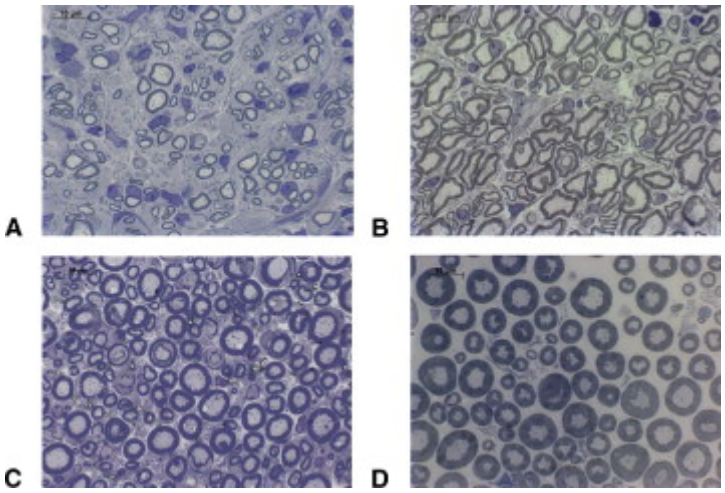

FIGURE 4. Representative photomicrographs of the regenerated nerve segments viewed at 1000×. **A** Empty. **B** Keratin. **C** Autograft. **D** Native tibial nerve.

Table 1. Complete histomorphometry data.

	Time Point	Nerve Area, μm^2	Total Axons per Nerve	Axon Density, Axons/μm^2	Myelinated Axon Diameter, μm
Empty	6 wk	15,558 ± 3,141	241 ± 49	1.55 ± 0.03	2.23 ± 0.19
Keratin	6 wk	130,006 ± 24,530	13,986 ± 2,639	10.76 ± 0.45	3.17 ± 0.11
Autograft	6 wk	74,389 ± 12,730	2,360 ± 404	3.17 ± 0.09	3.74 ± 0.15
Empty	3 mo	44,011 ± 2,937	626 ± 42	1.42 ± 0.07	3.83 ± 0.07
Keratin	3 mo	100,613 ± 12,741	1,806 ± 229	1.79 ± 0.05	4.28 ± 0.09
Autograft	3 mo	712,43 ± 3,206	1,237 ± 56	1.74 ± 0.09	3.66 ± 0.05
Empty	6 mo	124,560 ± 19,342	1,396 ± 217	1.12 ± 0.06	4.34 ± 0.07
Keratin	6 mo	86,457 ± 12,053	1,776 ± 248	2.05 ± 0.08	5.75 ± 0.06
Autograft	6 mo	110,994 ± 3,473	1,373 ± 43	1.24 ± 0.05	4.35 ± 0.07
		Linear coefficient between Keratin and Empty (p Value)			
		24,537 (.09)	3175 (.084)	2.52 (<.001)	0.987 (<.001)
		Linear coefficient between Keratin and Autograft (p Value)			
		10,361 (.90)	2434 (.119)	2.07 (<.001)	0.717 (<.001)
		Average difference between Keratin and Empty, %			
		40	4	185	28
		Average difference between Keratin and Autograft, %			
		12	1	101	18

Data are reported as mean ± SEM. Linear coefficients are the expected differences due to the difference in treatment. Average differences are calculated by dividing the linear coefficient by the average over the 3 time points

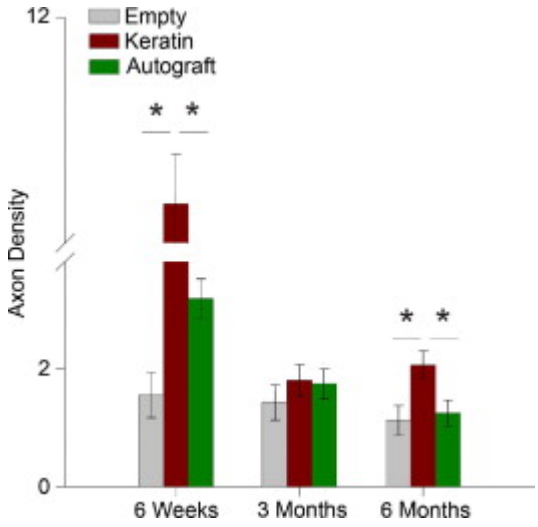

FIGURE 5. Average axon density. Pairwise comparisons were made for myelinated axon density for all time points and treatments. All results are reported as mean ± SEM. Significant pairwise comparisons are noted with *p < .05. Keratin-treated nerves showed significantly greater axon density at 6 weeks and 6 months, compared with both empty conduit and autograft.

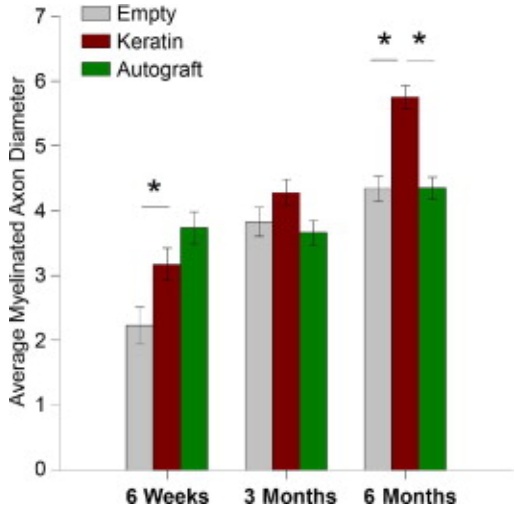

FIGURE 6. Average axon diameter. Pairwise comparisons were made for myelinated axon average diameter for all time points and treatments. All results are reported as mean ± SEM. Significant pairwise comparisons are noted with *p < .05. Axons from remodeled nerves at 6 months were of significantly larger diameter in the keratin-treated group, compared with both empty conduit and autograft.

Discussion

Successful nerve regeneration requires the coordination of physical, chemical, and biologic processes. Understanding the physical and temporal aspects of nerve regeneration within a conduit is important to the design of any bioengineered scaffold to be used as a luminal filler. Of equal importance, particularly for the model described here, careful surgical technique is essential when working with the small-scale anatomy of the mouse model.

The dynamic process of nerve regeneration has been well documented in the literature.[6] and [9] The endogenous provisional matrix produced is composed mostly of fibrin. If a matrix is not present[7] or is disorganized,[9] regeneration is extremely poor or does not proceed. Shortly after formation of the matrix, Schwann cells, macrophages, and nonneuronal elements migrate into the provisional matrix from the proximal and distal stumps. Axonal growth occurs 2 to 4 weeks after the repair, during which time the provisional fibrin matrix degrades. Later stages of neuromuscular recovery consist of establishment of neuromuscular connections, target-derived trophic feedback, myelination, resorption of the nonmyelinated axons (ie, axons not reaching their muscle target), and maturation of the regenerated neuromuscular unit.

A keratin-based scaffold facilitates nerve regeneration in several ways. First, surgical placement of a scaffold ensures that a matrix is present, so that the early infiltration of Schwann cells and macrophages can occur. Previous studies have demonstrated that keratin has fibronectin-like cell binding domains that facilitate adhesion,[5] supporting this hypothesized mechanism of action. Second, it has previously been shown that keratin-based biomaterials

increase the migration, proliferation and activity of Schwann cells,[8] suggesting that the scaffold has inherent biologic activity. Third, the keratin hydrogel used in this study is thought to degrade within 3 to 4 weeks, thus avoiding the inhibition of axonal ingrowth observed with other slow-degrading biomaterial scaffolds.[10] Timely degradation of a scaffold is necessary for the later stages of neuromuscular regeneration.[9] The time course of regeneration through a keratin hydrogel scaffold coincides with the normal degradation of endogenous fibrin matrix during physiological nerve regeneration.[6] Thus, the keratin hydrogel scaffold probably serves as a biologically active provisional matrix and facilitates the early stages of nerve regeneration while degrading in a manner that does not impede the later stages.

In the early stages of nerve regeneration, the axon produces numerous axonal sprouts that cross the nerve repair site, with as many as 3 to 4 sprouts per axon.[11], [12] and [13] Some of the sprouting axons reach endoneurial tubes in the distal segment and regenerate to the target sensory receptor or neuromuscular junction. Other sprouts do not reach target organs and subsequently die back for lack of a trophic signal.[14] Thus, contact with the target organ has a profound trophic effect on the regenerated axon.[15]

In the data presented here, this process is well documented, with a steady decline in axon density throughout the study period. There were, however, 2 significant effects of the keratin-based scaffold on this sprouting-death process. First, axon number and density were significantly higher in the keratin group at 6 weeks, supporting the idea that keratin facilitates initial axonal outgrowth. The second observation must be viewed in the context of the findings

of Kobayashi et al.,[16] namely, that the duration of muscle denervated directly correlates with re-establishment of functional synapses. The CMAP data presented here demonstrate that electrical recovery (ie, re-establishment of functional neuromuscular units) was greater in the keratin-treated group. Thus, the second significant histological observation is a logical consequence: more established neuromuscular contacts and greater target-derived trophism. Thus, it is not surprising that the steady decrease in axon density with time is attenuated in the keratin-treated group at 6 months, reflecting more mature axons due to earlier reinnervation and establishment of trophic neuromuscular junctions.

In the present study, the keratin-based scaffold significantly improved electrophysiological and histomorphologic outcomes, compared with empty conduits, as measured by both CMAP and histomorphometry. Many of the observed improvements in recovery can be attributed to the ability of the hydrogel to serve as a provisional matrix accelerating nerve regeneration. Early establishment of the matrix most likely led to the increased CMAP and axon density seen at 6 weeks. Subsequently, earlier myelination occurred, as evidenced by the decreased conduction delay, although this was not directly measured. The early establishment of more neuromuscular contacts in the keratin-treated group, as evidenced by the increased amplitude of the CMAP, may have further contributed to the increase in myelinated axon density and average diameter seen at 6 months. This late result due to early phenomena can be attributed to the establishment of neuromuscular contacts that stimulate myelination in a positive feedback mechanism. Myelination occurs later in neuromuscular regeneration, preferentially around axons that have an established neuromuscular connection.

Establishment of a neuromuscular connection at an early time point may lead to more functional connections with the target muscle, increasing CMAP amplitude and average myelinated axon number and diameter. In the present study, there was no difference in nerve area between groups or at different time points, possibly because of the physical limits of the silicone conduit in the empty and keratin groups and of the epineuria in the autograft group.

Numerous studies of peripheral nerve repair have explored the use of a variety of luminal fillers, Schwann cells, various stem cells, nearly all of the known nerve-related growth factors, and combinations thereof. Despite these studies, however, no conduit filler is currently available for clinical use that improves regeneration to a greater degree than empty or saline-filled conduits. Stem cell- and growth factor-based experiments, although executable in a laboratory setting, have major regulatory and financial limitations to clinical translation. The ideal conduit filler would be inexpensive, easy to use, inherently bioactive, and compatible with existing technologies. A keratin-based scaffold made from human hair meets many of these requirements and is a viable candidate for peripheral nerve repair. The present results suggest that a keratin-based biomaterial scaffold can positively affect peripheral nerve regeneration and promote neuromuscular recovery equivalent to the gold-standard, sensory nerve autografts. Although these results are encouraging, more extensive studies using a clinically relevant sized model are required before the translational opportunities of a keratin-based conduit filler are clear.

Acknowledgements

The authors thank the Wake Forest Orthopaedic Research Lab, Casey Northam, Jacquie Burnell, and Dr. Beth P. Smith for their contributions.

References

1 J. Noble, C.A. Munro, V.S. Prasad and R. Midha, Analysis of upper and lower extremity peripheral nerve injuries in a population of patients with multiple injuries, *J Trauma* **45** (1998), pp. 116–122.

2 R. Midha, Epidemiology of brachial plexus injuries in a multitrauma population, *Neurosurgery* **40** (1997), pp. 1182–1188 discussion 1188–1189.

3 A. Praemer, S. Furner and D.P. Rice, Musculoskeletal conditions in the United States, American Academy of Orthopaedic Surgeons, Rosemont, IL (1999), pp. 162–163.

4 H. Thomas, A. Conrads, K.H. Phan, M. van de Locht and H. Zahn, In vitro reconstitution of wool intermediate filaments, *Int J Biol Macromol* **8** (1986), pp. 258–265.

5 A. Tachibana, Y. Furuta, H. Takeshima, T. Tanabe and K. Yamauchi, Fabrication of wool keratin sponge scaffolds for long-term cell cultivation, *J Biotechnol* **93** (2002), pp. 165–170.

6 L.R. Williams, F.M. Longo, H.C. Powell, G. Lundborg and S. Varon, Spatial-temporal progress of peripheral nerve regeneration within a silicone chamber: parameters for a bioassay, *J Comp Neurol* **218** (1983), pp. 460–470.

7 Q. Zhao, L.B. Dahlin and M. Kanje, Repair of the transected rat sciatic nerve: matrix formation within implanted silicone tubes, *Restor Neurol Neurosci* **5** (1993), pp. 197–204.

8 P. Sierpinski, J. Garrett, J. Ma, P. Apel, D. Klorig and T. Smith *et al.*, The use of keratin biomaterials derived from human hair for the promotion of rapid regeneration of peripheral nerves, *Biomaterials* **29** (2008), pp. 118–128.

9 R.F. Valentini, P. Aebischer, S.R. Winn and P.M. Galletti, Collagen- and laminin-containing gels impede peripheral nerve regeneration through semipermeable nerve guidance channels, *Exp Neurol* **98** (1987), pp. 350–356.

10 R.O. Labrador, M. Butí and X. Navarro, Influence of collagen and laminin gels concentration on nerve regeneration after resection and tube repair, *Exp Neurol* **149** (1998), pp. 243–252.

11 B.J. Wong and D.E. Mattox, Experimental nerve regeneration: a review, *Otolaryngol Clin North Am* **24** (1991), pp. 739–752.

12 K.W. Horch and S.J. Lisney, On the number and nature of regenerating myelinated axons after lesions of cutaneous nerves in the cat, *J Physiol* **313** (1981), pp. 275–286.

13 B.G. Jiang, X.F. Yin, D.Y. Zhang, Z.G. Fu and H.B. Zhang, Maximum number of collaterals developed by one axon during peripheral nerve regeneration and the influence of that number on reinnervation effects, *Eur Neurol* **58** (2007), pp. 12–20.

14 T.M. Brushart, Motor axons preferentially reinnervate motor pathways, *J Neurosci* **13** (1993), pp. 2730–2738.

15 G. Terenghi, Peripheral nerve regeneration and neurotrophic factors, *J Anat* **194** (1999), pp. 1–14.

16 J. Kobayashi, S.E. Mackinnon, O. Watanabe, D.J. Ball, X.M. Gu and D.A. Hunter *et al.*, The effect of duration of muscle denervation on functional recovery in the rat model, *Muscle Nerve* **20** (1997), pp. 858–866.

CHAPTER VII

Repair of Critical Size Peripheral Nerve Defects in Rabbits Using Keratin Hydrogel Scaffolds

Paulina Sierpinski Hill[1], Peter J. Apel[2], Jonathan Barnwell[2], Tom Smith[2], L. Andrew Koman[2], Anthony Atala[1], Mark Van Dyke[1]

[1] Wake Forest Institute for Regenerative Medicine

[2] Department of Orthopaedic Surgery

The following manuscript has not been submitted. Paulina Sierpinski prepared the manuscript. Dr. Mark Van Dyke acted in an advisory and editorial capacity.

ABSTRACT

Limited satisfactory guidance strategies currently exist for bridging peripheral nerve defects. Entubulation of transected nerves using bioabsorbable nerve guides is a promising alternative to end-to-end coaptation and sural nerve autografting, but full functional recovery is rarely achieved using this technique. Numerous studies have suggested that scaffold-based conduit fillers may promote axon regeneration, but no neuroinductive biomaterial filler has been identified. Keratin biomaterials research in our lab has led to the development of a novel, potentially neuroinductive matrix filler made of proteins extracted from human hair. Previously, we showed that insertion of a keratin hydrogel scaffold into a nerve guide actively stimulates regeneration in a mouse model superior to that of empty conduits (1,2). The goal of the present study was to develop a critical size peripheral nerve defect model in a rabbit, and assess the effectiveness of a keratin hydrogel filler in the repair of larger gaps. Our results show that insertion of a keratin hydrogel into a bioabsorbable nerve guide promotes neuromuscular recovery, as determined by functional and histological outcomes. The presence of a keratin hydrogel resulted in a 79% improvement in conduction delay and a 74% increase in amplitude recovery over unfilled conduits. Histological assessment showed that keratin treated nerves were approximately 30% larger in size, had 47% more myelinated axons, and myelin sheaths that were 33% thicker than nerves that regenerated through empty conduits. This data supports the neuroinductive properties of keratin biomaterials reported previously, and suggests that keratin hydrogel fillers have potential to be used clinically.

INTRODUCTION

Peripheral nerve injuries can be caused by motor vehicle accidents, sports injuries, gunshot and stab wounds, work and home accidents, and tumor resection. Regardless of severity, nerve injuries are debilitating and interfere with an individual's ability to function at work and in daily life. Fewer than 60% of individuals return to work after suffering a median or ulnar nerve injury, and considerably less individuals regain a normal quality of life in cases of brachial plexus injury, even after undergoing surgical repair (3,4). The standard treatment for peripheral nerve injuries is primary repair or sensory nerve autografting. Unfortunately, conditions such as lack of autologous tissue, infection, delay in repair, and severe trauma often prevent these types of repairs from being possible (5).

Nerve conduits provide another option to this challenging problem but remain inferior to autografts in restoring functional recovery, even over short distances (6). Nerve conduits are advantageous because they allow for tension-free repair of even the most severe extremity injuries without requiring donor tissue to bridge the defect. Entubulation of damaged nerves has been shown to facilitate regeneration by preventing fibroblast invasion, supporting host Schwann cell migration and directing axonal sprouting (7). Bioabsorbable nerve guides made of collagen (NeuraGen, Integra LifeSciences), polyglycolic acid (GEM Neurotube, Synovis Micro Companies Alliance), and poly(dl-lactide-ε-caprolactone) (Neurolac, Polyganics) are currently approved for clinical use (8-10). However, empty conduits are limited in their ability to guide regenerating axons since they lack a scaffold across which regeneration can take place (11).

With the commercialization of biocompatible, bioabsorbable conduits, the experimental focus has recently shifted from the development of novel conduit materials to the addition of biologically active luminal fillers inside existing conduits. The insertion of luminal fillers composed of cellular, neurotrophic and scaffold based fillers has been shown to facilitate regeneration to varying degrees (12). Extracellular matrix (ECM) proteins such as collagen, laminin and fibronectin in the form of gels, fibers and sponges inserted into a nerve guide have been shown to be neuroconductive, in that they are capable of supporting axon growth without the addition of cellular or growth factor components (13-16). However, no neuroinductive scaffold-based fillers capable of acting directly on regenerative cells to promote regeneration beyond clinical limits currently exist.

Keratin has recently been identified as a promising biomaterial that may have neuroinductive properties (2). Keratins are a family of tough, fibrous proteins that form protective tissues such as hair, fur, feathers, nails and hooves. We have shown that keratins can be effectively extracted from human hair and processed into hydrogel scaffolds for use as nerve conduit fillers. Mouse nerves treated with a keratin gel resulted in a >300% improvement in conduction delay and ~150% increase in the compound muscle action potential (CMAP) at 6 weeks (2). Moreover, we showed that this regeneration was partly mediated by keratin's ability to act on Schwann cells by promoting their proliferation, migration and adhesion *in vitro*. In a follow up study assessing long-term functional outcomes, we showed that a keratin hydrogel filler resulted in permanent functional restoration comparable to that of autograft (1).

The goal of this study was to develop a critical size nerve defect model in a rabbit, and test the effectiveness of a keratin hydrogel filler in repairing clinically challenging gaps. To accomplish this, we developed a tibial nerve injury and repair model using Integra's FDA approved NeuraGen conduits, a leading product for entubulation repair. This model was used to test the ability of a keratin hydrogel to serve as a neuroinductive conduit filler over critical size peripheral nerve defects.

METHODS

Keratin Biomaterial Preparation

Keratin hydrogels were prepared as described previously (2). Briefly, human hair was obtained from a local barber shop and treated with peracetic acid to solubilize the keratins. Residual oxidant was removed and keratins were extracted into excess tris base and deionized (DI) water. The dialysate was neutralized, dialyzed, freeze dried and ground into a fine powder. The powder was reconstituted in phosphate buffered saline (PBS) at 15% (w/v) to generate keratin hydrogels. Gels were sterilized by γ-irradiation at 850 krad using a ^{60}Co

Animal Model

<u>Phase I – Critical size defect model development</u>

New Zealand White male rabbits (3.5-4 kg, n=22) were randomized into one of four groups: 1) 2 cm-2 months, 2) 2 cm-3 months, 3) 3 cm-3 months or 4) 3 cm-4 months. Animals were placed under general anesthesia and the left limb was shaved and cleansed with betadine. A longitudinal incision was made along the left hind limb and the sciatic nerve was exposed. The tibial nerve was isolated by microsurgical dissection and transected 1 cm proximal to its insertion into the gastrocnemius muscle. A 2 or 3 cm defect was generated by excising a carefully measured portion of the nerve and allowing the proximal and distal ends to retract. Each animal underwent repair with a NeuraGen nerve guide (1.5 mm internal diameter, 2 or 3 cm in length) composed of bovine type I collagen (Integra LifeSciences, Plainsboro, NJ), (Fig. 1A). The nerve conduit was secured in place with 8-0 non-absorbable nylon sutures. A horizontal mattress suture was used to pull the proximal and distal ends of the nerve into the conduit. A Tefla pad was placed over the surgical site and secured with skin staples. E-collars were placed around the necks of each rabbit to prevent self-mutilation. In a minority of cases, autotomy was noted. These animals were bandaged and monitored daily. Bandages were changed every 7-10 days and removed when autotomy subsided.

Phase 2 – Efficacy of keratin hydrogel as a nerve guide filler

After establishing the critical defect size, 40 New Zealand white male rabbits (3.5-4 kg) were randomized into 3 treatment groups: 1) Empty conduit (n=15), 2) Keratin-filled conduit (n=16) and 3) Sural Nerve Autograft (n=9). In the keratin group, collagen conduits were pre-filled with keratin gel under sterile conditions (Fig. 1B) and implanted as described above (Fig.

1C). In the autograft group, approximately 7 cm of the sural nerve was harvested and a 2 cm three-cable interpositional graft was used to bridge the defect using 10-0 non-absorbable nylon sutures. Wound dressings were applied over the incision site and E-collars were placed around the neck of each animal. Animals were closely monitored for autotomy of the toes and feet bandaged when necessary.

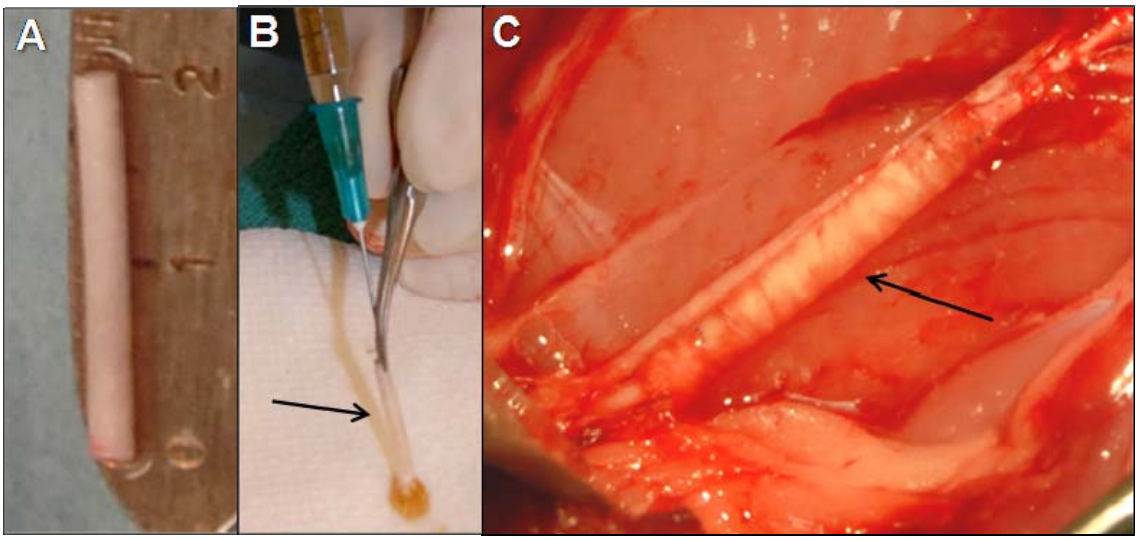

Figure 1. NeuraGen collagen nerve guides were rehydrated in PBS and measured to ensure accurate conduit length immediately prior to implantation (A). A pre-sterilized keratin hydrogel was injected into the lumen of rehydrated nerve guides (B), and microsurgically implanted across a tibial nerve defect in a rabbit (C).

Electrophysiology

Each animal underwent electrophysiological testing at their respective time point. Under general anesthesia, the nerve was exposed and the compound muscle action potential (CMAP) of the tibial nerve-gastrocnemius complex was measured using a Sierra Wave system (Caldwell Laboratories, Kennewick, WA). The peroneal nerve was transected prior to testing

to eliminate artifact. A bipolar stimulating electrode was placed on the tibial nerve proximal to the defect at the distance of the obturator externus tendon. A reference needle electrode was placed on the calcaneous and a surface recording electrode on the gastrocnemius muscle belly. The nerve was stimulated with a constant current of 1.0 mAmp for 0.1 ms. The contralateral limb was tested first and served as an internal reference for each animal. The experimental side was tested immediately afterwards. All parameters measured were expressed as a percentage of the contralateral internal reference control. Following testing, rabbits were sacrificed by intracardial injection of potassium chloride. The gastrocnemius muscles were isolated bilaterally and immediately weighed to determine degree of muscle atrophy.

Histology and Histomorphometry

All intact nerves, regardless of electrophysiological outcomes, were harvested for histological examination. A 6-0 Vicryl suture was inserted into the proximal end of the nerve at time of harvest to provide anatomical orientation during analysis. Nerves were fixed in 10% neutral buffered formalin (NBF) for 48 hours. Nerves were rinsed in phosphate buffered saline (PBS), osmium tetroxide treated, dehydrated in graded ethanol solutions and embedded in Epon resin. Sections (1 um) were cut in cross-section using an LKB III Ultramicrotome (LKB-Produkter A.B., Broma, Sweden), from the middle portion of the regenerated nerve (1 cm). Sections were stained with 1% toluidine blue and mounted on slides for analysis. Photomicrographs were captured on a Zeiss microscope (Carl Zeiss, Jena, Germany). Nerve

area and axon quantification was performed using Image J and SigmaScan Pro 5.0 (SYSTAT, Chicago, IL) semi-automated digital imaging software.

Statistical Analysis

All numerical data were analyzed and comparisons between treatment groups were made using SigmaStat. A single-factor analysis of variance (ANOVA) employing a Student-Newman-Keulls multiple comparison post-hoc test was used to determine statistical significance ($p<0.05$). All results are reported as mean ± standard error of the mean (SEM). A Fisher's exact probability test was used to determine differences in the total number of animals that regenerated across the critical size defect in each group.

RESULTS

Phase I – Critical size defect model

The critical size defect and time point at which less than 50% of empty conduit repaired animals had measurable regeneration by electrophysiology was found to be 2 cm at 3 months. Two out of five, or 40% of the animals had measurable action potentials at the gastrocnemius muscle following 3 months of regeneration across a 2 cm gap. No animals showed measurable regeneration across a 3 cm defect at 3 months, and only one animal in both the 2 cm-2 month and 3 cm-4 month groups showed detectable neuromuscular recovery at their respective time point.

Phase 2 – In vivo regeneration across critical size defect

Of the 40 rabbits, six were eliminated from the study due to premature death or euthanasia as a result of excessive autotomy of the foot. In the empty group, 5/15 (33%) of the animals had measurable regeneration by electrophysiology compared to 6/12 (50%) in the keratin group and 7/7 (100%) in the autograft group. A Fisher's exact probability test was used to determine if treatment had an effect on the number of animals that regenerated in each group. The number of animals with measurable neuromuscular recovery was significantly higher in the autograft group than in both the empty ($p=0.004$) and keratin ($p=0.034$) groups. No difference was observed between the total number of animals that regenerated across a 2 cm gap in empty versus keratin groups ($p=0.314$).

Post-op recovery and muscle tone

Incisional wounds were covered with a bandage and healed quickly with no signs of infection. Autotomy of the operated foot was observed in 17 of 40 rabbits, starting as early as 3-4 days after surgery. In some cases, autotomy was minor and temporary. In others, it was excessive, lasted for the duration of the study and led to amputation of toes due to bone exposure. Autotomy was especially prevalent in the autograft group where 77.8% of the animals displayed moderate to severe scratching, biting, or self-amputation of nails and/or digits. There

was no difference in the degree of self-mutilation between empty (40%) and keratin treated (36%) groups. Three animals developed decubitous pressure ulcers on the heels of their feet, two of which were in the autograft group.

Macroscopic observation at time of harvest showed that all 40 grafts were intact and continuous along the length of the nerve down to the gastrocnemius muscle. Closer examination under magnification showed an absence of inflammation and heavy scarring in all treatment groups. Non-absorbable sutures used to secure the proximal and distal nerve ends at time of repair were used to determine the location of the collagen conduit along the nerve. The collagen conduit itself was grossly indistinguishable from the proximal and distal nerve segments by 3 months. Gastrocnemius muscle tone was decreased and fatty tissue deposition was increased in all treatment groups compared to the contralateral side.

Electrophysiology

The two electrophysiological parameters measured were conduction delay and amplitude of the compound muscle action potential (CMAP). The conduction delay is the delay in nerve impulse transmission down the axon to the muscle, and, amplitude, or CMAP, is the magnitude of the impulse that reaches the muscle. Both parameters were expressed as a percentage of the contralateral control. Of the animals that did regenerate across the critical size defect, a significant improvement in functional recovery was observed in the keratin group compared to both empty and autograft groups. After 3 months of regeneration,

electrophysiology testing showed that the conduction delay was significantly better ($p<0.05$) in the keratin group (4.56%±2.23%) over both the empty (21.54%±2.17%) and autograft (36.93%±4.82%) groups (Fig. 2A). The amplitude recovery in the CMAP was significantly better in the keratin group (55.31%±11.92%) than in the empty group (14.51%±1.18%), (Fig. 2B). CMAP recovery was also larger in the keratin versus the autograft group (35.27%±4.12%) but this data did not reach statistical significance.

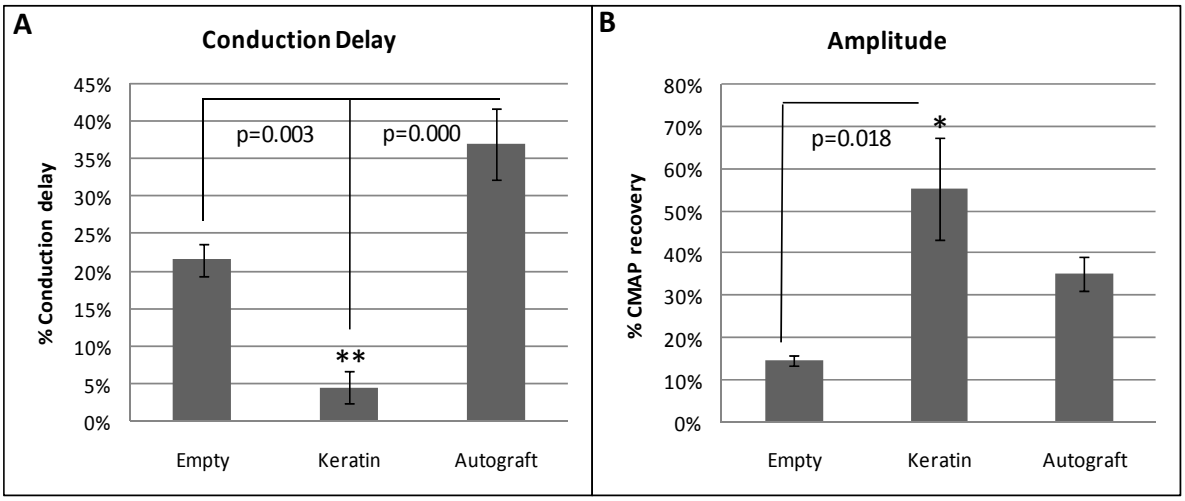

Figure 2. Three months following injury and repair, electrophysiological testing was performed to assess neuromuscular recovery. The presence of a keratin hydrogel filler resulted in a statistically significant improvement in the conduction delay over both empty and autograft groups (A), and a significantly higher amplitude compared to the empty group (B).

Preservation of muscle weight

There was no statistically significant difference in the gastrocnemius muscle weights between each group, indicating that the degree of muscle deterioration was equivalent independent of treatment. Muscle atrophy was slightly improved in the keratin group

(53.05%±5.27%), versus 60.92%±2.13% and 56.36%±1.54% in the empty and autograft groups respectively (Fig. 3).

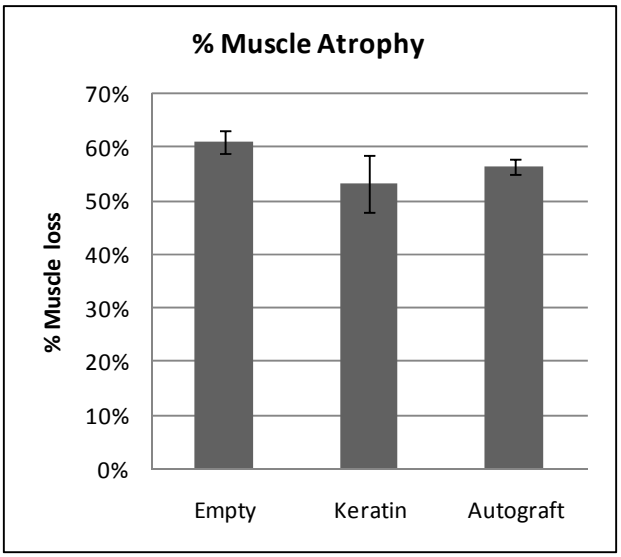

Figure 3. Percent gastrocnemius muscle atrophy following 3 months of regeneration. The gastrocnemius muscles of both legs were excised and weighed immediately following functional testing. No significant difference in percent muscle loss was observed between experimental groups.

Histology and Histomorphometry

Histological analysis was performed on all 34 animals that reached the 3 month time point without any major complications, even if functional regeneration was not detected by electrophysiology. The mid-portion of each graft was cross-sectioned and stained with toluidine blue. Myelinated axons were observed in all treatment groups at the mid portion of the graft (Fig. 4).

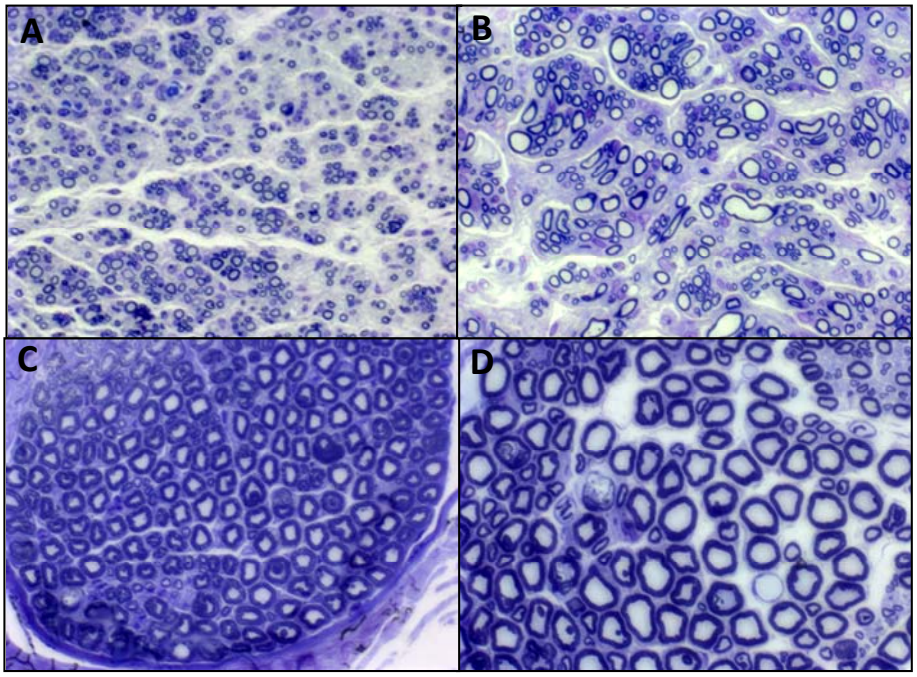

Figure 4. Representative images of toluidine blue stained cross sections of regenerated nerves in (A) empty, (B) keratin, (C) autograft, and (D) native nerve groups at 400X magnification.

Blinded quantitative analysis using image analysis software revealed an increase in the overall nerve area, total axons per nerve and total axon area in the keratin group compared to both the empty conduit and autograft groups (Fig. 5). Nerves that regenerated through an empty conduit had a mean area of 0.69±0.16 mm^2, and were approximately 30% smaller in size than keratin treated nerves (1.00±0.21 mm^2), (Fig. 5A). Autograft nerves were the smallest in size with an average area of 0.43±0.07 mm^2. The total number of axons per regenerated nerve was found to be 1.44±0.34 million in the keratin group, 0.77±0.22 million in the empty group, and 0.21±0.05 million in the autograft group (Fig. 5B). In addition, keratin treated nerves had a total axon area that was on average 47.6% and 76.1% larger than empty and autograft controls, respectively (Fig. 5C). There was no significant difference between the myelinated

axon size in the empty (4.340 ± 0.496 μm) and keratin (4.341± 0.548 μm) groups. However, the average myelinated axon diameter in the autograft group (7.196± 0.666 μm) was approximately 60% higher than in both the empty and keratin groups ($p<0.05$), (Fig. 5D). In the empty group, the myelin sheath of the regenerated axons was found to be thinner (0.55±0.03 μm) than in both the keratin (0.82±0.12) and autograft (0.89±0.04) groups (Fig. 5E). There was no statistical difference between the myelin thickness in keratin and autograft treated nerves ($p>0.05$), indicating that regenerating axons in the keratin group were equally well myelinated compared to the autograft group. The axon to nerve fiber ratio, commonly referred to as the G-ratio, was found to be statistically equivalent in all groups: Empty (0.85±0.03), Keratin (0.82±0.12), and Autograft (0.87±0.0.1), (Fig. 5F).

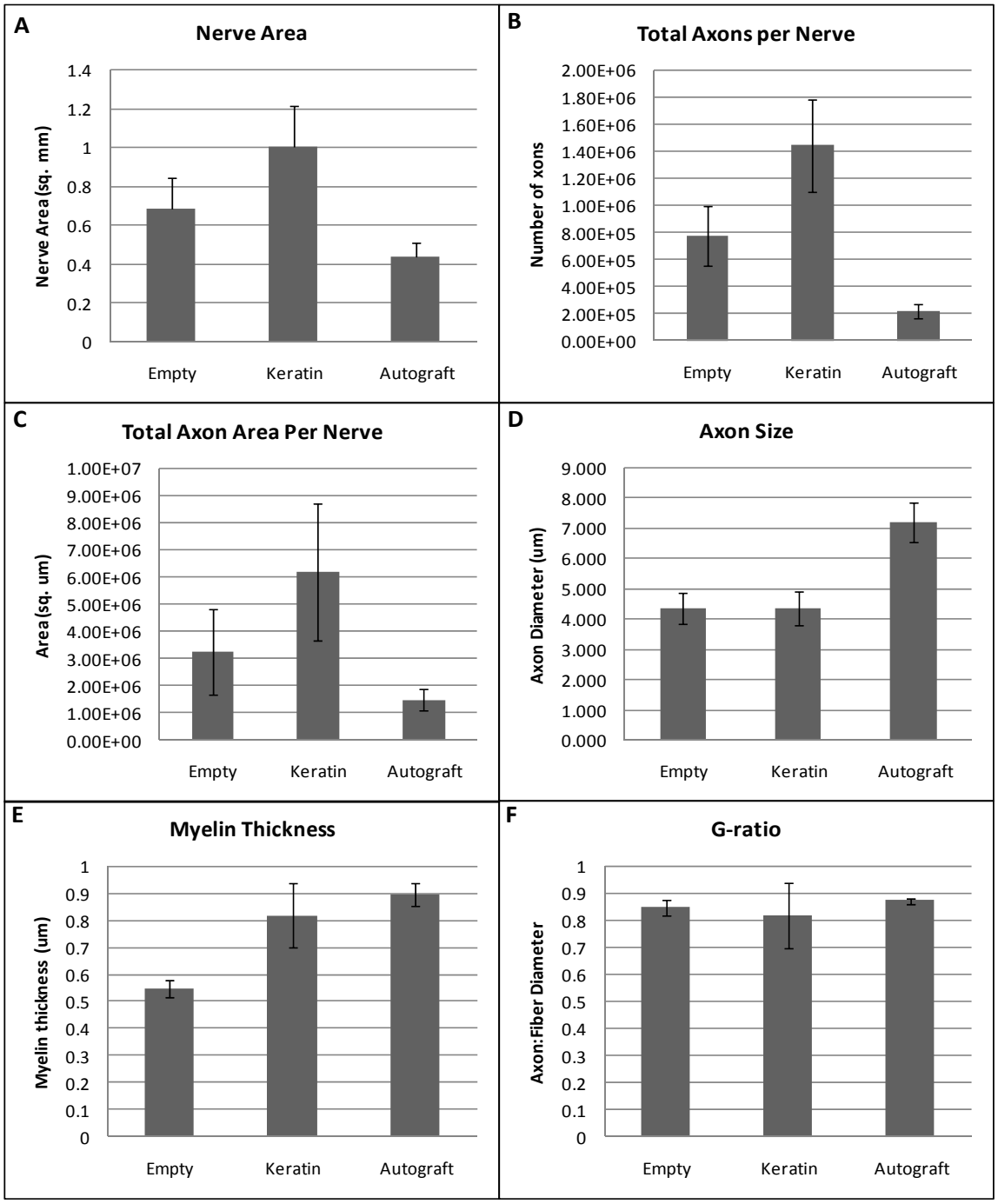

Figure 5. Histomorphometric analysis of nerve cross sections in empty, keratin and autograft groups. Keratin treated nerves were larger in size (A), had more axons (B) and a larger total axon area (C) than both empty and autograft controls. There was no difference in the average axon size between empty and keratin groups (D). The average myelin thickness of regenerated axons in keratin and autograft groups was statistically equivalent, and higher than in the empty group (E). The G-ratio was unchanged between treatment groups (F).

DISCUSSION

Establishing a reliable, large animal model of peripheral nerve injury and repair is critical to the development of conduit fillers for clinical use. The rat sciatic nerve defect model is the most commonly used model for assessing luminal fillers. As convenient as this model is in laboratory settings, rodents have a superior neuroregenerative capacity compared to other mammals, and are limited in their ability to predict therapeutic efficacy (17). Numerous synthetic and naturally derived matrices have been effective in supporting regeneration across 1-2 cm gaps in the rat (12). However, as promising as some of these therapies were in rodents, none of these experimentally tested fillers have been translated clinically.

In the present study, we sought to develop a critical size nerve defect model in a rabbit using clinically approved bioabsorbable nerve guides. Our definition of a critical size defect was the gap size and time point at which less than 50% of the empty conduit controls had measurable regeneration by electrophysiology. We found the critical size defect in a New Zealand White male rabbit tibial nerve model to be 2 cm at 3 months. The observed critical size defect is somewhat smaller than what is to be expected on the basis of rodent studies. However, when one takes into consideration the difference in the axon growth rate between the two species, and the stages of motor function recovery, such a small critical size defect is not surprising. The regeneration rate in a rat is approximately 3.5-4 mm per day, compared to 2 mm per day in a rabbit (18). After crossing the 2 cm defect, regenerating axons must re-grow through the distal stump down to the target muscle. Even then, axonal reinnervation of the

neuromuscular junction is not synonymous with return of function since a complex maturation process lasting up to 2 years, is known to precede functional recovery (19). Finally, return of motor function is last to take place, and follows sympathetic, pain, temperature and proprioception recovery (18). Thus, it is not surprising that motor functional recovery at 3 months could only be detected in less than 50% of control animals over a 2 cm defect. Since the average rate of outgrowth in middle-aged healthy human subjects is estimated to be 1 mm per day (20), the rabbit model developed here more closely resembles the regeneration rate of humans than the rat, and may be more predictive of clinical efficacy.

The main objective of this study was to assess the ability of a keratin hydrogel filler to serve as a neuroinductive provisional matrix over a critical size defect. The presence of a keratin gel was found to significantly improve regeneration, as measured by functional and histological outcomes. Although the total number of animals that regenerated across the defect was similar in empty and keratin groups, the quality of the regeneration was substantially improved when a keratin hydrogel was injected into the conduit. The conduction delay, or speed of electrical impulse transmission, improved by over 75% compared to both empty and autograft controls. The CMAP, or size of the electrical impulse, was 74% larger in the keratin treated nerves than in empty, and 36% larger than in autografts. This recovery of function is likely due to the provisional matrix provided by the keratin hydrogel filler. In empty conduits, formation of a fibrin clot - the body's own provisional matrix - is the rate limiting step in axon regeneration (21). When an exogenous scaffold such as keratin is not provided, fibrin matrix formation is initiated 24-48 hours following repair. By 5-7 days, sufficient fibrin material accumulates

within the conduit and a continuous bridge forms across the gap. Natural formation of such a matrix is dependent on many factors, including the size and severity of the injury, the degree of vascularization and the condition of peripheral tissues (22). In large defects, a homogenous fibrin matrix does not form, or if one forms, it is prematurely degraded prior to remodeling by Schwann cells (23). The fibrin matrix is enzymatically broken down by proteases secreted from infiltrating macrophages, Schwann and endothelial cells, as well as axonal growth cones (24). Since there are no known keratin proteases in mammals, the keratin hydrogel matrix is not degraded prematurely and permits host cells to lay down their own matrix, leading to the formation of bands of Bungner, or endoneurial tubes that guide sprouting axons. Importantly, with a degradation rate that is estimated to be approximately 1 month through a semi-permeable collagen conduit, the keratin hydrogel is not present long enough to impede axon growth into the distal stump as has been shown by other investigators (25).

One of the main shortcomings of other naturally derived scaffold based fillers is premature dissolution or prolonged persistence of the matrix. Many ECM protein based fillers are rapidly degraded by proteases which are readily secreted at the site of injury (26). Others, such a laminin-based gel, have been shown to be inhibitory to axon regeneration due to prolonged degradation rates *in vivo.* Madison, et al. found that a laminin-based gel significantly increased the initial rate of axonal outgrowth in a mouse model at 2 weeks (27), but that this same regeneration process is inhibited by the presence of the laminin filler at 6 weeks (28). Keratin fillers are advantageous because they are degraded by hydrolysis, and are unaffected by the proteolytic microenvironment of the regenerating nerve. As a result, the degradation rate of

keratin biomaterials is predictably consistent across species, and can be further optimized and controlled. This characteristic may be particularly important in cases where nerve regeneration is impaired, as in the elderly or in patients with underlying diseases that affect nerve growth. For such individuals, one may envision engineering a slower degrading keratin hydrogel filler that is capable of maximizing the diminished regenerative capacity seen in these patients.

In addition to providing a physical three dimensional matrix that degrades in a timely manner, keratin biomaterials may be superior to previously used nerve conduit fillers due to their ability to act as a mimic of the ECM. Keratin biomaterial substrates have been found to facilitate adhesion to a wide variety of cell types by providing fibronectin-like binding motifs (2,29,30). Further neuroinductive properties of keratin biomaterials could be due to the presence of residual growth-promoting factors extracted from the hair fiber (2).

Histologically, the presence of a keratin hydrogel filler resulted in nerves that were larger in size (Fig. 5A), had more axons (Fig. 5B) and a larger total axon area (Fig. 5C) than empty conduit controls. This histological data supports the observed functional improvements seen in animals treated with a keratin hydrogel filler. Taking into account that three months is an early time point in the regeneration process, and substantial remodeling must still take place, the presence of more axons in the keratin group suggests that the degree of functional recovery may be even more substantial over empty and autograft controls at later time points. It is well documented that regenerating axons are smaller in diameter and unmyelinated in the early stages of regeneration (2,31). As maturation progresses, axons acquire a myelin sheath that thickens over time and is followed by a gradual increase in axon diameter. The large myelin

thickness seen in the keratin group suggests that regenerating axons may be further along in the maturation process than those regenerating through empty conduits. This is further supported by the significant improvements seen in nerve impulse transmission, since conduction delay is directly dependent on myelin thickness (2,32).

One limitation of this study is the failure to histologically assess axonal regeneration in the distal nerve stump. All cross-sectional histology and histomorphometric analysis was performed at the mid-portion of the regenerated grafts. The time to reinnervation of the neuromuscular junction has been shown to be the single most important predictor to influence the level of outcome following nerve repair (33). Therefore, histological analysis of axon regeneration in the distal stump, immediately proximal to muscle innervation, will likely be more predictive of long-term functional outcomes. However, based on the significant improvement in motor function recovery in keratin treated nerves, it is expected that axons regenerating through a keratin hydrogel reached the neuromuscular junction faster and in larger numbers than those that regenerated through empty tubes.

This study shows that keratin biomaterials made from human hair actively stimulate regeneration over a critical size defect in a large animal model. Insertion of a keratin hydrogel into a collagen nerve guide resulted in significantly better neuromuscular recovery than in unfilled conduits, with functional restoration comparable to that of autografts. However, keratin treated nerves did not regenerate as consistently as autograft treated nerves where exogenous Schwann cells were present. Nevertheless, these data support the neuroinductive properties of keratin biomaterials previously reported by our lab, and suggests that

incorporation of a keratin hydrogel filler into existing nerve guides may promote nerve growth beyond current clinical limits with functional outcomes equivalent to or better than autograft in some cases.

ACKNOWLEDGEMENTS

The authors gratefully acknowledge the funding support provided by the Errett Fisher Foundation, as well as the Department of Orthopaedic Surgery and OREF foundation for funding support of co-authors Apel and Barnwell. The authors would like to thank Integra Life Sciences for supplying us with FDA approved collagen nerve guides and Rawad Hamzi for assistance with histomorphometry.

References

(1) Apel PJ, Garrett JP, Sierpinski P et al. Peripheral nerve regeneration using a keratin-based scaffold: long-term functional and histological outcomes in a mouse model. *J Hand Surg [Am].* 2008;33(9):1541-1547.

(2) Sierpinski P, Garret J, Ma J et al. The Use of Keratin Biomaterials for the Promotion of Rapid Regeneration of Peripheral Nerves. *Biomaterials.* 2007.

(3) Lundborg G. A 25-year perspective of peripheral nerve surgery: evolving neuroscientific concepts and clinical significance. *J Hand Surg [Am].* 2000;25(3):391-414.

(4) Kline DG. Surgical repair of brachial plexus injury. *J Neurosurg.* 2004;101(3):361-363.

(5) Terris DJ, Fee WE, Jr. Current issues in nerve repair. *Arch Otolaryngol Head Neck Surg.* 1993;119(7):725-731.

(6) Dahlin LB, Lundborg G. Use of tubes in peripheral nerve repair. *Neurosurgery Clinics of North America.* 2001;12(2):341-+.

(7) Belkas JS, Shoichett MS, Midha R. Peripheral nerve regeneration through guidance tubes. *Neurological Research.* 2004;26(2):151-160.

(8) Rosson GD, Williams EH, Dellon AL. Motor nerve regeneration across a conduit. *Microsurgery.* 2009;29(2):107-114.

(9) Farole A, Jamal BT. A bioabsorbable collagen nerve cuff (NeuraGen) for repair of lingual and inferior alveolar nerve injuries: a case series. *J Oral Maxillofac Surg.* 2008;66(10):2058-2062.

(10) Bertleff MJ, Meek MF, Nicolai JP. A prospective clinical evaluation of biodegradable neurolac nerve guides for sensory nerve repair in the hand. *J Hand Surg [Am].* 2005;30(3):513-518.

(11) Williams LR, Longo FM, Powell HC et al. Spatial-temporal progress of peripheral nerve regeneration within a silicone chamber: parameters for a bioassay. *J Comp Neurol.* 1983;218(4):460-470.

(12) Chen MB, Zhang F, Lineaweaver WC. Luminal fillers in nerve conduits for peripheral nerve repair. *Annals of Plastic Surgery.* 2006;57(4):462-471.

(13) Madison R, Dasilva CF, Dikkes P et al. Increased Rate of Peripheral-Nerve Regeneration Using Bioresorbable Nerve Guides and A Laminin-Containing Gel. *Experimental Neurology.* 1985;88(3):767-772.

(14) Toba T, Nakamura T, Shimizu Y et al. Regeneration of canine peroneal nerve with the use of a polyglycolic acid-collagen tube filled with laminin-soaked collagen sponge: A comparative study of collagen sponge and collagen fibers as filling materials for nerve conduits. *Journal of Biomedical Materials Research.* 2001;58(6):622-630.

(15) Lee DY, Choi BY, Park JH et al. Nerve regeneration with the use of PLGA coated collagen tube filled with collagen gel. *Journal of Cranio-Maxillofacial Surgery.* 2006;34:50-56.

(16) Madison RD, Dasilva CF, Dikkes P. Entubulation Repair with Protein Additives Increases the Maximum Nerve Gap Distance Successfully Bridged with Tubular Prostheses. *Brain Research.* 1988;447(2):325-334.

(17) Taras JS, Nanavati V, Steelman P. Nerve conduits. *J Hand Ther.* 2005;18(2):191-197.

(18) Lundborg G. Nerve Injury and Repair. Elsevier Inc., 1988.

(19) Ide C. Nerve regeneration and Schwann cell basal lamina: observations of the long-term regeneration. *Arch Histol Jpn.* 1983;46(2):243-257.

(20) Rummler LS, Gupta R. Peripheral nerve repair: a review. *Current Opinion in Orthopaedics.* 2004;15:215-219.

(21) McDonald D, Cheng C, Chen Y, Zochodne D. Early events of peripheral nerve regeneration. *Neuron Glia Biol.* 2006;2(2):139-147.

(22) Midha R, Zager EL. Nerve regeneration and nerve repair. *Neurol Res.* 2008;30(10):997-998.

(23) Johnson EO, Zoubos AB, Soucacos PN. Regeneration and repair of peripheral nerves. *Injury-International Journal of the Care of the Injured.* 2005;36:S24-S29.

(24) Williams LR. Exogenous Fibrin Matrix Precursors Stimulate the Temporal Progress of Nerve Regeneration Within A Silicone Chamber. *Neurochemical Research.* 1987;12(10):851-860.

(25) Valentini RF, Aebischer P, Winn SR, Galletti PM. Collagen- and laminin-containing gels impede peripheral nerve regeneration through semipermeable nerve guidance channels. *Exp Neurol.* 1987;98(2):350-356.

(26) Siebert H, Dippel N, Mader M et al. Matrix metalloproteinase expression and inhibition after sciatic nerve axotomy. *J Neuropathol Exp Neurol.* 2001;60(1):85-93.

(27) Madison R, Da Silva CF, Dikkes P et al. Increased rate of peripheral nerve regeneration using bioresorbable nerve guides and a laminin-containing gel. *Exp Neurol.* 1985;88(3):767-772.

(28) Madison RD, da Silva C, Dikkes P et al. Peripheral nerve regeneration with entubulation repair: comparison of biodegradeable nerve guides versus polyethylene tubes and the effects of a laminin-containing gel. *Exp Neurol.* 1987;95(2):378-390.

(29) Tachibana A, Furuta Y, Takeshima H et al. Fabrication of wool keratin sponge scaffolds for long-term cell cultivation. *Journal of Biotechnology.* 2002;93(2):165-170.

(30) Tachibana A, Kaneko S, Tanabe T, Yamauchi K. Rapid fabrication of keratin-hydroxyapatite hybrid sponges toward osteoblast cultivation and differentiation. *Biomaterials.* 2005;26(3):297-302.

(31) Jiang BG, Yin XF, Zhang DY et al. Maximum number of collaterals developed by one axon during peripheral nerve regeneration and the influence of that number on reinnervation effects. *Eur Neurol.* 2007;58(1):12-20.

(32) Sanders FK, Whitteridge D. Conduction velocity and myelin thickness in regenerating nerve fibres. *J Physiol.* 1946;105(2):152-174.

(33) Armstrong SJ, Wiberg M, Terenghi G, Kingham PJ. ECM molecules mediate both Schwann cell proliferation and activation to enhance neurite outgrowth. *Tissue Eng.* 2007;13(12):2863-2870.

CHAPTER VIII

Structural Dependence of Keratin Biomaterials on Integrin-Mediated Activation of Schwann Cells

Paulina Sierpinski Hill, Bernard Tawfik, Anthony Atala and Mark Van Dyke

Wake Forest Institute for Regenerative Medicine, Wake Forest University School of Medicine, Winston Salem, NC 27157.

The following manuscript has not been submitted. Paulina Sierpinski prepared the manuscript.

Dr. Mark Van Dyke acted in an advisory and editorial capacity.

ABSTRACT

Keratins are a family of structural proteins found in the protective tissues of vertebrates, including human hair. Human hair keratins (HHKs) consist mainly of alpha and gamma keratins, two protein families which possess distinct structural differences (1). Previous work has shown that HHKs can be extracted from hair fibers and processed into hydrogels that promote regeneration of peripheral nerves (2,3). We hypothesize that this rapid regeneration is due to keratin's ability to mediate Schwann cell behavior. The goal of this study was to investigate the mechanism by which HHKs activate Schwann cells, and to determine if this activation is dependent on HHK structure. A bioinformatics approach was used to analyze published HHK sequences for the presence of peptide binding domains, and revealed that HHKs are rich in amino acid motifs known to interact with cell surface integrins. Crude HHK preparations consisting of extractable alpha and gamma keratins were fractionated based on structural criteria, and characterized by quantitative amino acid analysis. The ability of crude and fractionated HHKs to promote Schwann cell proliferation was tested. The gamma family of HHKs were found to have the most pronounced stimulatory effect on Schwann cell growth, both in acidic and basic forms. The nature of the Schwann cell/keratin interaction was investigated by Western blot. Schwann cells were cultured on keratin substrates for 72 hours and analyzed for changes in integrin expression. Analysis showed upregulation of both β1 and αV integrins in Schwann cells cultured on keratin substrates versus uncoated dishes. Integrin αV receptors were barely detectable in cells cultured on uncoated plates. However, cells grown on alpha, gamma and basic gamma keratin substrates showed a 12- to 14-fold upregulation in

integrin αV. Phosphorylated mitogen-activated protein kinase (pMAPK) and MAPK expression was also affected by culture of Schwann cells on different keratins. The alpha fraction showed a 3.6-fold increase in pMAPK to MAPK ratio compared to the gamma fraction, suggesting a correlation between the binding motif-rich alpha keratin fraction and a mitogen activated pathway. This study shows that keratins can be effectively separated based on structural criteria, and that these structural characteristic appear to have an effect on the integrin mediated-signaling of Schwann cells.

INTRODUCTION

Keratins are a family of tough, structural proteins found in epidermal appendages such as hair, nails, wool, horns, beaks and hooves. Human hair is made up of approximately 90% keratin, the majority of which are alpha and gamma keratins (4). Alpha keratins are fibrous proteins that self-assemble into long filamentous bundles. They have an average molecular weight of approximately 50-85 kDa and are low in sulfur content. Gamma keratins are globular, lower in molecular weight (~15 kDa) but have a relatively high cysteine content (5). In addition to their structural differences, alpha and gamma keratins vary in function. The alpha keratins impart toughness to the hair fiber, whereas the gamma keratins function primarily as a disulfide crosslinker that holds the cortical superstructure of the hair fiber together (6). Alpha and gamma keratins can be further subdivided into acidic and basic keratins, based on their relative isoelectric points (7).

We, and others, have shown that alpha and gamma keratins can be extracted from end cut hair using oxidative and reductive chemistries (3,8,9). The resulting keratins can be processed into many different forms such as coatings, gels, sponges and films, and used for tissue engineering and regenerative medicine applications (10). Numerous cell types, and most recently Schwann cells, have shown excellent adhesion to keratin-based matrices provided in the form of sponges and coatings, suggesting that HHKs may act as a mimic of the extracellular matrix (ECM). Native ECM plays an important role in tissue regeneration, particularly in the peripheral nervous system, where it mediates Schwann cell adhesion, proliferation and migration following injury (11). These processes are facilitated by the binding of Schwann cell

surface integrins to specific amino acid motifs, such as Arginine-Glycine-Aspartic acid (RGD), presented by constituent nerve ECM proteins (12-14) . It has been shown that in addition to the widely known RGD motif, the "X"-aspartic-"Y" motifs, where X equals glycine, leucine, or glutamic acid and Y equals serine or valine, are also widely expressed in the nerve ECM (15,16). Alpha and gamma keratins derived from human hair contain these same binding domains, and likely promote Schwann cell adhesion by providing motifs specific to integrins expressed on the Schwann cell surface.

Schwann cells express integrins α1β1, α2β1, α3β1, α5β1, α6β1, α6β4, α7β1, αVβ3, and αVβ8. Of these, the αV and β1 subunits are abundantly expressed by primary Schwann cells *in vitro* (17). When bound to ECM ligands, these integrins cluster and form associations with various signal transducing molecules to activate specific signaling pathways, including those regulated by MAP kinase. As such, integrins transmit information across the cell membrane and are critical regulators of Schwann cell migration, attachment and growth, following nerve injury (18). Recently, we showed that in addition to facilitating binding, keratins have the ability to promote Schwann cell proliferation and chemotaxis, and cause upregulation of several important genes (3). We further showed that a keratin-based scaffold stimulates regeneration of peripheral nerves, resulting in short and long-term improvements in functional recovery (2). The mechanism of this activity is not known, but we hypothesize that it is due to keratin's ability to stimulate Schwann cell activity via integrin-mediated signaling. Our aim in this study was to evaluate the primary amino acid structure of known HHKs for peptide binding domains, devise fractionation schemes that allow separation based on this structural criteria,

and investigate the effect that structural characteristics have on Schwann cell activity at a mechanistic level.

METHODS

Extraction and purification of human hair keratins

Keratin proteins were prepared as described previously (3). Briefly, end cut human hair was obtained from a local salon, oxidized with peracetic acid and extracted with aqueous tris base and deionized (DI) water to yield a crude keratin extract. Fractionation of the crude keratin material into alpha and gamma keratin fractions was achieved by isoelectric precipitation. Further separation was achieved by anion exchange chromatography, as outlined in Fig. 1A. The alpha keratins were precipitated by addition of HCl until a pH of 4.6 was reached. The remaining gamma keratins were isolated by addition to an 8-fold excess of ethanol at a pH of approximately 2. Alpha and gamma fractions were dialyzed, concentrated, neutralized, lyophilized, and the resulting keratin solid ground into a fine powder. Alpha and gamma keratins were further fractionated by anion exchange chromatography yielding acidic and basic alpha and gamma keratin preparations. A DEAE-sepharose column was pre-conditioned with 10 mM tris base at pH 6. Lyophilized alpha keratin was dissolved at a concentration of 10 mg/mL in buffer and loaded onto the column (Fig. 1B). Unbound keratin material was washed off using an additional 2L of tris base and retained as a separate fraction. The bound material was eluted with 2L of 100mM Tris base + 2M NaCl at pH 12. The

column was cleaned, pre-conditioned and the process was repeated with gamma keratins. Acidic and basic alpha and gamma keratin fractions were neutralized, dialyzed against DI water and lyophilized. Lyophilized keratin powder was sterilized by gamma irradiation (850 krad) using a ^{60}Co source prior to reconstitution in cell culture media or phosphate buffered saline (PBS) for *in vitro* testing.

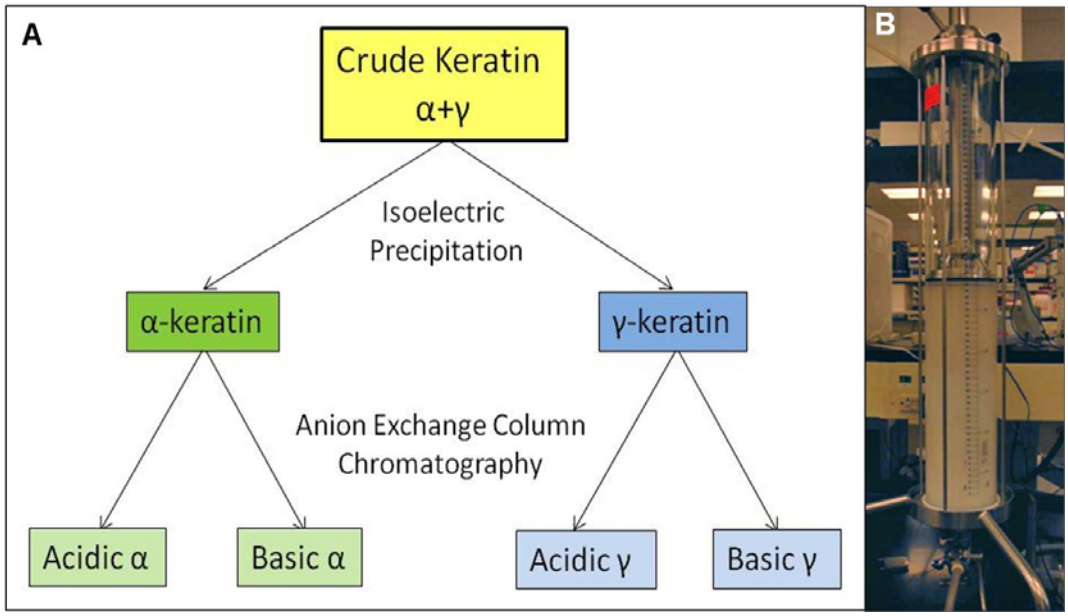

Figure 1. Overview of keratin fractionation process (A). The alpha and gamma fractions were separated by isoelectric precipitation at pH 4.6. Alpha and gamma keratins were further fractionated by anion exchange chromatography (B) yielding acidic and basic, alpha and gamma keratin preparations. All samples were dialyzed against DI water, concentrated, neutralized, and lyophilized.

Structural Analysis of HHK Amino Acid Sequences

Full-length published HHK amino acid sequences were analyzed using NCBI Blast for the presence of peptide binding domains that are known to promote cell adhesion. These

sequences were proposed structures based on cDNA data and were not confirmed by direct structural analysis of hair fiber extracts. As such it is most appropriate to consider them as probable structures and their analysis to be representative of actual HHKs. Primary amino acid structures were inspected for the following amino acid motifs: RGD, Glycine-Aspartic acid-Serine (GDS), Glycine-Aspartic acid-Valine (GDV), Leucine-Aspartic acid-Serine (LDS), Leucine-Aspartic acid-Valine (LDV), Glutamic acid-Aspartic acid-Valine (EDV), and Glutamic acid-Aspartic acid-Serine (EDS). Published HHKs were grouped into one of four sub-types: acidic alpha, basic alpha, acidic gamma and basic gamma based on their overall charge at neutral pH, and the number of cell binding sequences present on each proposed protein sequence was determined.

Amino Acid Analysis

Quantitative amino acid analyses were performed using the Pico-Tag method as described previously with slight modification (19). Briefly, crude and fractionated keratins were dissolved in ultrapure water at 1 wt. %. Samples (n=4) were hydrolyzed using 6 N HCl in 6 x 50 mm borosilicate glass tubes using a vapor-phase hydrolysis method. Samples were dried in the glass tubes which were then placed in a sealed glass vial with glass beads and 500 mL 6 N HCl. The vials were evacuated and flushed with nitrogen gas, then incubated at 110°C for 24 hours. Hydrolyzed amino acids were treated with phenylisothiocyanate to produce phenylthiocarbamyl-amino acid (PTC-AA) derivatives. The PTC-AA were separated and

quantified by reverse phase high performance liquid chromatography using a Waters HPLC system. These data are expressed as mean +/- standard deviation (n=4).

Schwann Cell Proliferation

A rat Schwann cell line, RT4-D6P2T, was obtained from the American Type Culture Collection (ATCC, Manassas, VA) and cultured as previously described (20). Schwann cell proliferation in response to crude and fractionated keratins was assessed using an MTS assay, a method that correlates metabolic reduction of a tetrazolium salt to cell number (21). RT4 cells were seeded on 96 well tissue culture plates at 1000 cells/well, allowed to attach overnight and exposed to keratin as an additive to media. Pre-sterilized keratin powders were reconstituted in serum-containing media at concentrations ranging from 0.0001-1 mg/mL (n=6 per group, per time point). At 24, 48 and 96 hours following addition of keratin to media, an MTS assay was performed according to the manufacturer's instructions (Promega, Madison, WI). Absorbance readings were taken using an ELX-500 UV plate reader (Bio-Tek, Winooski, VT) to determine relative cell numbers.

Western Blotting

The ability of a keratins to upregulate integrin expression and activate MAPK signaling was assessed by culturing Schwann cells on keratin substrates. Coating was achieved by

overnight incubation of plates with a 100 mg/mL solution of the keratin extract in PBS. Wells were rinsed three times with PBS to remove excess coating solution. RT4 Schwann cells were seeded at 5000 cells/cm^2. Uncoated and laminin-coated plates served as negative and positive controls, respectively. After 72 hours, protein was harvested from total cell lysates using RIPA extraction buffer, quantified by a Bradford assay, and analyzed by Western blot. Total proteins were resolved on a 12% SDS-PAGE gel and transferred to a PVDF membrane (Pierce, Rockford, IL). Membranes were blocked for at least one hour with 5% bovine serum albumin (BSA) dissolved in 1% Tween-20 Tris-buffered saline (TBST). Membranes were probed with antibodies to integrin β1 (1:500, Abcam, Cambridge, MA), integrin αV (1:500, Abcam, Cambridge, MA), MAPK (1:1000, Cell Signaling Technology) and pMAPK (1:1000, Cell Signaling Technology) by incubation at room temperature for one hour while shaking. Following three 5 minute washes in TBST buffer, membranes were incubated with secondary antibody (1:10,000) conjugated with horseradish-peroxidase (goat anti-rabbit IgG, Sigma, St. Louis, MO) for 40 minutes. Membranes were washed three times, 5 minutes each in TBST buffer, and detection was performed using the ECL plus Western blotting detection system (Amersham Biosciences, Piscataway, NJ. Relative changes in expression between treatment groups were quantified by performing densitometry measurements. All integrin and MAPK expression was normalized to a GAPDH or β-actin loading control.

RESULTS

Structural analysis

A total of 62 published HHK amino acid sequences were analyzed and grouped into acidic alpha, basic alpha, acidic gamma and basic gamma groups. Each HHK was screened for the following amino acid sequences: RGD, GDS, GDV, LDS, LDV, EDV, and EDS, which have been previously shown to promote binding to integrin sub-types on cell surfaces. Analysis showed that most HHKs have at least one peptide binding domain present in their proposed amino acid sequence (Fig. 2). On average, these cell binding domains are most prevalent in alpha keratins, 74% of which were found to have at least one binding motif. Of those, 100% of the acidic alpha keratins had at least one binding domain, 14.3% had two, and 8.6% had three integrin binding sequences. Of the basic alpha keratins, 35% had at least one binding domain, with 20% containing two or more. A total of 66.6% of the acidic gamma keratins contained binding domains but no such motifs were present in the basic gamma keratin family.

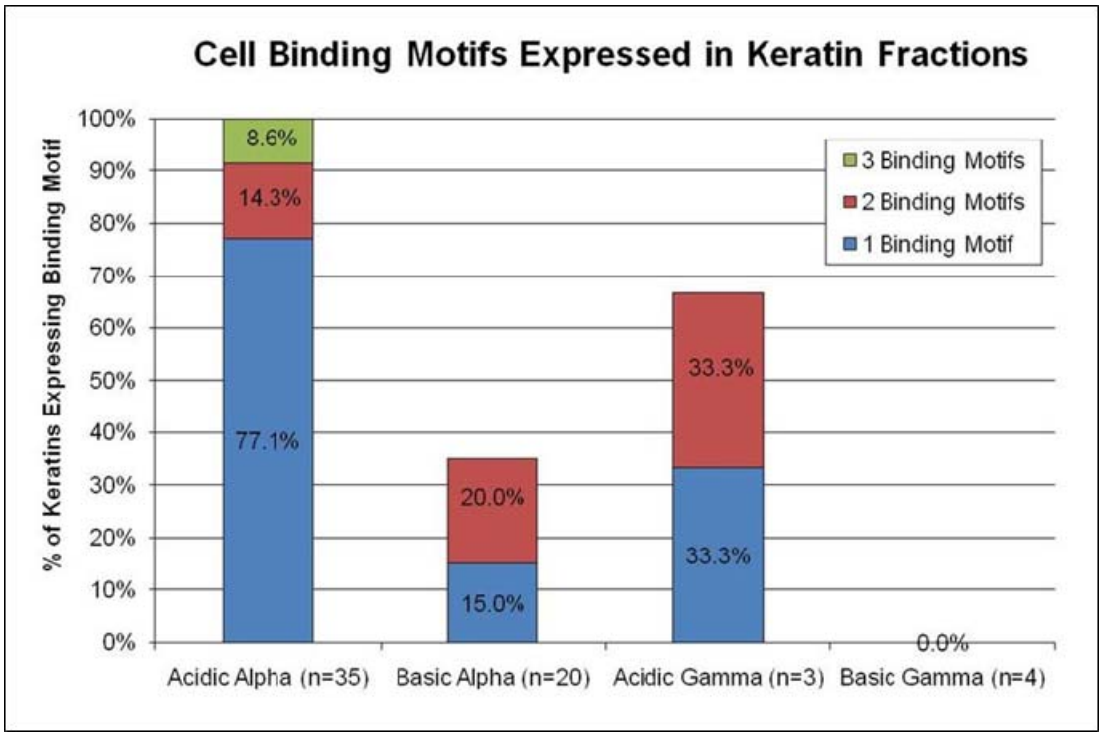

Figure 2. Structural analysis of proposed amino acid sequences of human hair keratins. Assessment reveals that with the exception of the basic gamma family of keratins, most HHKs have at least one peptide binding domain that interacts with cell surface integrins.

Amino acid analysis

The amino acid makeup of HHKs was consistent with earlier reports in the literature for wool and human hair keratins with the exception of higher methionine content (Table 1) (22,23). The methionine content of extracted keratins has been reported to be <1% of the total amino acid make-up. Our HHKs preparations contained 2.88-11.60% methionine, depending on the fraction assessed. Other differences can be seen in the amino acid composition of crude and fractionated HHKs, particularly in cysteine content. Alpha keratins which are known to be low in sulfur content, consistently contained less cysteine than gamma keratins. All gamma

keratin fractions had a high percentage of cysteine in their amino acid profile, confirming adequate separation of the two families of HHKs by isoelectric precipitation.

AMINO ACID	α + γ	α	Acidic α	Basic α	γ	Weakly Basic γ	Basic γ
Cysteine	16.08	7.43	4.72	9.77	23.63	9.81	26.83
Aspartic Acid*	6.83	11.17	10.18	9.18	3.84	9.09	3.91
Glutamic Acid*	11.55	16.18	15.49	15.29	9.38	15.13	9.77
Serine	11.57	8.70	7.66	8.15	13.46	8.86	14.11
Glycine	5.89	4.85	3.96	5.32	6.00	5.53	6.42
Histidine	1.02	0.87	0.84	0.85	0.90	0.83	0.96
Arginine	5.97	6.54	5.97	6.05	5.81	6.19	6.33
Threonine	7.32	4.74	4.44	5.43	9.20	5.46	9.57
Alanine	5.14	7.82	7.68	5.68	3.18	6.53	3.27
Proline	8.85	4.56	2.63	5.99	10.75	6.09	12.36
Valine	6.09	6.87	6.00	6.61	6.19	6.38	6.59
Methionine	6.88	2.61	11.60	3.56	8.23	3.40	2.86
Isoleucine	2.98	4.04	3.74	3.94	2.27	3.74	2.29
Leucine	6.97	10.62	10.14	9.94	3.83	9.70	3.68
Phenylalanine	1.80	2.18	1.92	2.33	1.29	2.28	1.07
Lysine	3.10	4.26	4.01	4.29	1.67	3.96	1.61

Table 1. Amino acid composition of crude (α + γ) and fractionated keratin biomaterials. Values are expressed as the mol % of the total identifiable amino acids +/- standard deviation (n=4). Of the 20 amino acids, 17 were identified using the process developed by Cohen *et al. (24)*. Tryptophan is irreversibly destroyed in the hydrolysis step and cannot be detected. Asparagine & glutamine side chains are hydrolyzed to form aspartic and glutamic acid, respectively. *Also includes asparagine and glutamine.

Schwann Cell Proliferation

The ability of keratin to induce cell multiplication was tested with RT4-D6P2T Schwann cells using the MTS assay, an established method for quantifying relative cell numbers. The cell line used in this assay has been shown to be similar to primary cultures of Schwann cells in previous studies (25). The growth response of the keratin-treated cells was measured and compared to basal media containing FBS (complete media) as the positive

control (Fig. 3). Dilutions of keratin, 1 mg/mL (Fig. 3A), 0.1 mg/mL (Fig. 3B), and 0.01 mg/mL (Fig. 3C), in basal media were added to cell cultures and incubated for 72 hours. Results showed statistically significant ($p<0.05$, $n=6$) increases in cell growth over complete media for several fractions at high and low concentrations. Gamma keratins had the largest effect on proliferation, more than doubling the proliferation rates over complete media. Gamma keratins exposed to cells at concentrations ranging from 0.01-1 mg/mL showed a 136% increase in cell number by 72 hours. The acidic and weakly basic gamma keratins also showed a substantial increase in cell number over a range of concentrations. Of the alpha keratins, the acidic alpha fraction stimulated proliferation the most. Schwann cells treated with acidic alpha keratins showed an average 91.5% increase in growth across concentrations.

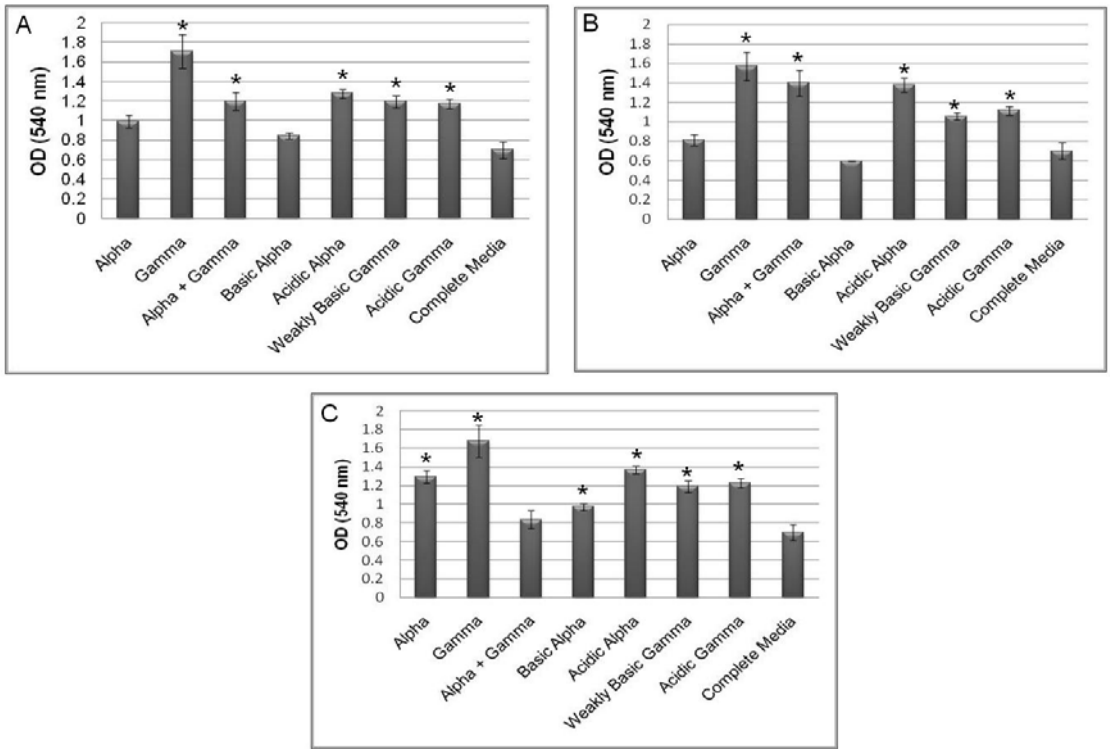

Figure 3. Schwann cell proliferation in response to fractionated keratins following 72 hours of growth. Keratin fractions were dissolved in serum-containing media at 1 mg/mL (A) and 0.1 mg/mL (B) and (C) 0.01 mg/mL. Relative cell numbers were determined using an MTS proliferation assay.

Integrin Expression

The levels of integrin-β1 and integrin-αV expression in the presence and absence of keratin were determined by Western blot. RT4 cells were cultured on crude and fractionated keratin substrates for 72 hours and immunoblotting of whole cell lysates was performed (Fig. 4A). Schwann cells cultured on keratin, laminin and uncoated substrates all expressed integrin-β1, which migrated as an immunoreactive band at the expected size of 150 kDa. Densitometry analysis showed that culture of Schwann cells on alpha and acidic gamma fractions resulted in a

1.7-1.8 fold upregulation in integrin-β1 expression that was equivalent to laminin (Fig. 4B). Half of the keratin fractions – gamma, weakly basic gamma, alpha+gamma and acidic alpha, resulted in slight decrease in integrin-β1 expression compared to uncoated dishes. Changes in integrin-αV expression were much more pronounced following culture on all keratin substrates compared to uncoated. A distinct immunoreactive band can be seen at the expected size of 135 kDa in all groups, except for uncoated where only a very faint band is present. Densitometry revealed that culture of Schwann cells on laminin and all keratin substrates increased integrin-αV expression. Cells grown on alpha, acidic alpha and basic alpha keratins had a 12-fold upregulation in integrin-αV expression over uncoated, indicating a structural effect of the alpha keratin binding motifs with integrin association.

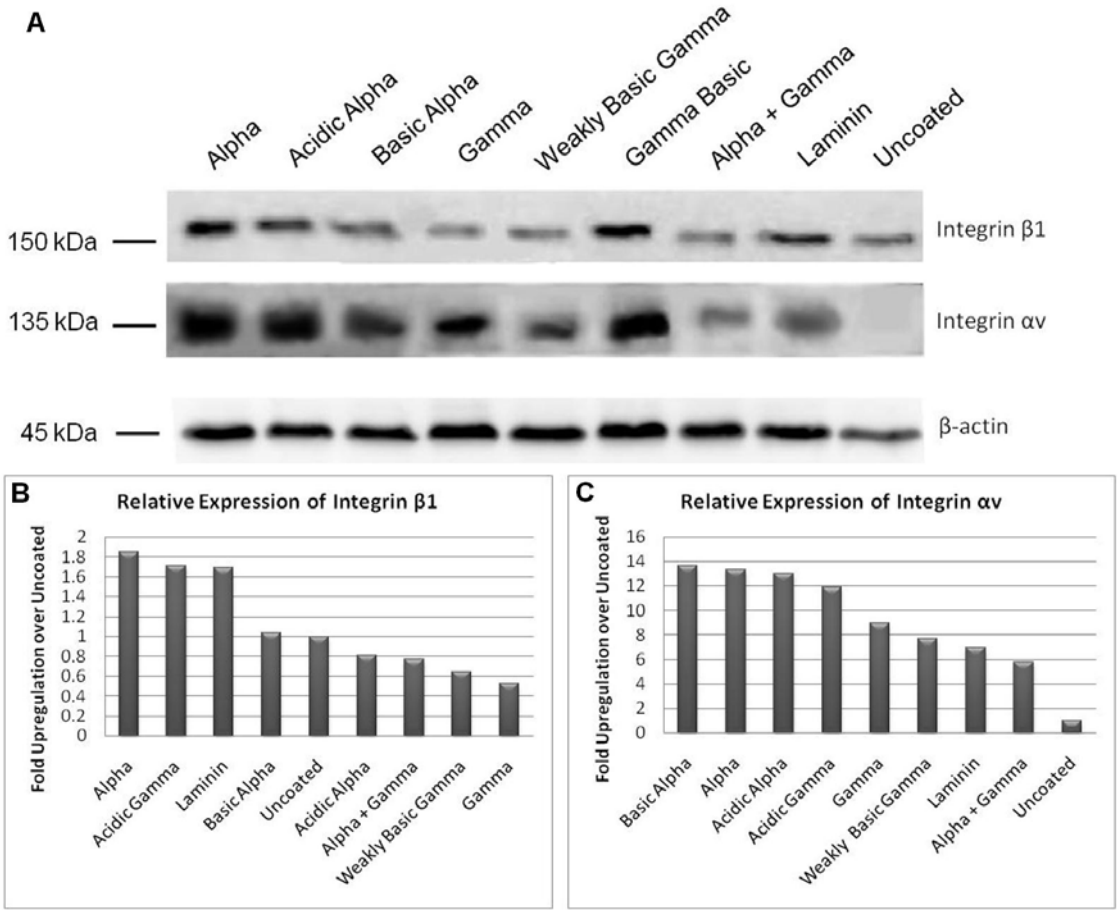

Figure 4. Immunoblot of Schwann cell lysates probed for integrins β1 and αV (A). Densitometry quantification of immunoblots probed for integrin β1 (B) and integrin αV (C) shows an increase in expression to varying degrees in RT4 cells cultured on keratin substrates.

MAPK signaling

Activation of the MAP kinase pathway in Schwann cells exposed to keratin substrates was analyzed by Western blot (Fig. 5). Erk1 and Erk2 MAPK sub-types were adequately separated by SDS-PAGE and detected as immunoreactive bands at 44 kDa and 42 kDa, respectively (Fig. 5A). For certain keratin fractions, immunoblotting appears to show

significant increases in pMAPK and MAPK compared to uncoated controls. However, quantification of expression by densitometry and normalization to the loading control GAPDH reveals that both pMAPK and MAPK expression decreased with culture on keratin coatings compared to tissue culture treated plastic. Nonetheless, distinct differences were observed in expression between different keratin sub-types (Fig. 5B). pMAPK expression was elevated in nearly all alpha keratins compared to the gamma keratins (Fig. 5C). In addition the pMAPK:MAPK ratio was higher in all alpha groups compared to the gamma keratins (Fig. 5D). In the alpha fraction, there was a 2.6-fold increase in pMAPK to MAPK ratio compared to the gamma fraction. The basic fraction showed a 2.4-fold increase in the pMAPK to MAPK ratio compared to the basic alpha fraction. This data further supports a structural effect of the alpha keratins.

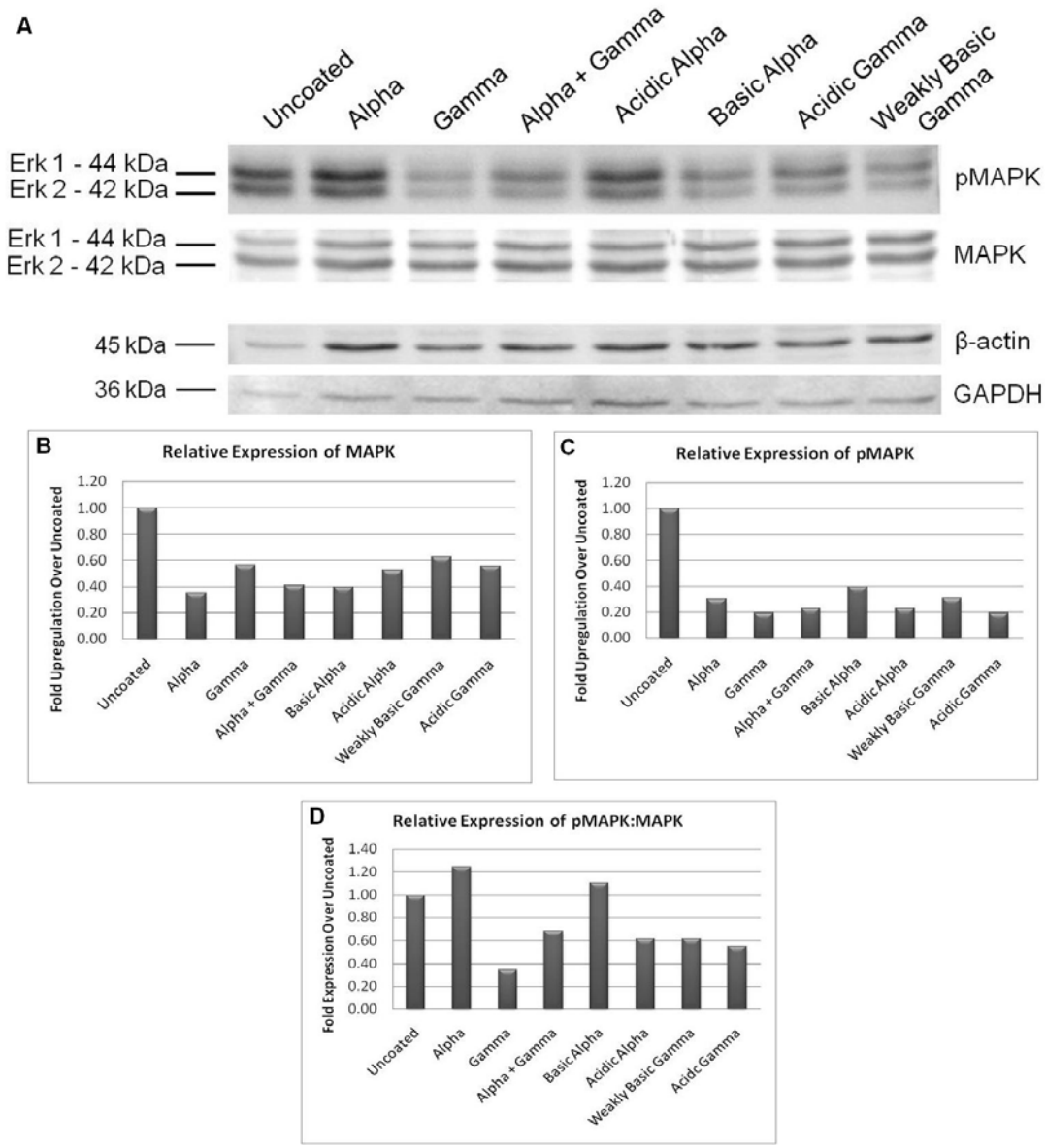

Figure 5. Immunoblot of Schwann cell lysates probed for MAPK and pMAPK (A). Relative expression of MAPK (B), pMAPK (C) and pMAPK:MAPK ratio (D) in RT4 cells cultured on keratin substrates.

DISCUSSION

The development of neuroinductive biomaterials for use in neural reconstruction is critical to overcoming current limitations in nerve repair. Existing materials provide a physical scaffold for regenerating nerves, but lack the ability to activate regenerative cells to enhance nerve tissue formation. Increasing the number of Schwann cells by promoting their adhesion and proliferation is known to improve functional healing of injured nerves. Thus, a biomaterial that is capable of acting directly on Schwann cells would be superior to previously tested materials.

This study shows that HHKs have the ability to activate Schwann cells both as a substrate and in soluble form, confirming previous observations that keratin biomaterials have neuroinductive properties. Furthermore, this study supports the hypothesis that HHK activation of Schwann cells is integrin mediated. Fractionation of crude HHK extracts by isoelectric precipitation and anion exchange chromatography generated six fractions of keratin family sub-types: alpha, acidic alpha, basic alpha, gamma, weakly basic gamma and basic gamma keratins. These fractions were characterized by amino acid analysis (Table 1) to confirm adequate separation. Assessment of keratin sub-types on Schwann cell proliferation revealed significant differences in growth rates in the presence of different keratins. The gamma keratins showed the highest increases in Schwann cell proliferation in basic, acidic or combined forms. More than a 100% increase in cell number was observed following exposure of Schwann cells to gamma keratins in soluble form for 72 hours. This suggests that the small molecular weight

globular keratins may have a more substantial effect on stimulating cell growth than the high molecular weight fibrous alpha keratins when presented to Schwann cells in soluble form.

Structural analysis of HHKs showed that alpha keratins, particularly acidic alpha keratins, are rich in peptide binding motifs similar to those found in the nerve ECM (26). We found that culture of Schwann cells on an alpha substrates resulted in upregulation of both β1 and αV integrins compared to both uncoated and laminin-coated plates, suggesting that alpha keratins may be even more effective in mediating Schwann cell adhesion than constituent nerve ECM proteins. Acidic alpha keratins resulted in a 14-fold upregulation in integrin αV but a slight downregulation (0.8-fold) of integrin β1 compared to uncoated dishes. This data is somewhat confounding. Sequence analysis of published keratins showed that LDV and EDS binding residues are most prevalent in acidic alpha keratins. These domains are known to associate with the β1 integrin sub-unit on cell surfaces (27,28). Thus, it would be expected that expression of β1 would be upregulated even more so than αV, and that intracellular signaling would be mediated by β1-subunit containing integrins such as α1β1, α2β1, α3β1, α5β1, α6β1 and α7β1 expressed on Schwann cells. However, it is possible that acidic alpha keratins contain binding motifs that have a higher affinity for the αV sub-unit versus β1, and mediate adhesion mostly via αVβ3 and αVβ8, two other integrins that are abundantly expressed on Schwann cells. In addition, it is quite probable that keratin does not promote adhesion via a single integrin sub-type. Fibronectin, for example, is capable of binding 20 distinct integrins to influence tissue repair (16). Since so many keratin homologs exist, it is reasonable to expect that the same is true for the keratin family of adhesion promoting proteins. Therefore, although these results are

suggestive of a structural dependence on Schwann cell activation, there is insufficient data to identify a definitive mechanism.

One limitation of this study is the failure to use primary cells instead of a Schwannoma cell line as an *in vitro* model system for studying Schwann cell-keratin interactions. In many *in vitro* studies of cell-biomaterial interactions, immortalized cell lines have been used in place of primary cells (29-32). This is mainly done for practical reasons since Schwann cells are difficult to isolate and have limited expansion potential, whereas immortalized cell lines are easy to obtain and grow for an indefinite number of passages. Although the expression patterns of the RT4-D6P2T have been shown to closely resemble that of primary Schwann cells (25), differences in phenotypic expression likely exist. It is well-established that the acquisition of a transformed or tumorigenic phenotype causes aberrant expression and activity of integrin receptors (33,34). Thus, assessment of integrin mediated signaling may be more appropriate using primary Schwann cells. Since integrin expression is usually elevated in immortalized cell lines, it is possible that keratins may have a larger effect on upregulating expression in primary Schwann cells. Furthermore, primary cells may show more of a structural dependence on HHK integrin-mediated activation.

Another limitation is that the nerve literature is overwhelmingly focused on laminin as the predominant basement membrane protein for Schwann cell function. Sequence analysis shows that keratin and laminin appear to have no common binding domains and share little structural similarities. The majority of the binding motifs present within keratins, such as LDV, EDS, are similar to those found in collagens and fibronectins (35). Therefore, keratins likely

bind to a completely different set of receptors than laminin, and activate Schwann cells via integrins and intracellular signaling pathways that are not as well characterized as those activated by the laminin family of ECM proteins.

In vitro experiments that cultivated primary Schwann cells on fibrin or ECM-based matrices showed that β1 and αV integrin mediated adhesion resulted in a strong activation of the MAP kinase pathway by demonstrating increased expression of ERK1 and ERK2 (36). In our study, upregulation of these integrins did not correspond to strong activation in MAPK signaling. This suggests that both the integrin expression patterns and integrin-mediated signaling is likely different in an RT4 Schwannoma model cell line, as was used in our experiments, than in a primary Schwann cell. In addition, it is possible that keratins may be activating cell proliferation via another intracellular signaling pathway such as those regulated by protein kinase C and the small GTPAses Rac and Rho, all of which have shown to be activated by association of integrins with ECM ligands (37,38).

One definitive conclusion that can be made is that different keratin sub-types have different effects on integrin upregulation and intracellular MAPK signaling. For example, even though only moderate to low upregulation of β1 was seen in the presence of keratins compared to uncoated plates, significant relative differences were observed between keratin of differing structure. For example, β1 expression was 3.5-fold higher in cells grown on an alpha substrate than on a gamma coating. This increase in β1 expression resulted in a higher activation of MAPK, as indicated by the 3.6-fold increase in the pMAPK:MAPK ratio in alpha treated cells vs. those grown on a gamma coating. Therefore, even though RT4 cells may not be the best *in*

vitro model for studying Schwann cell/keratin interactions, valuable information can still be obtained from these types of experiments. Such information can be used to design future studies aimed at optimizing the keratin hydrogel for use in neural reconstruction.

ACKNOWLEDGEMENTS

The authors would like to thank Lauren Van Dyke for assistance with sequence analysis of HHKs.

References

(1) Bradbury JH. The Structure and Chemistry of Keratin Fibers. In: Anfinsen CB, Edsall JT, Richards FM, editors. New York: Academic Press, 1973: 111-211.

(2) Apel PJ, Garrett JP, Sierpinski P et al. Peripheral nerve regeneration using a keratin-based scaffold: long-term functional and histological outcomes in a mouse model. *J Hand Surg [Am].* 2008;33(9):1541-1547.

(3) Sierpinski P, Garret J, Ma J et al. The Use of Keratin Biomaterials for the Promotion of Rapid Regeneration of Peripheral Nerves. *Biomaterials.* 2007.

(4) Yu J, Yu DW, Checkla DM et al. Human hair keratins. *J Invest Dermatol.* 1993;101(1 Suppl):56S-59S.

(5) Marshall RC. Characterization of the proteins of human hair and nail by electrophoresis. *J Invest Dermatol.* 1983;80(6):519-524.

(6) Ward WH, Lundgren HP. The Formation, Composition, and Properties of the Keratins. In: Anson ML, Bailey KB, Edsall JT, editors. New York: Academic Press Inc., 1954: 244-97.

(7) Plowman JE. The proteomics of keratin proteins. *J Chromatogr B Analyt Technol Biomed Life Sci.* 2007;849(1-2):181-189.

(8) Crewther WG, Fraser RDB, Lennox FG, Lindley H. The Chemistry of Keratins. Anfinsen CB, Anson ML, Edsall JT, Richards FM, editors. New York: Academic Press, 1965: 191-343.

(9) Lee YJ, Rice RH, Lee YM. Proteome analysis of human hair shaft: from protein identification to posttranslational modification. *Mol Cell Proteomics.* 2006;5(5):789-800.

(10) Kawano Y, Okamoto S. Film and gel of keratins. *Kagaku To Seibutsu.* 1975;13(5):291-292.

(11) Jessen KR, Mirsky R, Salzer J. Introduction. Schwann cell biology. *Glia.* 2008;56(14):1479-1480.

(12) Taylor AR, Geden SE, Fernandez-Valle C. Formation of a beta1 integrin signaling complex in Schwann cells is independent of rho. *Glia.* 2003;41(1):94-104.

(13) Chernousov MA, Stahl RC, Carey DJ. Schwann cell type V collagen inhibits axonal outgrowth and promotes Schwann cell migration via distinct adhesive activities of the collagen and noncollagen domains. *J Neurosci.* 2001;21(16):6125-6135.

(14) Herndon ME, Stipp CS, Lander AD. Interactions of neural glycosaminoglycans and proteoglycans with protein ligands: assessment of selectivity, heterogeneity and the participation of core proteins in binding. *Glycobiology.* 1999;9(2):143-155.

(15) Edgar D. Nerve growth factors and molecules of the extracellular matrix in neuronal development. *J Cell Sci Suppl.* 1985;3:107-113.

(16) Proctor RA. Fibronectin: a brief overview of its structure, function, and physiology. *Rev Infect Dis.* 1987;9 Suppl 4:S317-S321.

(17) Chernousov MA, Carey DJ. alphaVbeta8 integrin is a Schwann cell receptor for fibrin. *Exp Cell Res.* 2003;291(2):514-524.

(18) Venstrom KA, Reichardt LF. Extracellular matrix. 2: Role of extracellular matrix molecules and their receptors in the nervous system. *FASEB J.* 1993;7(11):996-1003.

(19) Bennett HP, Solomon S. Use of Pico-Tag methodology in the chemical analysis of peptides with carboxyl-terminal amides. *J Chromatogr.* 1986;359:221-230.

(20) Bansal R, Pfeiffer SE. Regulated galactolipid synthesis and cell surface expression in Schwann cell line D6P2T. *J Neurochem.* 1987;49(6):1902-1911.

(21) Mosmann T. Rapid colorimetric assay for cellular growth and survival: application to proliferation and cytotoxicity assays. *J Immunol Methods.* 1983;65(1-2):55-63.

(22) SIMMONDS DH. The amino acid composition of keratins. I. The amino acid analysis of merino 64's quality virgin wool. *Aust J Biol Sci.* 1954;7(1):98-110.

(23) Aluigi A, Zoccola M, Vineis C et al. Study on the structure and properties of wool keratin regenerated from formic acid. *Int J Biol Macromol.* 2007;41(3):266-273.

(24) Cohen SA, Strydom DJ. Amino acid analysis utilizing phenylisothiocyanate derivatives. *Anal Biochem.* 1988;174(1):1-16.

(25) Hai M, Muja N, DeVries GH et al. Comparative analysis of Schwann cell lines as model systems for myelin gene transcription studies. *Journal of Neuroscience Research.* 2002;69(4):497-508.

(26) Gong Q, Shipley MT. Expression of extracellular matrix molecules and cell surface molecules in the olfactory nerve pathway during early development. *J Comp Neurol.* 1996;366(1):1-14.

(27) Yokosaki Y, Matsuura N, Higashiyama S et al. Identification of the ligand binding site for the integrin alpha9 beta1 in the third fibronectin type III repeat of tenascin-C. *J Biol Chem.* 1998;273(19):11423-11428.

(28) Herard AL, Pierrot D, Hinnrasky J et al. Fibronectin and its alpha 5 beta 1-integrin receptor are involved in the wound-repair process of airway epithelium. *Am J Physiol.* 1996;271(5 Pt 1):L726-L733.

(29) Bosetti M, Santin M, Lloyd AW et al. Cell behaviour on phospholipids-coated surfaces *J Mater Sci Mater Med.* 2007;18(4):611-617.

(30) Bhatia SK, Arthur SD, Chenault HK, Kodokian GK. Interactions of polysaccharide-based tissue adhesives with clinically relevant fibroblast and macrophage cell lines. *Biotechnol Lett.* 2007;29(11):1645-1649.

(31) Ji Y, Li XT, Chen GQ. Interactions between a poly(3-hydroxybutyrate-co-3-hydroxyvalerate-co-3-hydroxyhexanoate) terpolyester and human keratinocytes. *Biomaterials.* 2008;29(28):3807-3814.

(32) Bhatia SK, Arthur SD, Chenault HK, Kodokian GK. Interactions of polysaccharide-based tissue adhesives with clinically relevant fibroblast and macrophage cell lines. *Biotechnol Lett.* 2007;29(11):1645-1649.

(33) Marco RA, Diaz-Montero CM, Wygant JN et al. Alpha 4 integrin increases anoikis of human osteosarcoma cells. *J Cell Biochem.* 2003;88(5):1038-1047.

(34) Duan X, Jia SF, Zhou Z et al. Association of alphavbeta3 integrin expression with the metastatic potential and migratory and chemotactic ability of human osteosarcoma cells. *Clin Exp Metastasis.* 2004;21(8):747-753.

(35) Humphries JD, Byron A, Humphries MJ. Integrin ligands at a glance. *J Cell Sci.* 2006;119(Pt 19):3901-3903.

(36) Ly DP, Corbett SA. The integrin alpha5beta1 regulates alphavbeta3-mediated extracellular signal-regulated kinase activation. *J Surg Res.* 2005;123(2):200-205.

(37) Schlaepfer DD, Hanks SK, Hunter T, van der GP. Integrin-mediated signal transduction linked to Ras pathway by GRB2 binding to focal adhesion kinase. *Nature.* 1994;372(6508):786-791.

(38) Aplin AE, Juliano RL. Integrin and cytoskeletal regulation of growth factor signaling to the MAP kinase pathway. *J Cell Sci.* 1999;112 (Pt 5):695-706.

CHAPTER IX

Discussion

Paulina Sierpinski Hill

The goal of this dissertation work was to develop, and investigate the effectiveness of, novel biomaterials for neural tissue engineering applications. Specifically, the objective was to develop neuroinductive scaffolds with the ability to act directly on regenerative cells to promote regeneration beyond current clinical limits. Two distinct scaffold-based guidance strategies were developed for bridging peripheral nerve defects. The first strategy was based on a classic tissue engineering approach, and involved the use of modified acellular grafts interposed across a nerve gap. The second strategy investigated the use of biomaterials made from human hair as a luminal filler for nerve guidance conduits. Both biomaterial scaffolds were characterized *in vitro* and ultimately tested in large animal models of peripheral nerve injury to assess their therapeutic potential. Although both approaches were developed from naturally derived tissues, they proved to be vastly different in terms of their material properties, bioactivity, and most importantly, ability to serve as inductive scaffolds for promoting functional regeneration of peripheral nerves.

In developing the first guidance strategy, we sought to understand why acellular grafts were incapable of supporting regeneration across large nerve gaps. One consideration that had been omitted in earlier allograft studies was scaffold architecture. Prior studies focused on preservation of the original architecture of the native ECM and failed to consider how the physical geometry of acellular grafts might counteract the presence of biological cues, prevent cell infiltration and inhibit axon growth (1-4). We hypothesized that acellular grafts were partly limited in their ability to support regeneration due to their dense architecture and requirement for extensive matrix remodeling upon implantation *in vivo*. To investigate this, we developed

chemical processing techniques to increase the porosity of decellularized nerves and tested the ability of such a scaffold to regenerate long segmental nerve gaps *in vivo*. We showed that the allografts could be modified using oxidative treatments to yield a more favorable microarchitecture without comprising their mechanical integrity. Furthermore, we showed that implantation of structurally modified grafts accelerated the remodeling process and lead to the formation of normal nerve tissue across large defects. Surprisingly, axon growth across the defect did not result in restoration of neuromuscular function. These findings showed that nerve allograft architecture is an important factor in regeneration across large defects and that modification of graft porosity may increase the effective length of acellular grafts. However, the lack of functional recovery suggested that acellular scaffolds are neuroconductive, but not neuroinductive, and are thus limited in their ability to promote functional regeneration. This study justified the search for another biomaterial with neuroinductive properties.

The majority of this dissertation work was dedicated to the development of the second guidance strategy, aimed at assessing the use of keratin biomaterials as a bioactive matrix filler for nerve guidance conduits. Due to the unique physical and biochemical properties of keratins, we hypothesized that keratin biomaterials could serve as a neuroinductive scaffold for bridging peripheral nerve defects. We hypothesized that keratins could do this by acting directly on regenerative cells and actively stimulating nerve growth. To assess this, we first performed basic characterization and biocompatibility testing on human hair derived keratin preparations, since keratins are a relatively new biomaterial in the regenerative medicine field. *In vitro* and *in vivo* testing showed that keratin biomaterials are highly biocompatible. Cell compatibility

assessment revealed that human hair keratins extracts are not cytotoxic, but instead have mitogenic properties. The host response to keratin scaffolds implanted subcutaneously was excellent, resulting in long-term maintenance of infiltrating host cells and generation of supportive vasculature.

The one disconnect in this thesis work is the establishment of biocompatibility with reductively-extracted keratins versus the oxidatively-derived keratin biomaterials used for all subsequent nerve experiments. Although both types of materials are derived from human hair and are considered to be highly biocompatible, oxidatively and reductively extracted keratins differ in their material properties and degradation rates. Reductively-derived keratins, or kerateines, were shown to have an *in vitro* and *in vivo* degradation rate that extended past 6 months, whereas oxidatively-extracted keratins, or keratoses, have an approximate degradation rate of 4 weeks. This difference in hydrolytic stability between the two types of preparations is critical for peripheral nerve regeneration, since it is postulated that the ideal scaffold-based nerve conduit filler should persist for approximately 4-5 weeks *in vivo* (5). Although the basic biocompatibility of keratoses was not characterized, *in vitro* testing with Schwann and endothelial cells, as well as *in vivo* nerve testing in small and large animal models, confirmed the high level of biocompatibility of oxidized keratins. Nevertheless, establishment of basic biocompatibility would have been more appropriate with oxidatively-derived keratins. This work is currently under way in the lab.

To evaluate the neuroinductive properties of keratin biomaterials, we performed a series of studies using cellular and animal models of nerve regeneration. *In vitro* assessment consisted of testing the ability of keratins to activate regenerative cells. We found that keratin biomaterials have the ability to promote Schwann cell proliferation, migration and adhesion. In later experiments using these same *in vitro* assays, we found that keratins are also able to activate endothelial cells (data not shown). In addition, we found that exposure of Schwann cells to keratin as a soluble factor dissolved in media, causes upregulation of several important genes. One example of such a gene is the Schwann cell integrin CD104, which mediates Schwann cell/axon interactions, and is known to be upregulated during nerve regeneration *in vivo* (6). To our knowledge, no other candidate nerve conduit filler matrix has been shown to activate both Schwann and endothelial cells to a similar degree.

Initial *in vivo* experiments were designed to test the safety and effectiveness of a keratin hydrogel in repairing small gaps in a mouse model. The ability of a keratin hydrogel to act at the early stages of regeneration was investigated, and found to result in a substantial improvement in functional recovery. At an early time point of 6 weeks, keratin treated nerves showed a >300% improvement in conduction delay and a ~150% increase in muscle action potential. Histological assessment revealed that keratin treated nerves were approximately 750% larger in size with higher average axon densities and larger axon diameters. Nerves were six times more vascularized and had newly formed blood vessels that were on average twice the size of those in the empty conduit group. Due to the remarkable improvements in neuromuscular recovery seen at 6 weeks, a follow up study was conducted to assess long-term functional outcomes.

Motor function was found to be permanently improved in the presence of a keratin gel. Assessment of regeneration at all time points showed that keratin had the most substantial effect on nerve growth during the early stages of regeneration, suggesting that a keratin-based hydrogel filler serves as a provisional matrix for infiltrating regenerative cells. This data provided further evidence for the neuroinductive properties of keratin biomaterials.

Recognizing that rodent models are limited in their ability to assess efficacy due to their enhanced neuroregenerative capacity (7), we developed a more clinically relevant animal model to assess keratin's performance over longer gaps. Specifically, we developed a critical size defect model of nerve injury and repair using clinically approved bioabsorbable nerve guides. We used this model to assess the ability of a keratin hydrogel filler to promote regeneration across a critical size defect. We found that injection of a keratin hydrogel into a collagen nerve guide was not only able to promote regeneration across large gaps, but resulted in significantly improved motor function recovery over empty conduits. Histological assessment confirmed electrophysiological outcomes by showing that keratin treated nerves were larger in size, had more axons, a larger total axon area, and thicker myelin sheaths than nerves that regenerated through unfilled collagen conduits.

The last portion of this dissertation work was focused on elucidating the mechanisms by which keratin biomaterials act on regenerative cells to promote nerve growth. Based on earlier reports suggesting that keratins act as a mimic of the ECM, and our own data supporting these observations, we hypothesized that activation of Schwann cells by keratins is structurally dependent and integrin-mediated. We first evaluated the primary amino acid structure of

known keratins for peptide binding motifs, and developed fractionation schemes to separate out different families of keratins contained within whole human hair extracts based on structural criteria. These purified keratins were tested for their ability to activate Schwann cells using a combination of cellular and molecular assays, and found to upregulate expression of integrins β1 and αV, that led to intracellular changes in MAPK signaling. Although we were not able to identify a specific structurally-dependent mechanism, we showed that keratins could be effectively separated based on structural criteria, and that these structural characteristics have an effect on the integrin-mediated signaling of Schwann cells.

This dissertation work demonstrates the development of allograft- and keratin-based scaffolds for bridging peripheral nerve defects. Although the two technologies were not tested side-by-side in the same animal model, the data presented here suggests that keratins are neuroinductive, whereas acellular grafts are neuroconductive. Keratins were found to promote Schwann cell proliferation, migration and adhesion, via mechanisms that appear to be integrin-mediated. Although we and others, have shown that acellular grafts are neuroconductive in that they are able to support axon growth, no studies have documented the ability of acellular grafts to activate regenerative cells in a similar manner to keratin biomaterials.

Thus, this work represents the first study investigating the use of structurally modified allografts and biomaterials made from human hair for regeneration of peripheral nerves. More importantly, this work has resulted in the development and characterization of a novel neuroinductive biomaterial that can be used as a luminal conduit filler in peripheral nerve repair. Numerous studies have explored the use of cellular, growth factor, and scaffold-based

nerve conduit fillers, however none of these experimentally tested fillers have been translated clinically. More than two decades have passed since insertion of a matrix into the lumen of a nerve conduit was shown to promote nerve regeneration, but today surgeons are still bridging defects using empty or saline-filled nerve conduits. This work presents the development of a scaffold-based filler that may be capable of overcoming many of the limitations associated with previously tested luminal fillers. Unlike other fillers, keratins are neuroinductive in that they are able to directly stimulate nerve growth by acting on regenerative cells. Furthermore, keratin biomaterials meet many of the scientific and regulatory criteria of the ideal biomaterial. Since they are derived from one of the few human tissues that are commonly discarded, they are readily available, easy to obtain and represent a plentiful supply of growth-promoting proteins. Furthermore, keratins are non-xenogenic, cell instructive and have the optimal degradation characteristics of a peripheral nerve scaffold. In addition, keratins are highly biocompatible and do not have to be tissue-matched for each individual.

In summary, keratin biomaterials made from human hair represent a novel, neuroinductive, scaffold-based conduit filler that may be used as an "off-the-shelf" product for treatment of peripheral nerve injuries. The results of this dissertation work justify the translation and clinical development of a keratin-based hydrogel filler as a complimentary product for use in existing nerve conduits. Moreover, this work suggests that keratin biomaterials are a promising scaffold-based conduit filler that may be capable of overcoming current clinical limitations in peripheral nerve repair.

References

(1) Frerichs O, Fansa H, Schicht C et al. Reconstruction of peripheral nerves using acellular nerve grafts with implanted cultured Schwann cells. *Microsurgery.* 2002;22(7):311-315.

(2) Haase SC, Rovak JM, Dennis RG et al. Recovery of muscle contractile function following nerve gap repair with chemically acellularized peripheral nerve grafts. *J Reconstr Microsurg.* 2003;19(4):241-248.

(3) Kim BS, Yoo JJ, Atala A. Peripheral nerve regeneration using acellular nerve grafts. *J Biomed Mater Res A.* 2004;68(2):201-209.

(4) Krekoski CA, Neubauer D, Graham JB, Muir D. Metalloproteinase-dependent predegeneration in vitro enhances axonal regeneration within acellular peripheral nerve grafts. *J Neurosci.* 2002;22(23):10408-10415.

(5) Valentini RF, Aebischer P, Winn SR, Galletti PM. Collagen- and laminin-containing gels impede peripheral nerve regeneration through semipermeable nerve guidance channels. *Exp Neurol.* 1987;98(2):350-356.

(6) Frostick SP, Yin Q, Kemp GJ. Schwann cells, neurotrophic factors, and peripheral nerve regeneration. *Microsurgery.* 1998;18(7):397-405.

(7) Taras JS, Nanavati V, Steelman P. Nerve conduits. *J Hand Ther.* 2005;18(2):191-197.

SCHOLASTIC VITAE

PAULINA SIERPINSKI HILL

Wake Forest University School of Medicine
Medical Center Boulevard
Winston-Salem, NC 27157-1083
psierpin@wfubmc.edu

EDUCATION

May 2009	Ph.D. in Molecular Medicine and Translational Science Wake Forest Institute for Regenerative Medicine Wake Forest University School of Medicine, Winston-Salem, NC
2004	B.S. in Biology, Biochemistry & Neuroscience B.A. in Chemistry Honors Thesis in Neuroscience East Carolina University, Greenville, NC

INTERNSHIPS

04/2008-12/2008	Office of Technology Asset Management (OTAM) Wake Forest University Health Sciences, Winston-Salem, NC

HONORS AND AWARDS

2008	Wake Forest University Alumni Student Travel Award to attend TERMIS 2008 - San Diego, CA
2008	Grand Prize Winner of Charlotte Biotechnology Conference Research Commercialization Plan Competition – Charlotte, NC
2008	Marie Curie Foundation Scientist Travel Award to attend 5th International Stem Cell School & Conference - Berlin, Germany

2008	Selected as 1 of 200 pre-doctoral students to attend 3rd Annual NIH Graduate Student Research Festival – Bethesda, MD
2008	Society for Biomaterials Student Travel Achievement Recognition Award Honorable Mention
2008	Wake Forest Institute for Regenerative Medicine Annual Retreat Pre-doctoral Poster award
2008	Article highlighted in *Clinical Neurology News*. **Sierpinski P**, et al. *Biomaterials* 29: 118-128 (2008).
2007	Article highlighted in ***Science*** 2007; 23:1219. **Sierpinski P**, et al. *Biomaterials* 29: 118-128 (2008).
2007	Tissue Engineering & Regenerative Medicine International Society (TERMIS) Student Travel Award – Toronto, ON
2006	Winner of Wake Forest Institute for Regenerative Medicine Annual Retreat Pre-doctoral Poster Competition
2004	Summa Cum Laude – East Carolina University
2004	Honors in Neuroscience, East Carolina University
2004	Winner of East Carolina University Undergraduate Thesis Research Competition
2003 & 2004	East Carolina University Outstanding Scholar-Athlete Award
2002	East Carolina University Summer Medical Research Program
2002	Conference USA Annual Commissioners Award for Outstanding Scholar-Athlete
2001	East Carolina University Service Award for commitment to community service
2001-2004	Conference USA All Academic Team
2000 & 2001	Chancellor's List – East Carolina University
2002 & 2003	Dean's List – East Carolina University
2000-2004	East Carolina University Women's Tennis Scholarship

LEADERSHIP AND SERVICE

2005-present	Undergraduate, Medical and Graduate Student Research Mentor

2005-present	Wake Forest University Matching Matriculants with Return Students (MMARS) Program Representative
2008	North Carolina DNA Day 2008 Ambassador
2006-2007	Graduate Student Association (GSA) Athletics Chair
2005-2007	Graduate Student Association (GSA) Departmental Representative
2005-2006	Crosby Scholar Advisors for High School Students
2003-2004	Golden Key International Honors Society, Vice-President of East Carolina University chapter
2003-2004	East Carolina University Student Athletic Council, Vice-President
2002-2004	Fellowship of Christian Athletes Leader for High School Students
2002-2004	East Carolina University Women's Varsity Tennis Team Captain
2001-2003	Pitt County Memorial Hospital Volunteer

PROFESSIONAL MEMBERSHIPS

2006-present	Society for Biomaterials
2006-present	Tissue Engineering and Regenerative Medicine International Society
2004-present	International Student Society for Stem Cell Research (ISSSCR)
2003-present	Golden Key International Honors Society
2003-present	Phi Kappa Phi Honors Society
2000-2004	East Carolina Honors Society

PUBLICATIONS

Sierpinski P, Tawfik B, Van Dyke ME. Structural dependence of keratin biomaterials on integrin-mediated activation of Schwann cells (manuscript in preparation).

Sierpinski P, Apel PJ, Barnwell J, Smith T, Koman LA, Atala A and Van Dyke ME. Repair of critical size peripheral nerve defects in rabbits with keratin hydrogel scaffolds (manuscript in preparation).

Sierpinski P, Brantley H, Van Dyke ME. Some properties of keratin biomaterials Part I: Kerateines (manuscript in preparation).

Sierpinski P, Apel PJ, AbouShwareb T, Yoo J, Atala A, Van Dyke ME. Regeneration of peripheral nerves using structurally modified acellular grafts (in review by *Tissue Engineering*).

Apel PJ, Garrett J, **Sierpinski P,** Smith T, Koman LA, Van Dyke ME. Peripheral nerve regeneration using a keratin-based scaffold: Long-term functional and histological outcomes in a mouse model. *J. Hand Surgery* 33(9):1541-1547 (2008).

Sierpinski P, Garrett J, Ma, J, Apel PJ, Klorig D, Smith T, Koman, LA, Atala A and Van Dyke ME. The use of keratin biomaterials made from human hair for the promotion of regeneration of peripheral nerves. *Biomaterials* 29: 118-128 (2008).

Murashov AK, Chintalgattu V, Islamov RR, Lever TE, Pak SE, **Sierpinski PL**, Katwa LC, Van Scott, MR. RNAi pathway is functional in peripheral nerves. *FASEB J*. 21: 656-70 (2007).

Murashov AK, Pak ES, Hendricks WA, Owensby JP, **Sierpinski PL**, Tatko LM, Fletcher PL. (2005) Directed differentiation of embryonic stem cells into dorsal interneurons; *FASEB J*. 19: 252-4 (2005).

ABSTRACTS – PODIUM PRESENTATIONS

Sierpinski P. Keratin Biomaterials Activate Schwann Cells via Integrin-Mediated Signaling and Promote Regeneration of Large Peripheral Nerve Defects in a Rabbit Model. *Society for Biomaterials,* April 2009 (San Antonio, TX).

Sierpinski P. Structurally Modified Acellular Scaffolds Promote Peripheral Nerve Regeneration in a Rabbit Model. *Tissue Engineering and Regenerative Medicine International Society (TERMIS-NA)*, December 2008 (San Diego, CA).

Sierpinski P. A Biomaterial Derived from Human Hair Keratins Can Serve as a Scaffold for Tissue Engineering in Orthopaedic Applications. *Orthopaedic Research Society*, October 2007 (Honolulu, HI).

Sierpinski P. Human Hair Derived Keratins Mediate Schwann Cell Behavior *in vitro* and Facilitate Rapid Peripheral Nerve Regeneration *in vivo, Tissue Engineering and Regenerative Medicine International Society (TERMIS-NA),* June 2007 (Toronto, ON).

Sierpinski P. Human Hair Derived Keratins Mediate Schwann Cell Behavior *in vitro* and Facilitate Rapid Peripheral Nerve Regeneration *in vivo*, *Society for Biomaterials*, April 2007 (Chicago, IL).

Sierpinski P. Biocompatibility of Keratin Biomaterials Derived from Human Hair, *North Carolina Tissue Engineering & Regenerative Medicine (NCTERM),* September 2006 (Durham, NC).

Sierpinski P. Rapid Peripheral Nerve Regeneration Using Self-Assembled Human Hair Keratin Scaffolds, *Society for Biomaterials*, April 2006 (Pittsburgh, PA).

ABSTRACTS - POSTER PRESENTATIONS

Sierpinski P, Tawfik B, Atala A, Van Dyke ME. Keratin Biomaterials Show a Structural Dependence on Schwann Cell Activation. *Tissue Engineering and Regenerative Medicine International Society (TERMIS-NA)*, December 2008.

Sierpinski P, Apel PJ , Garrett J, Ma J, Klorig D, Smith T, Koman LA, Atala A, Van Dyke ME. Growing Nerves From Human Hair – The Road to Commercialization. *Charlotte Biotechnology Conference,* October 2008.

Sierpinski P, Apel PJ , Garrett J, Ma J, Klorig D, Smith T, Koman LA, Atala A, Van Dyke ME. Neural Tissue Engineering Scaffolds Made From Human Hair Activate Regenerative Cells and Nerve Regeneration. *5th International Stem Cell School & Conference*, October 2008.

Sierpinski P, Apel PJ , Garrett J, Ma J, , Klorig F, Smith T, Koman LA, Atala A, Van Dyke ME. Keratin Biomaterials Activate Regenerative Cells and Promote Peripheral Nerve Regeneration at Early and Late Stages in a Mouse Model. *Society for Biomaterials*, September 2008.

Sierpinski P, Burnell J, Yoo J, Atala A, Van Dyke ME. Peripheral Nerve Regeneration through Structurally Modified Acellular Scaffolds in a Rabbit Model. *Society for Biomaterials*, September 2008.

Sierpinski P, Garrett J, Ma J, Apel PJ, Klorig D, Smith T, Koman LA, Atala A, Van Dyke ME. Keratin Biomaterials Mediate Schwann Cell Activity *in vitro* and Promote Rapid Regeneration of Peripheral Nerves *in vivo. NIH Graduate Student Research Festival*, September 2008.

Sierpinski P, Burnell J, Apel PJ, Klorig D, Bobba V, DeLeo S, Smith T, Van Dyke ME. Keratin Biomaterials Made from Human Hair Mediate Schwann and Endothelial Cell Activity *In vitro*. *Orthopaedic Research Society*, October 2007.

Sierpinski P, Apel PJ, Burnell J, Yoo J, Atala A, Van Dyke ME. Peripheral Nerve Regeneration Using Structurally Modified Acellular Grafts. *North Carolina Tissue Engineering & Regenerative Medicine (NCTERM),* September 2007.

Sierpinski P, Garrett J, Ma J, Apel PJ, Smith T, Koman LA, Atala A, Van Dyke ME. Human Hair Derived Keratins Mediate Schwann Cell Behavior *in vitro* and Facilitate Rapid Peripheral Nerve Regeneration *in vivo. North Carolina Tissue Engineering & Regenerative Medicine (NCTERM),* September 2007.

Sierpinski P, Garrett J, Ma J, Apel PJ, Smith T, Koman LA, Atala A, Van Dyke ME. Human Hair Derived Keratins Mediate Schwann Cell Behavior *in vitro* and Facilitate Rapid Peripheral Nerve Regeneration *in vivo. Experimental Biology*, April 2007.

Sierpinski P. & Van Dyke ME. Biocompatibility of Keratin Biomaterials Derived from Human Hair, *Society for Biomaterials*, April 2007.

Sierpinski P, Garrett J, Ma J, Apel PJ, Smith T, Koman LA, Atala A, Van Dyke ME. Peripheral Nerve Regeneration Using Human Hair Derived Keratin Scaffolds, *Wake Forest University School of Medicine Surgical Sciences Research Day,* November 2006.

Sierpinski P. & Van Dyke ME. Biocompatibility of Keratin Biomaterials Derived from Human Hair, *Experimental Biology*, April 2006.

Sierpinski P. & Van Dyke ME. Biocompatibility of Keratin Biomaterials Derived from Human Hair, *Tissue Engineering & Regenerative Medicine International Society (TERMIS-NA)*, April 2006.

Sierpinski P, Ma J, Garrett J, Burnell J, Lee SJ, Smith T, Atala A & Van Dyke M. Neural Tissue Engineering Scaffolds from Self-Assembled Human Hair Keratins, *North Carolina Tissue Engineering & Regenerative Medicine,* February 2006.

Sierpinski P. Ma J, Ma J, Garrett, J, Burnell J, Lee SJ, Smith T, Atala A, Van Dyke ME. Tissue Engineering Scaffolds from Self-Assembled Human Hair Keratins, *Regenerate Meeting,* June 2005.

INVITED PRESENTATIONS

Sierpinski P. Regeneration of Peripheral Nerves Using Neuroinductive Biomaterial Scaffolds. MIT, March 2009.

Sierpinski P. Regeneration of Peripheral Nerves Using Neuroinductive Biomaterial Scaffolds. Johns Hopkins, February 2009.

Sierpinski P. Regeneration of Nerve Tissues Using Biomaterials Made From Human Hair. Stanford University, December 2008.

Sierpinski P. Peripheral Nerve Regeneration Using Novel Biomaterial Scaffolds. Wake Forest Health Sciences, March 2008.

Sierpinski P. Growing Nerves with Human Hair – Is it possible? *Babcock Graduate School of Management,* Wake Forest University, February 2008.

Sierpinski P. Wound Healing with Keratin Biomaterials Made from Human Hair. *Babcock Graduate School of Management,* Wake Forest University, February 2008.

Sierpinski P. Peripheral Nerve Regeneration using Tissue Engineering Strategies, Wake Forest Health Sciences, April 2005.

Sierpinski P. Molecular Targeting of Glioblastoma Multiforme (GBM) with Recombinant Fusion Proteins, December 2004, Wake Forest Health Sciences.

Sierpinski P. Inhibition of Axonal Protein Synthesis by RNA Interference (RNAi) Mechanisms, April 2004, East Carolina University.

GRADUATE COURSES

Molecular Biology I & II
Proteins & Enzymes
Molecular Basis of Human Disease I & II
Clinical Molecular Medicine
Regenerative Medicine I & II
Research Techniques in Microscopy
Introduction to Statistics
Contemporary Issues in Molecular Medicine
Scientific Development & Business of Science
Fundamentals of Scientific Integrity
Metabolism & Bioenergetics
Physiology/Pharmacology
Immunology
Advanced Topics - Molecular Medicine
Biochemical Techniques
Biomaterials
Scientific Communication
Commercializing Innovation
Professional Development
Translational Science Seminar Series

Topics in Clinical Trials Workshops I & II